People's Democratic Republic of Algeria Ministry of Higher Education and Scientific Research
University of Ibn Khaldoun Tiaret
Faculty of Nature and Life Sciences
Department of Nutrition and Agri-food Technologies

End of studies dissertation
In view of obtaining the Master's degree
Field: Nature and Life Sciences
Sector: Nutrition and Agri-food Technologies
Speciality: Precision Agriculture

Presented by:

-BENOUADAH OUSSAMA

-TLIDJI ABDELKADER

THEME

Estimating water irrigation consumption for wheat crop using remote sensing data in the region of Tiaret

Defended in: 06/26/2023.

Jury:

President: Dr. KADDAR BACHIR **« MCB, University of Tiaret,»**

Supervisor: Dr BOUACHA ISLEM **« MCB, University of Tiaret »**

Examiner: Dr. BENSALAH LAOUISSATE **« Research Director, CRSTRA (taouiala) »**

Academic year: 2022-2023

Acknowledgements

We thank above all "ALLAH", for having given us faith and courage and for having guided us for the accomplishment of this work. First of all, we thank for their moral, spiritual and material support, our parents, brothers, sisters, friends and companions who helped, advised and encouraged us find here the expression of our deepest gratitude.

Thus, we would like to express our deep gratitude to our promoter **Mr. Bouacha Islam Mohamed** doctor at the faculty of natural and life sciences at Ibn Khaldoun University of Tiaret, for his supervision, his precious advice as well as his encouragement and confidence.

We extend our heartfelt thanks to:

Mr. KADDAR BACHIR doctor the Ibn Khaldoun University of Tiaret and **Mr. BENSALAH** doctor at the Amar Telidji University of laghouat for their precious time and their presence as members of the juries.

Special appreciation goes to **Mrs. Saida**, the laboratory engineer, for her exceptional technical assistance, dedication, and support during the experimental phase. Her expertise and willingness to help have been invaluable in achieving accurate and reliable results.

We are grateful to the director of the pilot farm Cherif Eddine, for granting permission to conduct research on-site. His cooperation and logistical support

My sincere appreciation to **Dr. Issam Chaaban** for his valuable advice, suggestions, and expertise. His mentorship and guidance have played a significant role in shaping the overall quality and contribution of this research.

We also express our thanks and our great gratitude to all the professors of the Faculty of Natural and Life Sciences at Ibn Khaldoun University of Tiaret who accompanied us in this educational journey.

Dedication

I dedicate this dissertation to the incredible individuals who have been pillars of support and inspiration throughout my academic journey. First and foremost, I express my deepest gratitude and love to my parents for their unwavering encouragement, sacrifices, and belief in my abilities. Their unconditional love and constant support have been the driving force behind my accomplishments.

I am grateful to my siblings, my brothers Hichem and Ibrahim for their constant presence, encouragement, and understanding. Their unwavering support and belief in my potential have been a source of motivation and strength throughout this challenging process.

A special dedication goes to **Mrs. Mihoub Fatma**, my second mom, for her invaluable guidance, patience, and selfless devotion to my academic growth. Her unwavering belief in my abilities and her countless hours spent providing guidance and support have been truly transformative.

I would like to express my heartfelt appreciation to my cousin **Rostom** for his valuable advice, constructive criticism, and academic insights. His guidance and mentorship have played a crucial role in shaping the quality and direction of this research.

I am grateful to my friends **Youcef, Merouan, farouk, Khalido, Cherif, Alilo, Basset, Kebbich, bouzian** and all my other friends for their constant encouragement, understanding, and companionship. Their unwavering support, intellectual discussions, and moments of laughter have made this journey more enjoyable and meaningful.

Lastly, I extend my heartfelt thanks to all my family members and loved ones for their unwavering support, understanding, and belief in my potential. Their love, encouragement, and presence have been the cornerstone of my success.

This dissertation is dedicated to all the individuals mentioned above. Their love, support, guidance, and friendship have made this achievement possible, and I am forever grateful for their presence in my life.

Dedication

It is with deep gratitude and sincere words that I dedicate this modest end-of-studies work to my dear parents who sacrificed their lives for my success and enlightened me by their judicious advice and their douaa. I also dedicate this work to my brothers, sisters and friends.

Abbreviations List

AMSR : Advanced Microwave Scanning Radiometer
ANRH : Agence Nationale des Ressources Hydriques (National Agency for Water Resources)
API : Application Programming Interface
AquaStat : FAO's global information system on water and agriculture
ASCAT : Advanced SCATterometer
BCM : Billion Cubic Meters
BM : Banque Mondiale (World Bank)
CFT : Center for Forestation Techniques
CH_4 : Methane
CNIS : Centre National de l'Informatique et des Statistiques
CO_2 : Carbon Dioxide
CWSI : Crop Water Stress Index
DHW : Directorate of Hydraulic Works
DRE : Direction des Ressources en Eau (Water Resources Directorate)
ET : Evapotranspiration
ETr : Reference crop evapotranspiration
EVI : Enhanced Vegetation Index
FAO : Food and Agriculture Organization
G : Soil heat flux
GDP : Gross Domestic Product
GDPA : Gross Domestic Agricultural Production
GEE : Google Earth Engine
GHG: Greenhouse Gas
H : Sensible heat flux
ha : hectare
IPCC : Intergovernmental Panel on Climate Change
K : potassium
KCl : potassium chloride
LDCM : the Landsat Data Continuity Mission
LSWI : Land Surface Water Index
Madr : Ministry of Agriculture and Rural Development
MADRP : Ministère de l'Agriculture, du Développement Rural et de la Pêche
MAP : Mean Annual Precipitation
MAT : Mean Annual Temperature
MATE: Ministry of Energy and Mining (Algeria)
MCM : Million Cubic Meters
Mha : million hectares
mm/hr : millimeters per hour
MMP : monthly mean precipitation
MMT : Monthly Mean Temperature
MODIS : Moderate Resolution Imaging Spectroradiometer
N : nitrogen
N_2O : Nitrous Oxide
NDMI : Normalized Difference Moisture Index
NDVI : Normalized Difference Vegetation Index

NIR : near-infrared
OLI : Operational Land Imager
P : phosphorus
PDI : Programme pour le Développement de l'Investissement Agricole (Program for the Development of Agricultural Investment)
pH : potential hydrogen
PNDR : Programme National de Développement Rural (National Agricultural and Rural Development Program)
q : quintal (unit of weight equal to 100 kilograms)
RGPH : Recensement Général de la Population et de l'Habitat (General Population and Housing Census)
RL↑ : Outgoing longwave radiation
RL↓: Incoming longwave radiation
Rn : Net radiation flux at the surface
RS : Remote Sensing
RS↓ : Incoming shortwave radiation
SEBAL : Surface Energy Balance Algorithm for Land
SMOS : Soil Moisture Ocean Salinity
SR : Surface Reflectance
SWIR : shortwave infrared
UNEP : United Nations Environment Programme
USD : United States Dollar
USDA : United States Department of Agriculture
USGS : United States Geological Survey
VIC : Variable Infiltration Capacity
A : Surface albedo
εo : Surface thermal emissivity
λ : Latent heat of vaporization
λET : Latent heat flux

List of figures

List of tables

Table of content

Abstract

Cereal and wheat crops play a vital role in global and Algerian agriculture, providing a staple food source and contributing to food security. However, the increasing incidence of drought poses significant challenges to wheat production. This necessitates the adoption of innovative approaches, such as remote sensing, to monitor and manage agricultural resources effectively.

This study explores the importance of remote sensing in agriculture and its role in mitigating the impacts of drought on wheat crops. It begins by discussing the significance of cereal and wheat crops for global food production, highlighting their importance in ensuring food security and sustainable development, particularly in Algeria.

The work done in this study is employing remote sensing (Landsat 8 images), laboratory analysis, and modeling techniques. The study utilized the SEBAL model and the AquaCrop software to calculate evapotranspiration, quantify water needs, and optimize water irrigation practices.

Overall, this study demonstrates the importance of cereal and wheat crops, highlights the challenges posed by drought, underscores the significance of remote sensing in agriculture, and provides an overview of the work conducted to estimate water irrigation consumption for wheat crops using remote sensing data. The findings have the potential to inform decision-makers, farmers, and researchers in adopting sustainable water management strategies and enhancing the resilience of wheat crops in the face of climate change and water scarcity.

Keywords: cereals, wheat, water irrigation, remote sensing, SEBAL model, AquaCrop software, precision agriculture, decision-making

ملخص

تلعب محاصيل الحبوب والقمح دورًا حيويًا في الزراعة العالمية والجزائرية، حيث توفر مصدرًا للغذاء الأساسي وتساهم في الأمن الغذائي. ومع ذلك، فإن زيادة حدوث الجفاف تشكل تحديات كبيرة لإنتاج القمح. وهذا يستلزم اعتماد نهج مبتكر، مثل الاستشعار عن بعد، لرصد وإدارة الموارد الزراعية على نحو فعال.

تستكشف هذه الدراسة أهمية الاستشعار عن بعد في الزراعة ودوره في التخفيف من آثار الجفاف على محاصيل القمح. ويبدأ بمناقشة أهمية محاصيل الحبوب والقمح لإنتاج الغذاء العالمي، وإبراز أهميتها في ضمان الأمن الغذائي والتنمية المستدامة، لا سيما في الجزائر.

العمل المنجز في هذه الدراسة هو استخدام الاستشعار عن بعد (صور LANDSAT 8)، والتحليل المخبري، لحساب التبخر، وتحديد الاحتياجات المائية، AquaCrop وبرنامج SEBAL وتقنيات النمذجة. استخدمت الدراسة نموذج وتحسين ممارسات الري المائي.

بشكل عام، توضح هذه الدراسة أهمية محاصيل الحبوب والقمح، وتسلط الضوء على التحديات التي يفرضها الجفاف، وتؤكد على أهمية الاستشعار عن بعد في الزراعة، وتقدم لمحة عامة عن العمل الذي تم إجراؤه لتقدير استهلاك مياه الري لمحاصيل القمح باستخدام بيانات الاستشعار عن بعد. النتائج لديها القدرة على إطلاع صناع القرار والمزارعين والباحثين على تبني استراتيجيات إدارة المياه المستدامة وتعزيز مرونة محاصيل القمح في مواجهة تغير المناخ وندرة المياه.

الكلمات المفتاحية: الحبوب، القمح، الري بالمياه، الاستشعار عن بعد، نموذج SEBAL، برنامج AquaCrop، الزراعة الدقيقة، اتخاذ القرار.

Résumé :

Les cultures céréalières et le blé jouent un rôle vital dans l'agriculture mondiale & *al*gérienne, en fournissant une source alimentaire essentielle et en contribuant à la sécurité alimentaire. Cependant, l'augmentation des périodes de sécheresse pose des défis importants à la production de blé. Cela nécessite l'adoption d'approches innovantes, telles que la télédétection, pour surveiller et gérer efficacement les ressources agricoles.

Cette étude explore l'importance de la télédétection en agriculture et son rôle dans atténuer les impacts de la sécheresse sur les cultures de blé. Elle commence par discuter de l'importance des cultures céréalières et du blé pour la production alimentaire mondiale, en mettant en évidence leur importance pour assurer la sécurité alimentaire et le développement durable, notamment en Algérie.

Le travail réalisé dans cette étude utilise la télédétection (images du satellite Landsat 8), l'analyse en laboratoire et des techniques de modélisation. L'étude a utilisé le modèle SEBAL

et le logiciel AquaCrop pour calculer l'évapotranspiration, quantifier les besoins en eau et optimiser les pratiques d'irrigation.

Dans l'ensemble, cette étude met en évidence l'importance des cultures céréalières et du blé, souligne les défis posés par la sécheresse, met en évidence le rôle crucial de la télédétection en agriculture et donne un aperçu des travaux réalisés pour estimer la consommation en eau pour l'irrigation des cultures de blé en utilisant des données de télédétection. Les résultats ont le potentiel d'informer Les décideurs, les agriculteurs et les chercheurs dans l'adoption de stratégies de gestion durable de l'eau et d'améliorer la résilience des cultures de blé face au changement climatique et à la rareté de l'eau.

Mots clés: céréales, blé, eau d'irrigation, télédétection, modèle SEBAL, logiciel AquaCrop, agriculture de précision, prise de décision

General Introduction

Natural resource demand has increased significantly over the past few decades, primarily as a result of population growth that is exponential, economic expansion, and a society that values consumption more and more. In particular, agriculture places a significant stress on water resources as it consumes more and more water to meet the expanding need for crops, which is by far the largest use of freshwater on Earth **(Anderson *&* *al.*, 2012)**. Irrigation water is limited and scarce in many areas of the world. Agriculture is the major consumer of fresh water.

Agriculture is a vital sector for the economy of Algeria, and it has been an important part of the country's history and culture for centuries. The agriculture sector contributes to the livelihoods of millions of people and provides food security for the country. In Algeria, agriculture accounts for approximately 13% of the country's GDP, and it employs approximately 25% of the population **(FAO, 2021**). In fact, irrigated agriculture uses more than 70% of the freshwater resources that are mobilized globally **(Foley *&* *al.*, 2011)**, and in semi-arid and dry areas, it even uses more than 80–90%. **(Chehbouni *&* *al.*, 2008)**. Because of this, freshwater supplies are getting scarcer in many places of the world **(Anderson *&* *al.*, 2012)**. The water resources availability is particularly sensitive in Mediterranean regions **(figure1)**, **(Giorgi, 2006)** which are considered one of the most sensitive areas to climate change due to a large decrease in annual precipitation with increasing temporal variability and an observed trend to warmer conditions **(IPCC, 2014)**. Among human activities, agriculture is undoubtedly the most directly influenced by Climate Change therefore it will impact the biotechnical component of agricultural production processes **(Seguin, 2010)**.

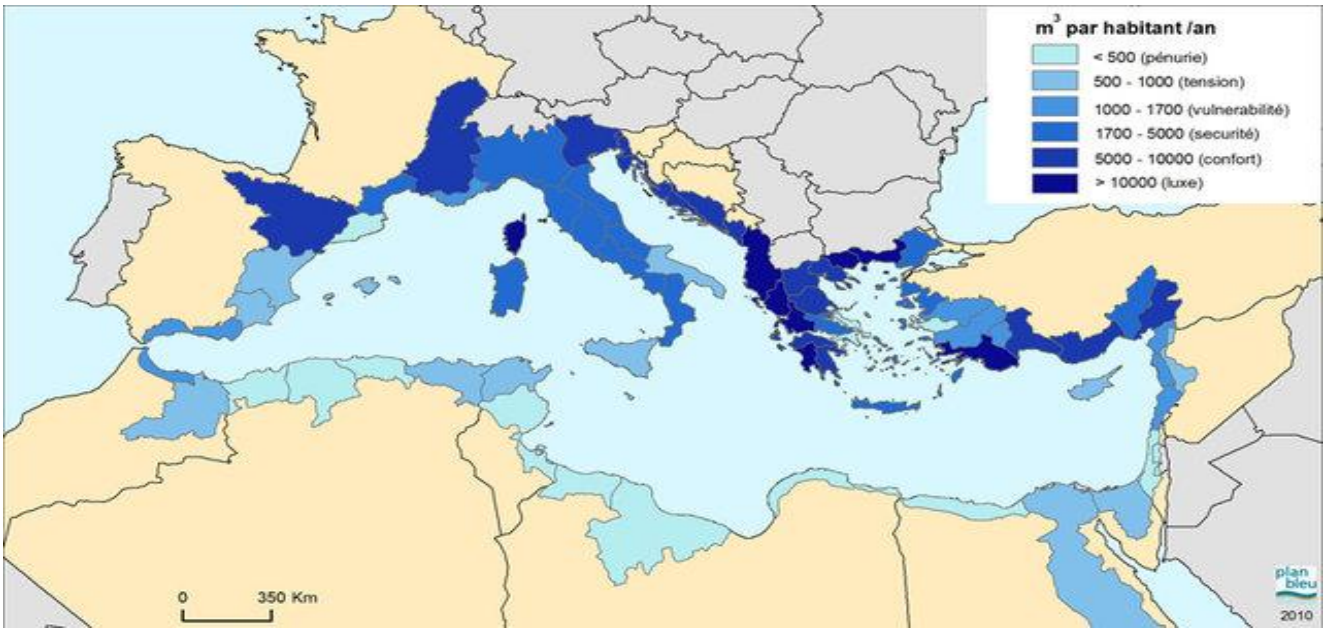

Figure 1: Water resources in the Mediterranean region (Source: **Nicolas Da Silva,2018)**

Increasing the water use efficiency in agriculture has been regarded as one of the main topics connected to water scarcity and droughts **(Werner *& al.*, 2012)**. therefore, monitoring and quantifying water resources over extended areas are critical for an efficient management of water resources.

According to the real needs of the crop, requires a good characterization of the evapotranspiration. This term is still very poorly understood on a global scale (**Jasechko *& al.*, 2013)**. Water losses through evapotranspiration are often the largest component of the water balance and can account for up to 60% of the total pluviometry contribution **(Oudin, 2004)**. The estimation of crop water requirement is a basic step used in planning and designing for an efficient crop production system. Crop models proved to be a great help towards this end. **(Pereira *& al.*, 2002)**.

An important key point for improved water use efficiency is to devise a site-specific protocol for optimum irrigation schedule, where measured quantity of irrigation is applied after a specific interval which checks the percolation of water beyond root zone and ensures the higher water use efficiency. Best irrigation schedule demands a clear understanding of crop response to water stress throughout the growing season.

Integration of ancillary ground information with remote sensing imagery is often able to provide repetitive and synoptic views of crucial parameters characterizing land surface interactions, surface energy fluxes, and surface soil moisture. Various methods have been developed for this purpose using a wide range of remote sensing data **(Yuei-An Liou *& al.*, 2014)**.

During this decade, several approaches have been developed in order to benefit from the contribution of remote sensing in agriculture:

- use to be able to make farm plans, useful for measuring areas and yield potentials for insurance premium purposes **(Alhousseune Diara, 2019)**
- detection of anomalies in crop development. By comparing footage from the current season to previous seasons. This allows farmers to see the impact of cultural practices. However, this does not provide quantitative recommendations that can be directly applicable **(Vintrou, 2012)**
- exploring the relationships that exist between electromagnetic remote sensing measurements and certain biophysical variables specific to the crop (leaf area, vegetation temperature, etc.) or to the soil (humidity, soil temperature, etc.).

Remote sensing technology has the potential to improve water management in agriculture by providing accurate and timely information about crop water requirements. by providing ET estimations for large land surface areas using a minimal amount of ground data. This information can help farmers and water managers to make informed decisions about water use and to optimize water management practices **(Lopez-Urrea *& al.*, 2020)**.

Several studies have shown that remote sensing can be an effective tool for estimating crop water consumption. **(Ahmadi *& al.*, 2021)** for example, used remote sensing data to estimate water consumption for wheat crops in Iran, while **(Wang *& al.*, 2020)** used remote sensing to estimate water consumption for maize crops in China.

Water loss via evapotranspiration (ET) is a crucial feature of the water budget study of a region and possibly the most difficult component to measure. At both the spatial and temporal scales, accurate calculation of ET is crucial for effective water management.

Wheat is a cereal of paramount importance throughout the world, from an economic point of view, it is one of the three major cereals with corn and rice. It is, with around 600 million tons annually, the third largest harvest in the world. World wheat production has more than tripled in the space of 60 years, rising from 222 million tons in 1961 to over 771 million tons in 2021 **(FAO, 2023)**.

Algeria still remains among the major importers of cereals (durum wheat and soft wheat) on the world market due to the weak capacity of the national sector to meet the growing consumption needs of the population. In fact, local cereal production covers just over 30% of the country's needs. In 2021, cereal imports totalled 3.9 billion dollars, against 1 billion dollars in 1961, the quantities imported has tripled **(FAO, 2023)**. The main natural cause of falling wheat and barley productivity in Algeria is drought.

In Algeria, the Tiaret region provides one-third of the national wheat production. **(Rezzoug *& al.*, 2008)**.

In this study, we plan to use and include our experimental measurements, surface energy balance model, requiring little in terms of input parameters and remote sensing data (optical and thermal, low and high spatio-temporal resolution) for the mapping of the evapotranspiration (evapotranspiration modelling). so, we can quantify wheat irrigation water needs and consumption using meteological dataset in the region of Tiaret.

This research is divided into 7 chapters:

Part 1: bibliographic synthesis

Chapter 1: represents a bibliographic study and a general overview about drought and water resources in Algeria.

Chapter 2: general overview on the agricultural sector in Algeria.

Chapter 3: the impact of climate change on agriculture in Algeria

Chapter 4: precision agriculture and remote sensing in agriculture

Part 2: Experimentation

Chapter 5: Description of the study area

Chapter 6: Methodology

Chapter 7: Results and Discussion

Chapter I: Water resources and draught in agriculture

Drought and climate change are major challenges for the agriculture sector in Algeria. The country has been experiencing more frequent and severe droughts in recent years, which have had a significant impact on agricultural production and food security. Climate change is also expected to exacerbate these challenges, with predictions of increasing temperatures and changing rainfall patterns.

Water management is one of the priorities of environmental policies in developed countries and, increasingly, in developing countries. The very low availability of fresh water, which represents only 3% of the total water on earth (figure 2), its unequal distribution on the scale of the planet (wet and arid regions), combined with the strong population growth world, As well as to climate change, especially the episodes of drought, make it necessary and urgent to optimize the use of water **(Alhousseine Diarra, 2019)**.

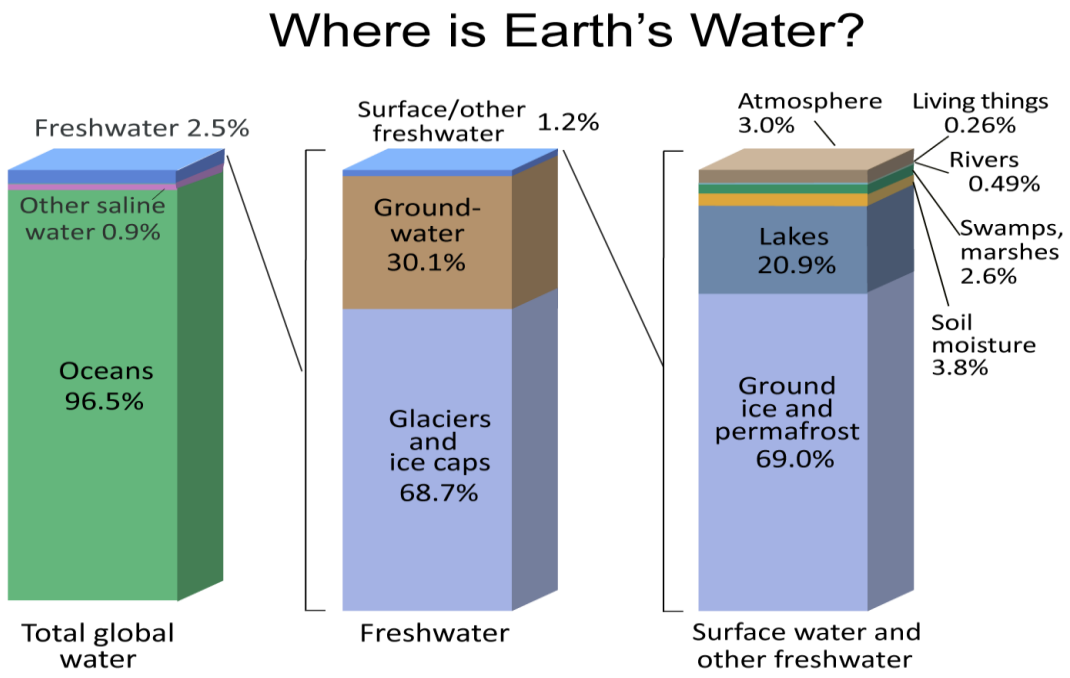

Figure 2: water distribution on, in and above the Earth. Source**: (web master 1)**

1.1 Climatic stages in Algeria

In Algeria, all Mediterranean bioclimates are represented, from humid in the north to Saharan in the south for the bioclimatic stages, and from cold to hot for the thermal variants. five Mediterranean bioclimate stages have been defined for Algeria: Saharan, arid, semi-arid, sub-humid and humid. These are subdivided into variants on the basis of thermal thresholds for

the coldest month. The Mediterranean influence diminishes with distance from the sea. The aridity gradient is also observed from east to west. The bioclimatic domains show a climatic and bioclimatic diversity that favors great biological diversity. All bioclimatic stages and sub-stages are present **(Arfa, 2008)**.

Table 1: Bioclimatic stages in Algeria **(Kerrache, 2011)**

Bioclimatic floors	Rainfall (mm)	Area (ha)	Percentage (%)
Per-humid	1200-1800	185275	0.08
Humid	900-1200	773433	0.32
Sub-humid	600-900	3401128	1.43
Semi-arid	300-600	9814985	4.12
Arid	100-300	11232270	4.72
Saharan	<100	212766944	89.3

1.2 Algerian Surface water

In the whole of Algeria there are 80 dams, with a capacity of 8.6 billion m3, providing an annual volume of 20 billion m3 of water for human consumption, industry and irrigation.

Due to losses from evaporation, heavy sedimentation, and leakage, the majority of Algerian dams only last thirty years on average **(Benfetta and Ouadja, 2017)**. Only eight major dams are present in the (arid) south, while 57 major dams are operational in the coastal and central regions.

(Figure 3) provides an overview on the Algerian water sources.

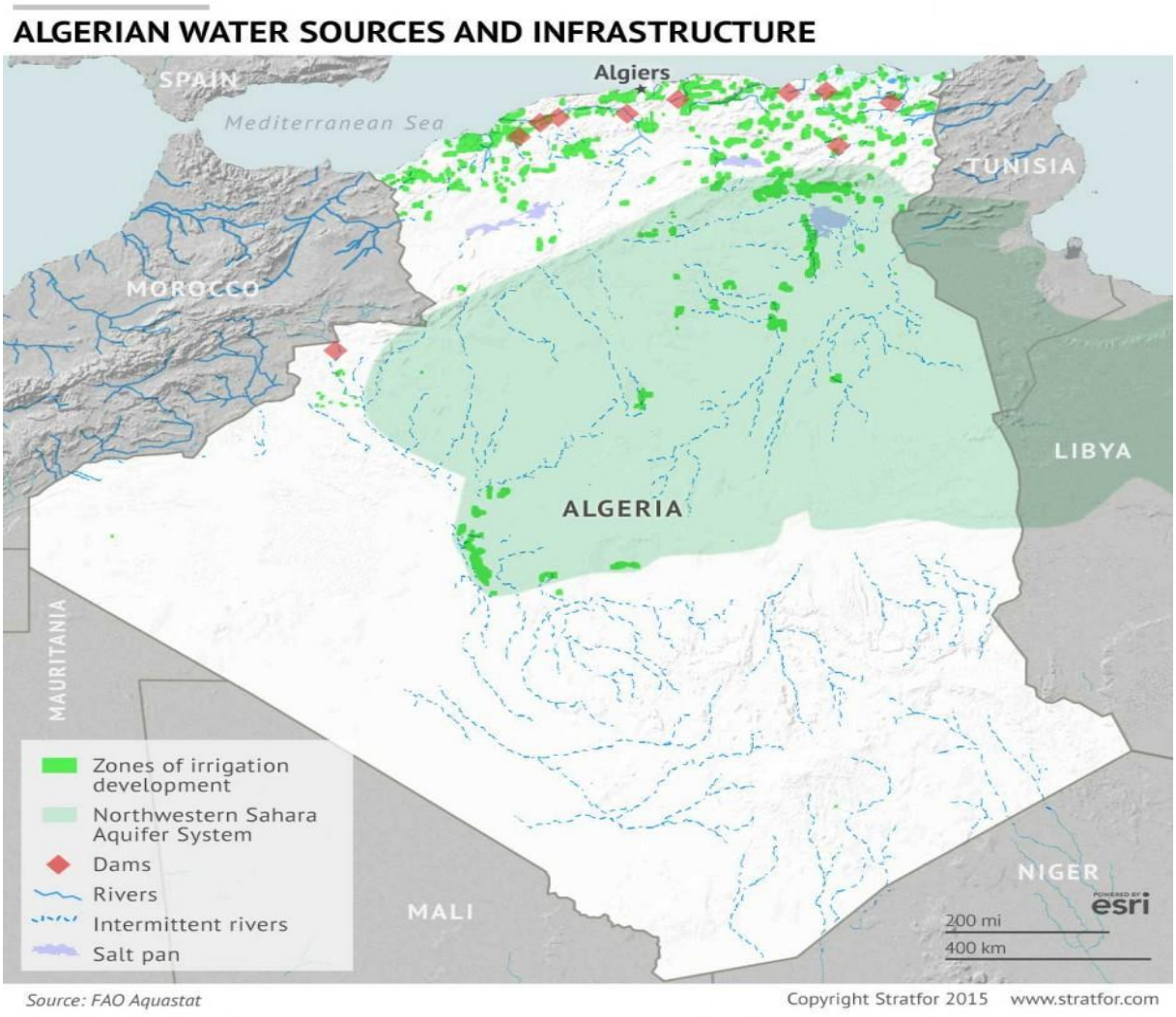

Figure 3: Zones of irrigation development and major dams in Algeria. In transparent green overlay, the extent of the North-western Sahara Aquifer system. Source : **(Victor Langenberg & *al.*, 2021)**.

1.3 Draught in Algeria

The Mediterranean basin, particularly the region of North Africa, is one of the area's most vulnerable to climate change, according to IPCC. Nevertheless, there is very little information available about the region of North Africa, and until recently, studies on climate change have not been carried out in Algeria, Algeria is classified as a climate change hotspot by the IPCC **(IPCC,2007)**.

Drought is a recurrent phenomenon in Algeria, particularly in the arid and semi-arid regions of the country. Droughts in Algeria are caused by various factors, including natural climatic variability, such as the El Niño-Southern Oscillation (ENSO), and human activities, such as overexploitation of water resources and land degradation **(Bouguerra *& al.*, 2019)**.

Droughts in Algeria have had a severe impact on agricultural production, particularly for rainfed crops, such as cereals.

The most severe drought in Algeria in recent decades occurred between 2016 and 2019. The drought affected over half of the country's agricultural land and caused significant crop losses and food insecurity **(FAO, 2019)**.

Effects of draught on agriculture

The effects of climate change are clearly observed in the regions of North Africa, with an increase of 0.9° C in annual temperatures and a decrease in annual precipitation of 26% on average over the period 1900-2010, These variations will be significantly revised upwards with warming above the global average and a greater decrease in precipitation. Dramatic consequences could result from this, such as an increase in periods of drought, a low filling rate of dams **(Bates *& al.*, 2008)** and therefore a decline in agricultural production.

In addition to the direct impact on agricultural production, climate change is also expected to affect the distribution and spread of plant diseases and pests, further reducing crop yields **(FAO, 2018)**. This highlights the need for effective adaptation strategies to minimize the impact of climate change on the agriculture sector in Algeria.

Significant spatio-temporal diversity is an indication of rain. The northern Mediterranean strip receives up to 1,200 mm annually, with annual rainfall varying and decreasing toward the west. The transitional central regions have 100–400 mm of yearly rainfall on average. Less than 100 millimeters of rain fall in the desert each year. From 1,000 mm in the north-east to over 3,000 mm in the south-east, the natural losses due to possible evapotranspiration **(figure 4).**

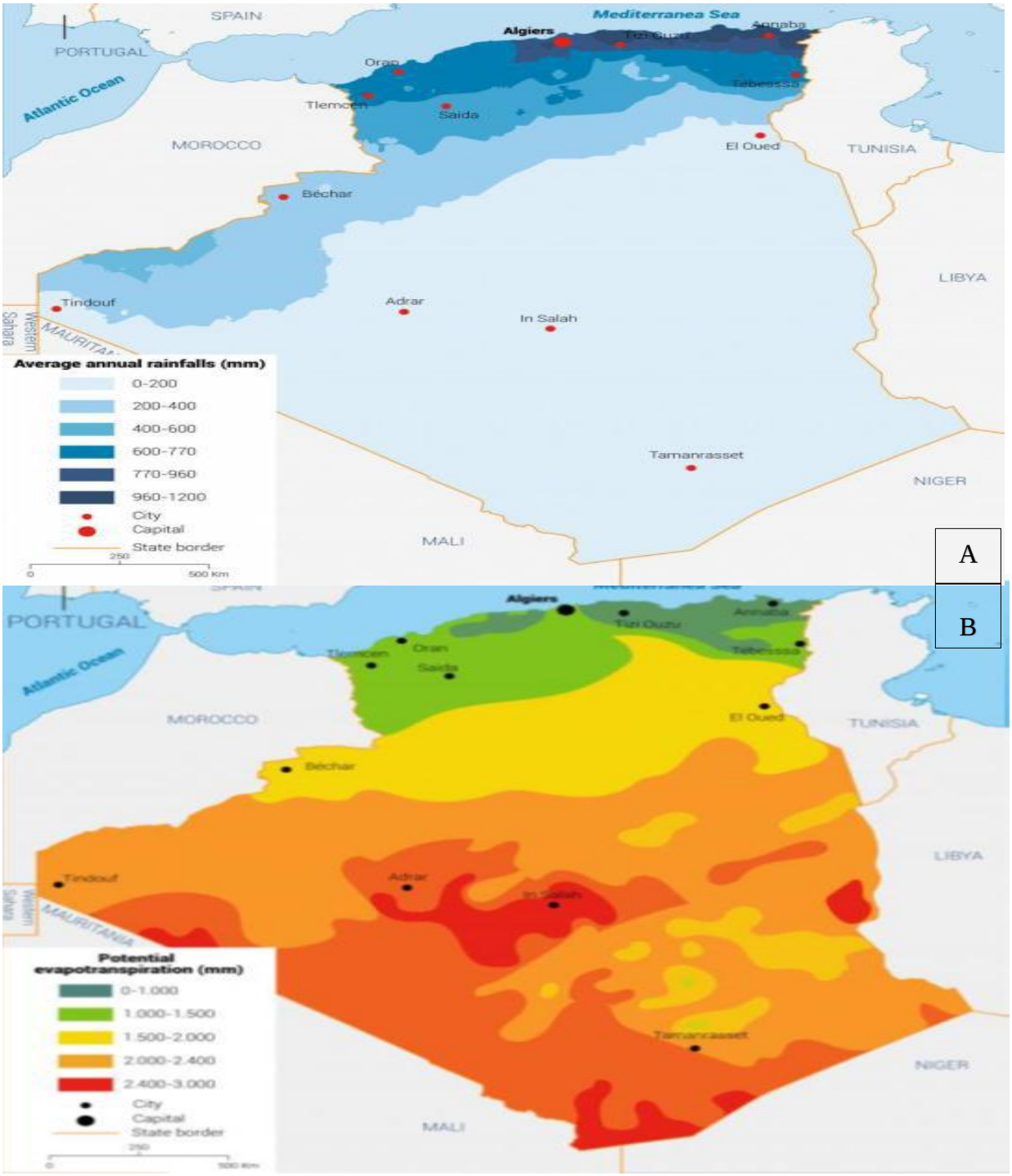

Figure 4: A: Annual average precipitation in mm, B: annual potential evapotranspiration. **(Victor Langenberg & *al.*, 2021)**

Drought can also affect the quality of agricultural products. For instance, drought stress can lead to poor fruit quality and lower nutritional value, drought stress can reduce the content of essential minerals, vitamins, and antioxidants in crops such as wheat, rice, and maize

(Farooq *& al.*, 2017). Moreover, drought can increase the susceptibility of crops to pests and diseases, which can further reduce the quality of agricultural products.

The effects of drought in agriculture extend beyond crop yield and quality reduction. Drought can also result in economic losses for farmers and agricultural industries **(Debnath *& al.*, 2018)**.

Increasing the agricultural product while rationalizing irrigation water. One of the solutions for saving water in this area consists in managing demand, i.e. optimizing the supply, according to the real needs of the crop at a given moment in its development, taking into account environmental conditions. This requires a good characterization of evapotranspiration. a good characterization of evapotranspiration also presents major challenges for understanding the processes of the hydrological functioning of catchment areas. This concept of irrigation management is part of the development of modern agriculture capable of ensuring a good level of productivity.

The winter cereal season is ongoing in Algeria and has been marked by above-average temperatures **(Figure 5)** and a large rainfall deficit **(Figure 6)**.

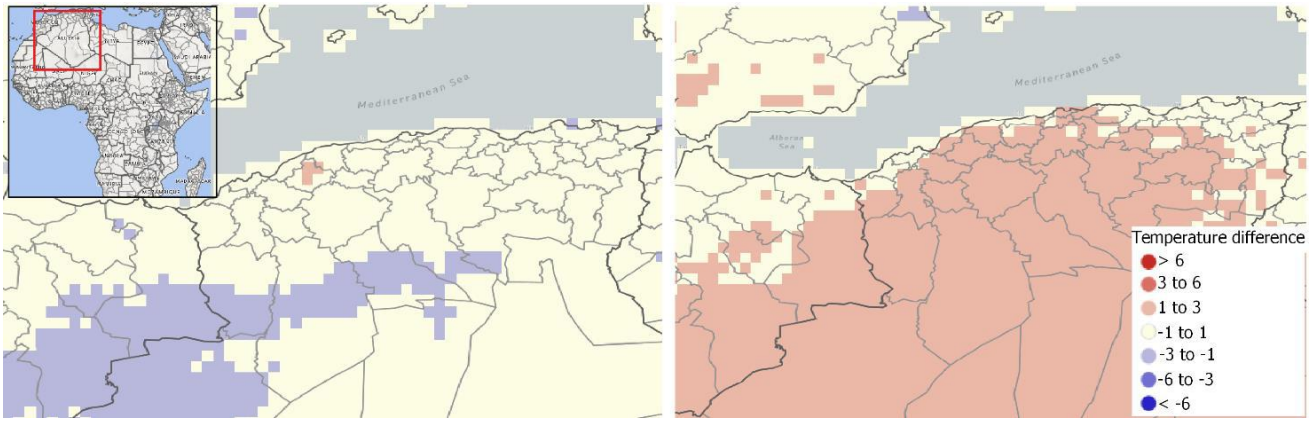

Figure 5: Difference of cumulative mean air temperature with historical average for March (left) and April (right) in ºC. Source: **(asap, 2021)**

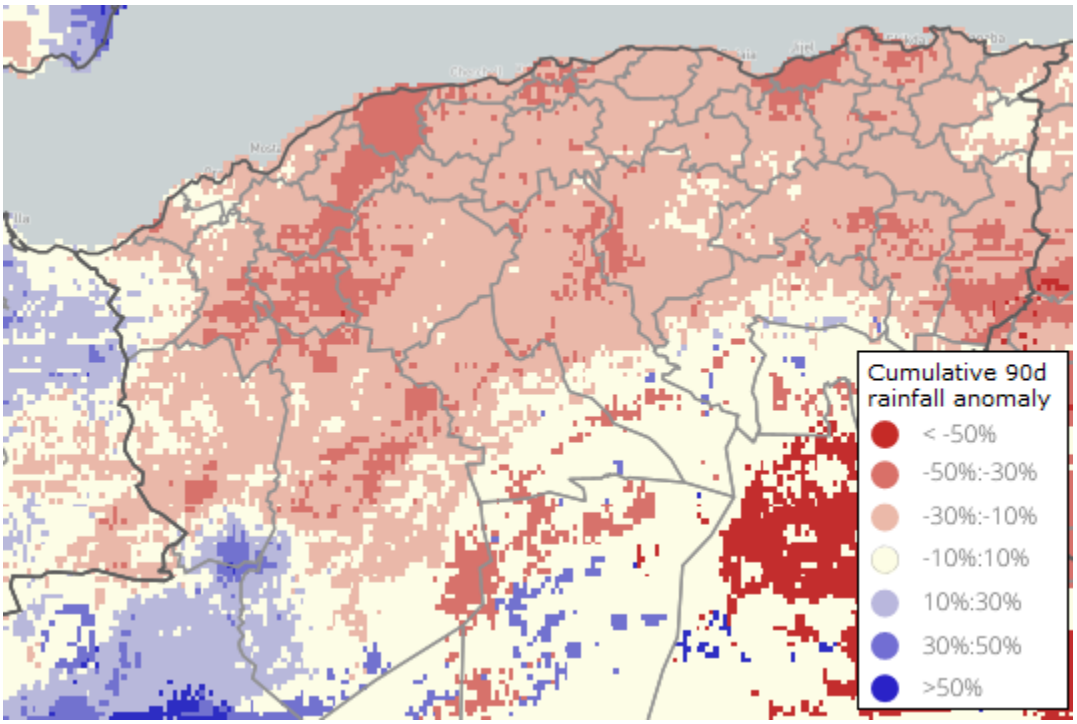

Figure 6: Cumulative rainfall anomaly for February/March/April in %. Source: **(asap, 2021)**

The predominant red pattern in Figure 3 at the end of April shows that crops and rangelands have not gotten enough rain to meet their water needs. In the western and central regions of the country, crops and rangelands were badly impacted by the combined impacts of little rainfall and above-average temperatures. The hot and dry weather had an adverse effect on cereals during flowering and grain filling, especially by causing grain filling to proceed more quickly than biomass build-up.

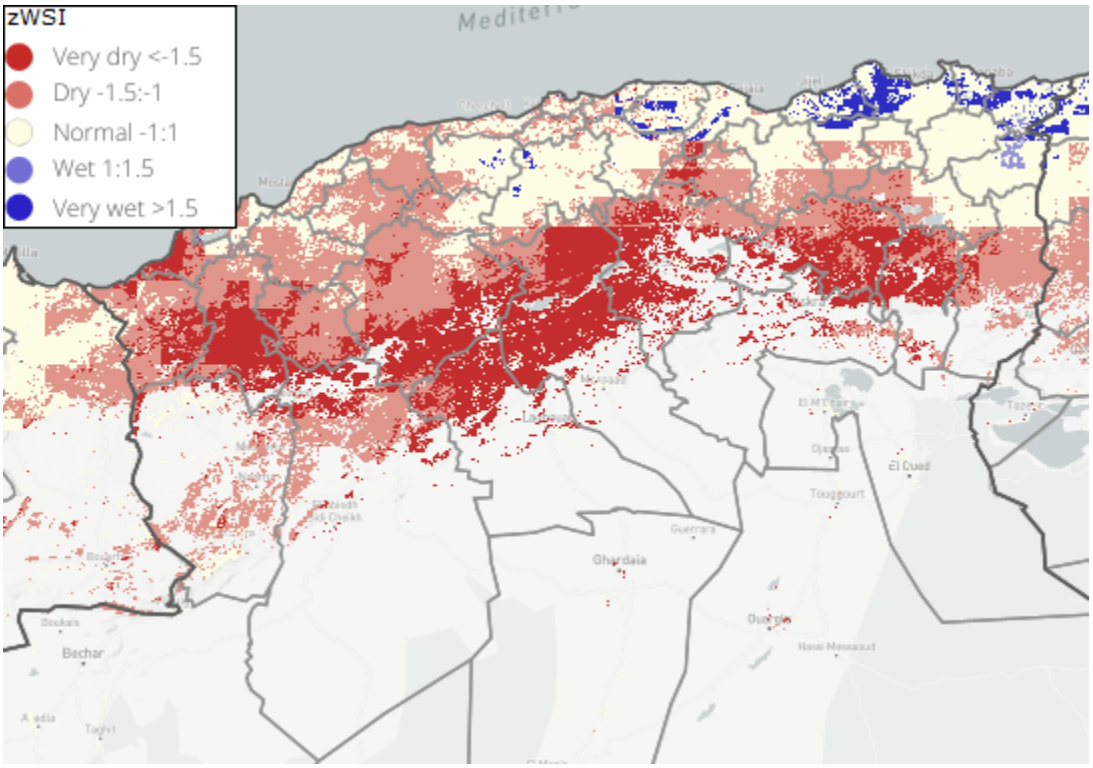

Figure 7: Spatial distribution of anomalies in the Water Satisfaction Index for crops from the start of the growing season until the end of April 2021. Source: **(asap, 2021)**

1.4 Role of Remote Sensing in Drought and Climate Change Monitoring

Remote sensing technology has the potential to provide valuable information for monitoring drought and climate change in agriculture. Satellite images can be used to monitor vegetation indices, such as the normalized difference vegetation index (NDVI), which is an indicator of vegetation greenness and health. Changes in NDVI over time can provide information on the impact of drought and climate change on agricultural productivity **(Wu & *al.*, 2018)**.

Remote sensing can also be used to monitor changes in land use and land cover, which can provide information on the extent of land degradation and the impact of human activities on the environment **(UNEP, 2019)**. This information can be used to develop effective land management strategies to reduce the impact of drought and climate change on agriculture.

Chapter II: Agricultural sector in Algeria

Algeria has approximately 8.7 million hectares of agricultural land, of which 3.8 million hectares are cultivated **(FAO, 2020)**.

Agriculture is an important sector for the economy of Algeria, contributing approximately 13% of the country's GDP and employing around 25% of the population **(FAO, 2021)**. This weakness of agricultural production places Algeria among the world's largest importers of food products, with a food bill that amounts annually to nearly $ 4 billion (with a clear predominance of cereals on which the national food intake is based).

Algeria has experienced high demographic growth: the population, which was around 13 million at independence, has risen to almost 45 million 60 years later. Since the 1960s, the Algerian state has therefore attempted to modernize agriculture in order to increase and stabilize agricultural and food production **(Bencharif, 2018)**.

2.1 Evolution of agricultural sector in Algeria

The Algerian population is estimated at 44.6 million inhabitants as of 1 January 2021**. (World Bank, 2021)**, and the natural increase in the birth rate (+1.9% per year) is leading to a regular and significant increase in food requirements. Algeria is largely desert: out of a total surface area of 238 million hectares (Mha), the area used for agriculture is 48.7Mha, or 20%. Of these 48.7 million hectares, it is customary to distinguish the southern part, composed of high plateaus and oases, which represents an area of 32.7 million hectares essentially devoted to nomadic and pastoral sheep farming, from the Tell, the northern plains of the Tullian Atlas. The Tell, with a surface area of 16Mha, is divided between 4.7Mha of forest areas, 2.8Mha of alfalfa areas and 8.5Mha of useful agricultural area (UAA). These 8.5Mha are divided into 5.8Mha of private land and 2.7Mha of state land, largely entrusted to farmers through concessions.

Over the past 15 years (2000-2014), gross domestic agricultural production (GDPA) has increased, as a percentage of GDP, from 8.3% in 2000 to 9.2% in 2010 and 11.2% in 2014, an increase attributed to an increase in market gardening and animal production. The gross domestic product of the agri-food sector stabilized at around 5.6% of national GDP at the end of the last five-year plan **(Bessaoud *& al.*, 2019)**

Table 2: main Indicator 2017. Source: Data Bank 2018 (BM). CNIS (Algeria). MADRP (Algeria). (*AquaStat 2018)

Share of agriculture in GDP (in %)	12.5
GDPA growth rate (at constant factor prices, in %)	2.5
Agricultural production growth rate (average 2000-2015, in %)	6.4
Agri-food trade balance (current USD 106)	-8.2
Arable agricultural land (million hectares, in 2017)	8.5
% Irrigated land of total agricultural land	15
Internal renewable water resources per capita. (m3/cap./year) *	600
Rural population (millions) Rural population growth (annual %)	11 -0.3

the agricultural sector has been the engine of the country's economic growth since between 2004-2014 it experienced an annual growth rate of 7.06%, while during the same period this rate was only 2.72 % for the whole economy. The added value of the agri-food sector, which generates the equivalent of 19% of the agricultural value added, represents nearly half (46%) of the added value of the industrial sector excluding hydrocarbons and 40% of industrial employment excluding hydrocarbons **(Bessaoud & *al.*, 2019)**.

2.2 Major Crops in Algeria

The main crops grown in Algeria include cereals, vegetables, fruits, and legumes. Among these crops, cereals, particularly wheat and barley, are the most important and widely cultivated **(FAO, 2021b)**. According to FAO statistics, wheat production in Algeria was estimated at approximately 3.8 million tonnes in 2020, making Algeria one of the largest wheat producers in North Africa **(FAO, 2021a)**. Wheat is a staple food for Algerians, and it is also a significant export crop.

The Government notes that production forecasts for 2025 are in the order of 55 million q and an area of 3.75 million ha.

In the development of strategic crops in the South, an initial land portfolio has been allocated under the concession for an area of 134,000 ha for the benefit of 140 investors, while an ongoing program of 97,000 ha is planned during 2022.

Other important crops in Algeria include vegetables and fruits, such as tomatoes, potatoes, citrus fruits, and dates. These crops are grown mainly in the northern regions of the

country, which have a more favorable climate and more abundant water resources than other regions **(FAO, 2021)**.

The production of fruits and vegetables has also increased in recent years due to government support programs, which has led to an increase in the area devoted to potatoes by 68% between 2010 and 2017 and a 143% increase in production **(USDA)**

Figures 5 and 6 provides an overview of wheat and barley production in Algeria.

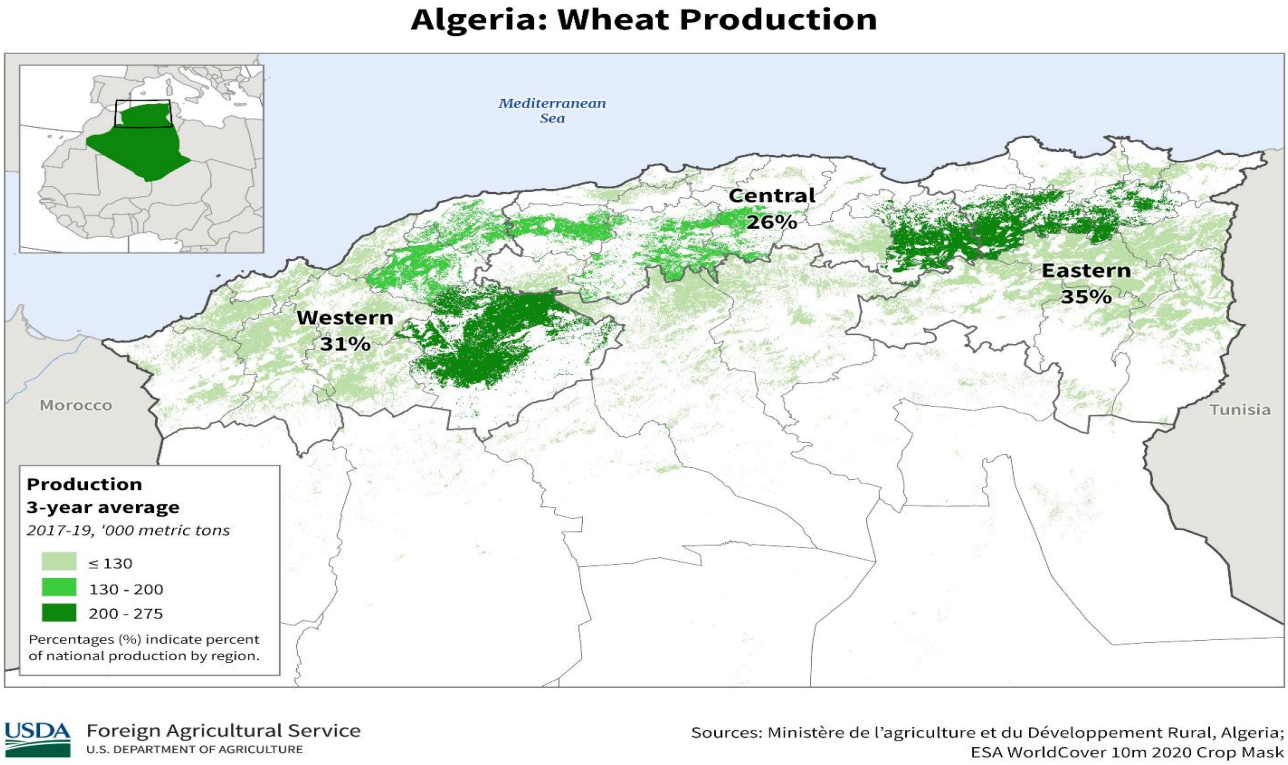

Figure 8: wheat production in Algeria. Source: **(MADR).**

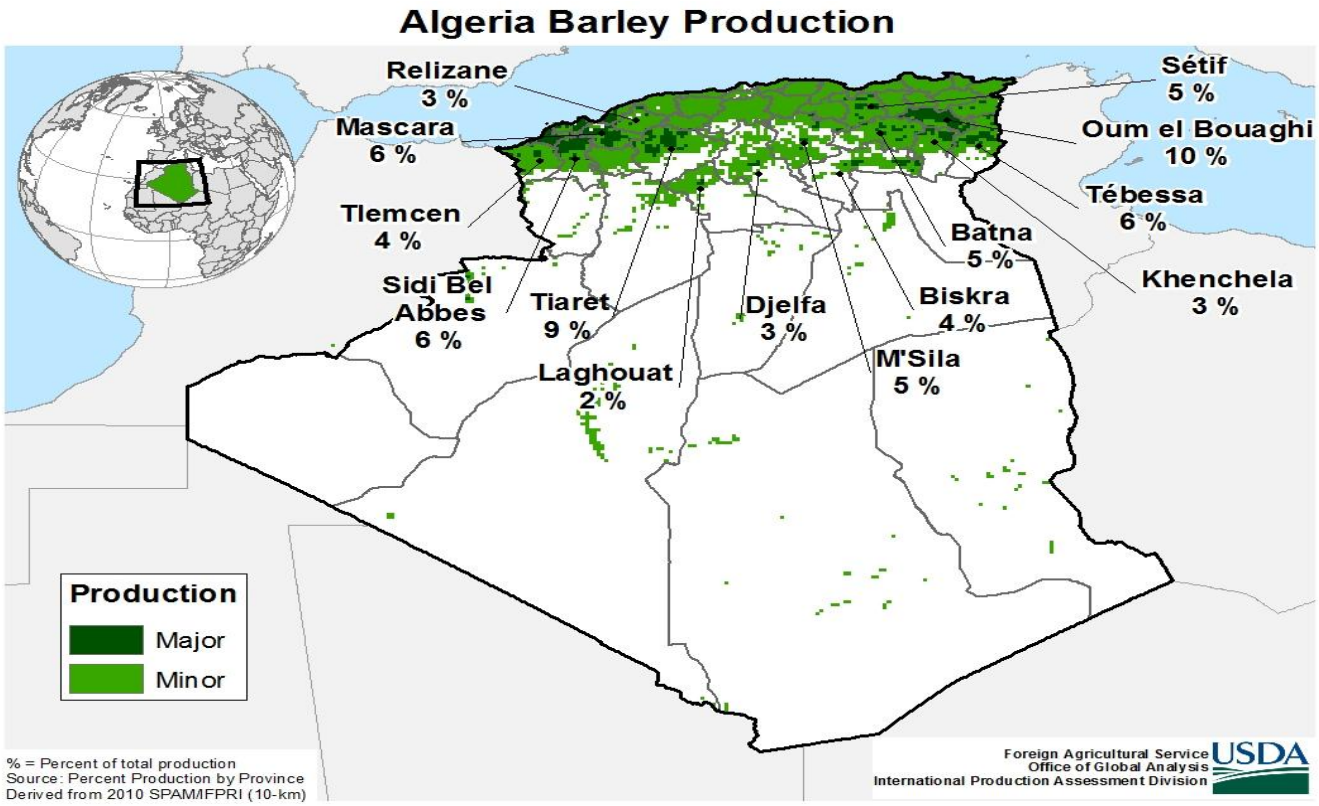

Figure 9: Barley production in Algeria. Source: **(MADR).**

2.3 Water Scarcity in Algeria

Water scarcity is a significant challenge in Algeria, particularly in arid and semi-arid regions. The country's water resources are limited, and they are unevenly distributed across the country. The northern region of Algeria, which includes the coastal areas, receives the majority of the rainfall and has the highest water availability. In contrast, the southern region of Algeria, which includes the Sahara Desert, has very limited water resources and is prone to frequent droughts **(UNDP, 2016)**.

The agriculture sector is the largest consumer of water resources in Algeria, accounting for approximately 84% of the country's total water consumption **(FAO, 2021a)**. Irrigated agriculture, in particular, is a major water user, and it accounts for approximately 70% of the total water used in agriculture **(UNDP, 2016)**. The country's limited water resources are under stress due to the high-water demand for irrigation in agriculture, which also adds to water scarcity and water stress.

The table 3 provides an overview of the estimated water use of different sectors in Algeria. The numbers show a clear overexploitation of the non-renewable groundwater resources. In this overview, the water scarcity on a monthly scale is hidden by the annual analysis of demand versus supply. A monthly assessment of the water balance could show

severe shortages in water supply vs demand. Also, the numbers in **Table 3** consider water quantity but not water quality. The total water resources available will lower when taking into account certain water quality standards.

Table 3: Overview of water resources and water use (with BCM=billion cubic metre). Source: **(Victor Langenberg *& al.*, 2021).**

Type	**Algeria**
Total water ressources	19 BCM/yr
Estimated water demand for all sectors	10.5 BCM/yr
Estimated renewable water ressources	13.6 BCM/yr
Estimated withdrawals for irrigation	6 BCM/yr
Estimated non-renewable used groundwater resources	2 BCM/yr
Estimated water use for domestic purposes	2.9 BCM/yr
Estimated yearly water use for livestock 2016-2018	42.7 MCM/yr

2.4 Water Management in Agriculture

Efficient water management in agriculture is essential to ensure the sustainability of agricultural production and to enhance water-use efficiency. Water management practices in agriculture include both supply-side and demand-side measures

The Algerian government has implemented various policies and programs aimed at modernizing the agricultural sector and improving productivity, including the National Agricultural and Rural Development Program (PNDR) and the Program for the Development of Agricultural Investment (PDI**) (International Food Policy Research Institute).**

Remote sensing technology has the potential to improve water management in agriculture by providing accurate and timely information about crop water requirements. Remote sensing data, such as satellite images, can be used to estimate crop water requirements and to monitor the water status of crops. This information can help farmers and water managers to make informed decisions about water use and to optimize water management practices **(Lopez-Urrea *& al.*, 2020)**.

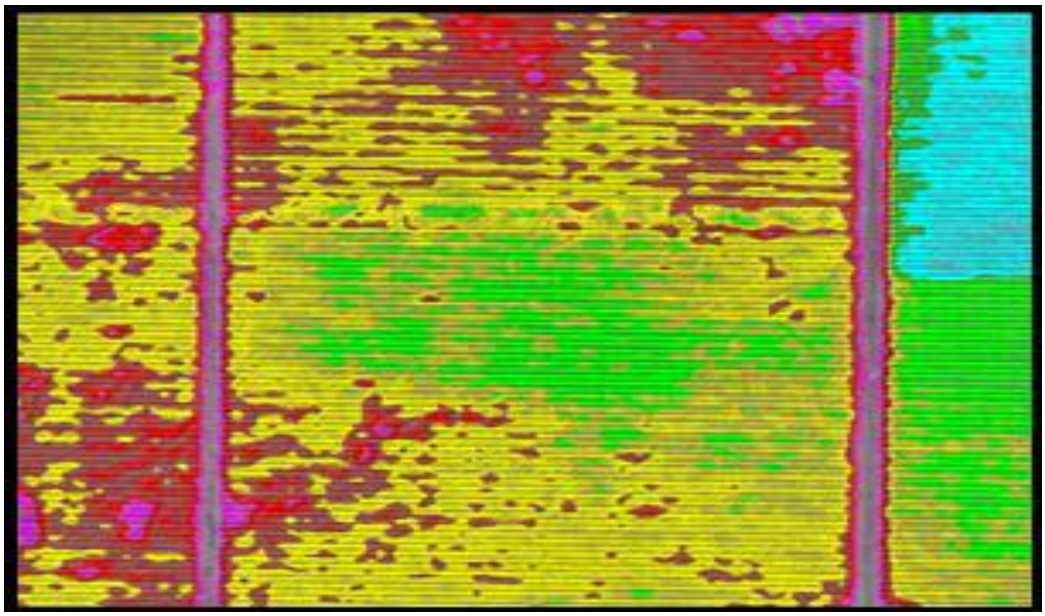

Figure 10: Pattern of variable requirements for irrigation within one field (green is high, yellow is average, red is low water content) as seen from the QuckBird satellite. Source: **(Digital globe).**

The accompanying graphic demonstrates the variation in irrigation needs within a single field. While the red sections of the field are in desperate need of irrigation, the green areas in the middle of the field are adequately watered. Even though QuickBird lacks the thermal bands needed to assess water content, simple vegetation indices can still be used to detect the signs of a water shortage. With this knowledge, the farmer will be able to determine which areas need more water and change the irrigation system accordingly**. (figure 10)**

Chapter III: The impact of climate change on agriculture in Algeria

3.1 Climate change effecting the globe

The climate is a crucial element that determines various characteristics and distributions of managed and natural systems, including hydrology and water resources, marine and freshwater ecosystems, terrestrial ecosystems, forestry and agriculture. **(Rosenzweig, C. *&* *al.*, 2007).**

Global warming is a serious problem facing the world today. It has reached record breaking levels as evidenced by unprecedented rates of increase in atmospheric temperature and sea level. According to the World Meteorological Organization (WMO), the world is now about one degree warmer than before widespread industrialization. The Intergovernmental Panel on Climate Change (IPCC). also reported that each of the last three decades has been increasingly warmer, with the decade of the 2000s being the warmest. **(Field, C.B. *&* *al.*, 2014).**

Based on a range of global climate models and development scenarios, it is expected that the Earth could experience global warming of 1.4 to 5.8 °C over the next century.**(Pachauari, R.K. *&* *al.*, 2007).**

The main cause of global warming is increased concentrations of greenhouse gases in the atmosphere. The most prevalent atmospheric gases are carbon dioxide (CO_2), methane (CH4), and nitrous oxide (N2O), which are caused by many anthropogenic activities including burning off the fossil fuels and land-use change **(Yoro, K.O. *&* *al.*, 2020).**

Scientists within the Intergovernmental Panel on Climate Change (IPCC) expect that the present increase in greenhouse gas concentrations will have direct first-order effects on the global agricultural production.

Climate change and global warming are of great concern to agriculture worldwide and are among the most discussed issues in today's society. Climate parameters such as increased temperatures, rising atmospheric CO_2 levels, and changing precipitation patterns have significant impacts on agricultural production. In fact, temperature, rainfall changes, winds and floods have all hampered agricultural sector, which is one of the most vulnerable sectors to climate change. **(Aryal, J. P., and Stirling, C. 2019)**

Agriculture is the most vulnerable sector to climate change, due to its huge size and sensitivity to weather parameters, thereby causing huge economic impacts. **(Mendelsohn, R 2009).** the changes in climatic events such as temperature and rainfall significantly affect the

yield of crops. The effect of rising temperatures, precipitation variation, and CO_2 fertilization varies according to the crop, location, and magnitude of change gin the parameters. The temperature increase is found to reduce the yield, while the precipitation increase is likely to offset or reduce the impact of increasing temperature **(Adams, R.M. *&* *al.*, 1998)**.

Agriculture, often referred to as an open-air factory, is an economic activity that depends heavily on climate and certain weather conditions to produce food and many other goods necessary to sustain human needs. Moreover, agriculture is an activity that is exceptionally vulnerable to climate change and the impacts of climate change are characterized by various types of uncertainty. **(Deshar, R *&* *al.*, 2019).**

Climate change is estimated to have both positive and negative impacts on agricultural systems at the global level, with negative impacts outweighing the positive ones (**Müller, C. *&* *al.*, 2013).**

Temperature increases, altered precipitation patterns, and increased CO_2 concentrations have a significant impact on ecosystems, ranging from species to ecosystem levels. **(Stevens, C.J. *&* *al.*, 2004).**

Study conducted by **(Howard *&* *al.*, 2016)** revealed that the short-run and long-run changes in precipitation and temperature affect crop productivity. It also demonstrated that global warming has bad effects on the environment and human activities. For example, **(Zaveri *&* *al.*, 2019)** used a fixed effects technique to examine the implications of climatic changes on India's wheat output. The obtained findings imply that irrigation can help to mitigate the negative repercussions of these variations.

3.2 Climate change effecting Algeria

In recent years, climate change has been documented in many locations throughout the world **(Moonen *&* *al.*, 2002).** Climate changes have affected considerably temperature, precipitation intensity geographical distribution, drought and flood frequency all over the world (Intergovernmental Panel on Climate Change, IPCC 2007).

In its 2007 report, the IPCC combined 25 global climate models to assess the impacts of climate change in 2050 and 2100. In the Mediterranean region, there is forecast a temperature rise by 2-3°C by 2050 and by 3-5°C by 2100. The incidence of rainfall will be less frequent but more intense, while droughts more common and longer. The spatial and temporal

distribution of precipitation would change, which will directly affect agriculture and water resources.

Algeria lies in one of the most vulnerable regions facing climate change impacts during the twenty-first century. But in the recent years. Algeria has experienced a persistent decline in annual rainfall associated with the significant increase in temperature all because of climate change.

By comparing the emission per inhabitant, Algeria is among important emitters from developing countries **(Figure 11).** In comparison, the average annual global emission of CO_2 is 4.7 T/inhab., Qatar 55.4 T inhab., UAE 31.1 T/inhab., U.S. 19.8 T/inhab., France 6.1 T/inhab., Lebanon 20.3 T/inhab, Tunisia 2.4 T/inhab., Morocco 1.5 T/inhab. and India 1.4 T/inhab.

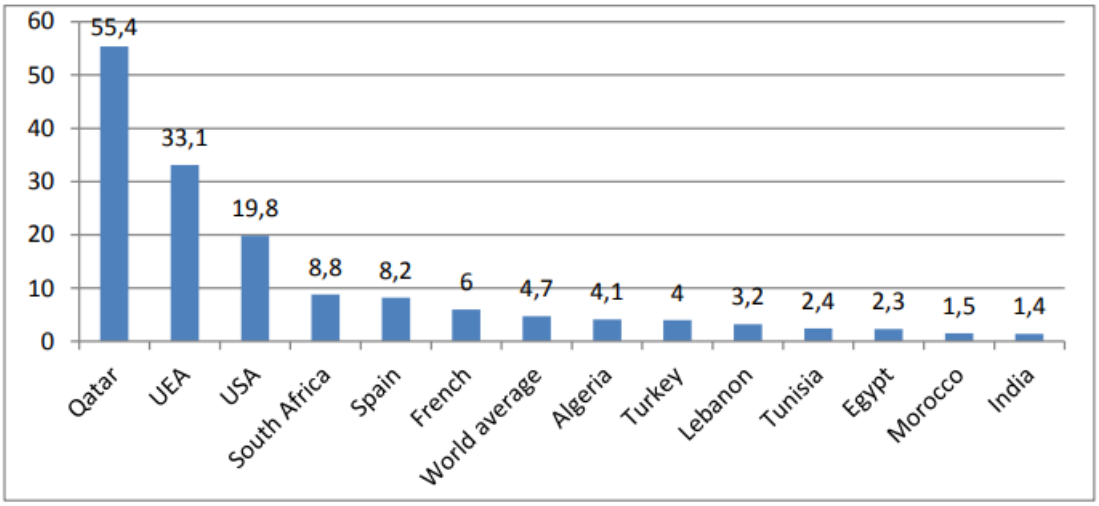

Figure 11: Comparison of CO_2 emissions per capita among other countries. Source: Author's own elaboration based on World Bank data [WB]

The economy of Algeria relies on the energy sector (production and consumption) which contribute in about ¾ of the total emissions of greenhouse gases **(Figure 12).**

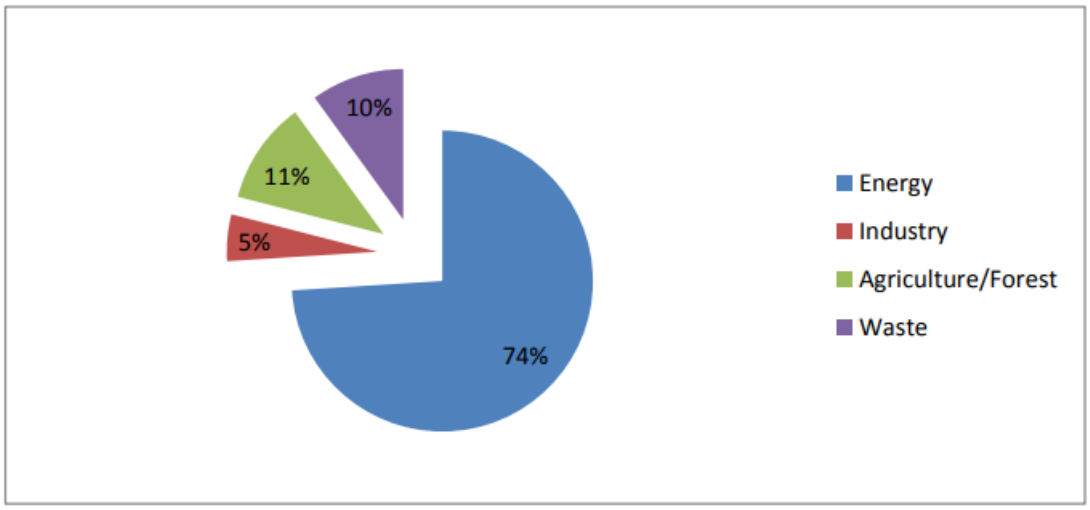

Figure 12: Total GHG emissions by sector in Algeria. Source: Author's own elaboration based on **(MATE, 2010)**

By the rising of temperatures and decreasing of rainfall climate change is reaching the Mediterranean basin. Algeria is the most affected country in North Africa by these factors. **(Niang *& al.*, 2014).** Despite the increasing grain demand due to the high population density, Algerian's agricultural production has shown, in the last decades, high output productivity and crop variability has contributed greatly to Algeria's economic growth. In 2019, it contributed by 12.3 percent of the total GDPs and enhanced the living conditions of around 30 % of the national rural population by creating more employment opportunities, **(Bessaoudet *& al.*, 2019).** Despite the importance of this sector, the Algerian agricultural sector depends on precipitation, as revealed by **(Schilling *& al.*, 2012).** In fact, rainfed land accounts for 50% of the entire area of grain production **(Bensemane *& al.*, 2011).**

Past analyses **(Kostopoulou and Jones, 2005)** and GCM simulations for the next decades **(Giannakopoulos *& al.*, 2009)** show that the Mediterranean region, characterized by rainy winters and dry summers, is experiencing increasing temperatures and large changes in the frequency of extreme climatic events for both temperature and rainfall.

Climate change influences the start and length of growing seasons **(Fiwa *& al.*, 2014; Zhao *& al.*, 2015; Lemma *& al.*, 2016)** and the duration and magnitude of heat and water stress in agricultural production systems **(Lobell *& al.*, 2015; Saadi *& al.*, 2015; Schauberger *& al.*, 2017).** Growth acceleration due to higher average temperature results in less radiation

interception and less biomass production **(Rosenzweig and Hillel, 2015).** Besides, above-optimal temperatures directly harm crop physiological processes.

Algeria suffers from bad environmental factors (e.g., temperature rise and rainfall decline) which deteriorated the agricultural production. Given the importance of agriculture in the country's economy.

Land used by agriculture, which occupies nearly 21% of the total land area, is estimated at 49 million ha distributed as follows: 8.4 million ha of agricultural area, 33 million ha used as routes, 6.6 million ha of forests and steppes of Alfa. Irrigated land accounts for 11% of the agricultural area, an area of 929.000 ha. Algeria therefore has only 3.5% of the total area of the country as arable and irrigated land. The ratio "availability / capita" agricultural land rose from 0.75 ha / cap in 1962 to 0.24 ha / cap in 2008. This enormous loss of farmland is not only the result of human pressures (industrial, construction, pollution), but also the result of desertification, soil erosion or vegetation cover loss. Climate change will degrade biodiversity and contribute to the weakening of the soil and reduced vegetation cover resulting in gradual desertification. In the steppe, the effect of climate change is reflected by the change in the cyclical nature of drought from one year to three years in the 1960s to two years out of five in the 1970s and the 1980s and to seven out of ten years now. **(Touitou MOHAMMED *& al.,* 2018).**

Chapter IV: Precision agriculture and Applications of Remote Sensing in Agriculture

Precision Agriculture (or Precision Farming) is a collection of agricultural practices that focus on specific areas of the field at a particular moment in time. This is opposed to more traditional practices where the various crop treatments, such as irrigation, application of fertilizers, pesticides and herbicides were evenly applied to the entire field, ignoring any variability within the field.

Remote sensing is a powerful tool that can be used to monitor agricultural crops and improve farm management practices.

Satellite images provide an excellent means for mapping and observing ground and cultivated areas, having great potential for improving irrigation management and yield predicting, by providing real time data such as (soil conditions, crop health and needs, drought zones alongside with warnings and intervention location) estimations for large land surface areas. Some recent studies have used remote sensing (RS) models successfully to monitor and improve agriculture**. (Foster *& al.,* 2019)**.

4.1 Monitoring Water Conditions

Irrigation is defined as the full or partial application of water by artificial means (either surface or groundwater resources) to counter the precipitation deficit during the crop growth periods **(Ozdogan *& al.,* 2010)**. Irrigation is the largest consumer of freshwater resources, with the usage of approximately 70% of the groundwater withdrawals **(Bastiaanssen *& al.,* 2000)**.

Water absorbs radiation in the red and near-infrared regions of the electromagnetic spectrum, and no reflectance signal is detectable from a clear body of water from wavelengths at 750 nm or longer **(Zhang *& al.,* 2014)**.

Satellite remote sensing is increasingly being used as a complementary source of information to in situ monitoring networks and, in many cases, is the only feasible source. Satellite-based sensors are now capable of making direct and indirect measurements of nearly all components of the hydrological cycle **(Lettenmaier *& al.,* 2015; McCabe *& al.,* 2017; Y. Zhang *& al.,* 2016)**. These include precipitation, evaporation, lake and river levels, surface water, soil moisture, snow, and total water storage (surface and subsurface water). These sensors are therefore capable of providing critical information in support of managing water and monitoring the evolution of hazards and their impacts **(Van Dijk, and Renzullo, 2011)**.

Figure 13 represent two different observations of the same place (Nile River and Aswan reservoir) in two periods dry period 20 August where you can clearly see low water level and

in watery period 17 January where you can see a significant increase in water level in the reservoir.

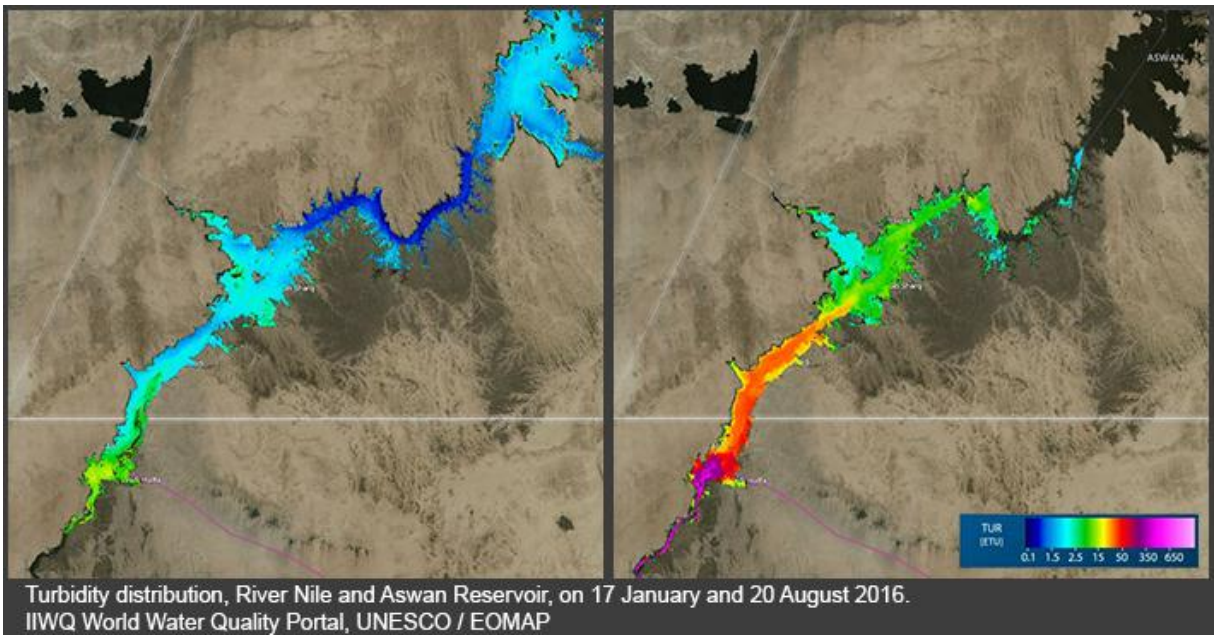

Figure 13: Satellite observation of Nile River and Aswan reservoir in two different periods. Source: **UNESCO/EOMAP**

The Sentinel-2 mission launched in 2015 provides unprecedented information from which surface water fluctuations can be derived **(Drusch *&* *al.*, 2012)**. In particular, the revisit time of 10 days for the current satellite (Sentinel-2A) and 5 days when the second satellite was launched in early 2017 will enable monitoring of rapid changes. It monitors across a range of 13 spectral bands from visible and NIR to SWIR at a range of resolutions from 10 to 60 m, and a 290-km field of view, which provides an unprecedented combination of spectral and spatial resolution and coverage. The sensor also has the potential to provide information on water quality and pollution through chlorophyll concentrations, algal blooms, and turbidity **(Gernez *&* *al.*, 2015)**.

Remote sensing information contributes to irrigation research by either identifying the irrigated areas or quantifying the amount of water required/supplied. Optical/thermal reflectance information collected over several years is subjected to either supervised or unsupervised classification algorithms to identify the irrigated areas. Derived products such as NDVI, NDMI, EVI, LSWI are also used in classification schemes for this purpose. Similar classification schemes are applied to backscatter timeseries from radar sensors for detecting irrigation. In the case of passive microwave sensors, the soil moisture obtained measures the

moisture changes due to rainfall as well as irrigation events. Therefore, attempts are made to use soil moisture products to identify the spatial and temporal patterns of irrigated areas. ET is an essential variable for quantifying the irrigation water requirement. Energy balance methods are popular in determining ET using optical/thermal reflectance from satellites. On the other hand, the identification of irrigation water supplied to a farm is a primary function of soil moisture. Recent efforts have focused on extracting the irrigation information by using satellite soil moisture and precipitation datasets. **(L. Karthikeyan *&* *al.,* 2020)**.

Three main methodological approaches to the estimation of irrigation water use are describe down below based on 41 studies that reflect the primary type of satellite data used to derive estimates of irrigation water use.

First, 20 out of 41 studies use remotely sensed thermal infrared imagery (e.g., from MODIS—Moderate Resolution Imaging Spectroradiometer—or Landsat) to estimate crop ET rates, which are then converted in to estimates of consumptive irrigation water use by subtracting an estimate of effective rainfall. Variations on this approach involve calculating the difference between estimated ET fluxes for irrigated locations with those for neighboring rainfed pixels **(Romaguera *&* *al.,* 2014; Van Eekelen *&* *al.,* 2015; Vogels *&* *al.,* 2020**) or, alternatively, with ET fluxes simulated by land surface hydrology models. The latter typically do not include representations of irrigation practices, meaning that the additional ET "observed" in reality through satellite remote sensing can be attributed to irrigation water consumption **(Anderson *&* *al.,* 2015; Droogers *&* *al.,* 2010; Lopez Valencia *&* *al.,* 2020)**. Estimates of consumptive irrigation water use are converted to applied or abstracted water by applying efficiency adjustment factors to account for non-consumptive losses such as deep percolation or runoff. Typically, these factors are conditioned on the types of irrigation technology used by farmers in the region and do not vary between farmers operating the same technology or over time. For example, **(Msigwa *&* *al.,* 2019)** and **(Van Eekelen *&* *al.,* 2015)** both assume a constant irrigation application efficiency of 75% for case studies in southern Africa based on assumptions about prevailing irrigation technology mixes across their study areas.

A second category of models estimate irrigation water use based on satellite soil moisture observations from either passive (e.g., SMOS—Soil Moisture Ocean Salinity and AMSR—Advanced Microwave Scanning Radiometer) or active (e.g., ASCAT—Advanced SCATterometer and Sentinel-1) microwave sensors. Similarly, to thermal-infrared models, two broad methodological approaches are applied in soil moisture-based models of irrigation water use. First, "observed" soil moisture changes can be used in conjunction with meteorological

data and soil moisture balance models to solve for the unknown rate of irrigation **(Brocca *&* *al.*, 2018; Jalilvand *&* *al.*, 2019)**.

ET fluxes used in the inversion of soil water balance models are typically estimated using empirical relationships between ET and soil moisture. However, some studies also utilize satellite-based ET time series, combining information from thermal-infrared and microwave sensors. An alternative approach for isolating effects of irrigation is to compare observed soil moisture changes detected using microwave sensors with soil moisture changes predicted for the same location by land surface models that omit irrigation processes **(Zaussinger *&* *al.*, 2019; Zohaib and Choi, 2020)**. A variation on this approach is adopted by (**Abolafia-Rosenzweig *&* *al.*, 2019)**, who assimilate satellite soil moisture data within a land surface hydrological model Variable Infiltration Capacity model (VIC) to derive estimates of the underlying rate of irrigation water use. As for thermal-infrared models, additional adjustment factors based on technical system efficiencies may subsequently be applied to determine applied or abstracted rates of water, in particular to account for non-consumptive losses of irrigation water before entering the soil profile (e.g., surface runoff and canopy evaporation) that are not captured by satellite soil moisture data.

Finally, the third category of models used to estimate irrigation water use are crop coefficient models. These models utilize reflectance-based estimates of crop coefficients, which capture crop vegetation condition on a given day obtained as a function of vegetation indices (e.g., normalized difference vegetation index [NDVI] and enhanced vegetation index [EVI]) derived from different combinations of spectral bands captured by satellite imagery **(Campos *&* *al.*, 2017)**. Crop coefficients are then inputted, along with meteorological data, to soil water balance models to estimate rates of irrigation given assumptions about the level of soil moisture depletion at which irrigation will be triggered and expected application and conveyance efficiencies of water use. A key difference between crop coefficient and thermal-infrared or soil moisture-based models is that reflectance-based crop coefficient models are most commonly used to provide estimates of crop irrigation requirements rather than actual abstraction rates **(Abuzar *&* *al.*, 2017; Campos *&* *al.*, 2017; Foster *&* *al.*, 2019; Gonçalves *&* *al.*, 2020; Santos *&* *al.*, 2010; Segovia-Cardozo *&* *al.*, 2019; Vuolo *&* *al.*, 2015)**. This is because reflectance-based crop coefficients capture reductions in crop ET caused by suboptimal crop development over the growing season but do not provide direct information about additional reductions in crop ET as a result of water stress limiting plant transpiration. Instead, underlying soil water balance models typically assume that farmers' trigger irrigation when soil moisture depletion reaches the level at which stomatal closure would be triggered **(Foster *&* *al.*, 2019;**

Gonçalves *& al.*, 2020), thus generating an estimate of the amount of irrigation that would need to have been applied to avoid water stress. Where these assumptions are violated, or if uncertainties exist in the assumed threshold for initiation of stomatal closure or other model inputs (e.g., irrigation application efficiencies), then estimates of irrigation water use are likely to diverge from true abstraction rates **(Peña-Arancibia *& al.*, 2016).**

Figure 14 represent a satellite image captured by Landsat 8 showing how enhanced vegetation index can help detect vegetation.

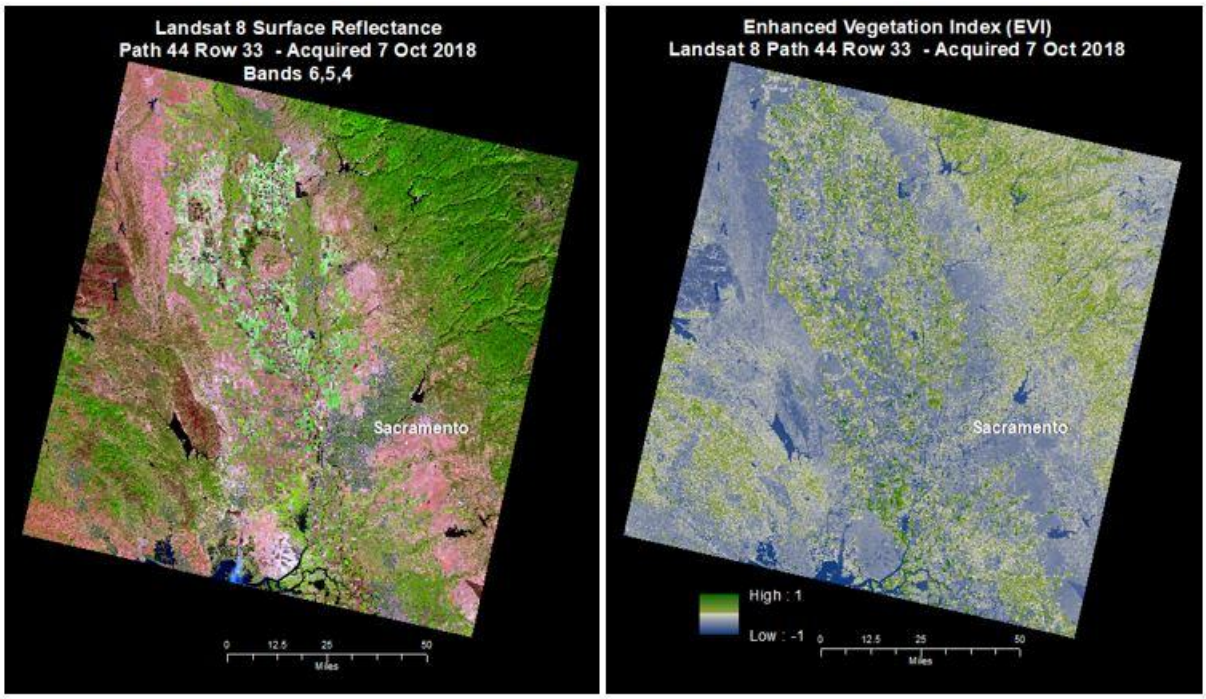

Figure 14: Landsat Surface Reflectance and Enhanced Vegetation Index This image displays a (left) Landsat 8 Surface Reflectance (SR) and (right) the SR-derived Enhanced Vegetation Index (EVI). Source: public domain USGS

The use of remote sensing to monitor soil moisture levels and optimize irrigation schedules. Can help farmers reduce water waste, improve crop yields, and save on irrigation costs.

4.2 Monitoring of Drought

Drought is a common hydrometeorological phenomenon **(Hayes *& al.*, 2012)**, and a pervasive hazard, second only to flooding in its impact on social and economic security (Nagarajan, 2009). Since the turn of the century, several socio-economically significant regional droughts have occurred, for example in Australia (2000–2009), USA (2000–2016), Southern and Sub-Saharan Africa (2015–2017), China (2007–2012) and Europe (2007–2010) **(Ummenhofer *& al.*, 2009; Ault *& al.*, 2016; Chao *& al.*, 2016; Cook *& al.*, 2016; Baudoin *& al.*, 2017)**. There

is no universal definition of a drought **(Lloyd-Hughes, 2014)**, but in its simplest form a drought event represents a deficit of water relative to normal conditions. Unlike floods which have a clear and sudden start and end **(Wang *&* *al.*, 2016)**, droughts can be characterised by slow development and prolonged impacts. How spatio-temporally variable rainfall deficits propagate through the land surface to register deficits in soil moisture, runoff and recharge is complex and heterogeneous. While droughts can be ended by sudden extreme precipitation, how to precisely identify the termination point of a drought event is contested **(Parry *&* *al.*, 2016)**. These attributes mean that drought is a phenomenon that is challenging to quantify and analyse. Impacts from recent droughts reveal high levels of exposure and vulnerability of both natural and human systems **(Van Loon *&* *al.*, 2016)**. This is significant as with future climate change it is likely that many areas will start to experience more frequent and intense dry conditions, with irreversible impacts for people and ecosystems **(IPCC, 2014)**. Consequently, drought monitoring and mitigation have become urgent scientific issues **(Liu *&* *al.*, 2016)**.

Generally, drought is classified into meteorological drought, agricultural drought, hydrological drought, and socio-economic drought **(Figure 15).** Meteorological drought refers to the water deficit caused by an imbalance between precipitation and evaporation. Agricultural drought reflects the extent to which soil moisture is lower than the least requirement of plants by analyzing the characteristics of soil moisture and morphology of plants during growth. Hydrological drought occurs when river flow is lower than the normal value or when the water level of an aquifer decreases; and socio-economic drought is the phenomenon in which production and consumption are affected by the lack of water in both the natural system and human socio-economic system **(Chen *&* *al.*, 2009).**

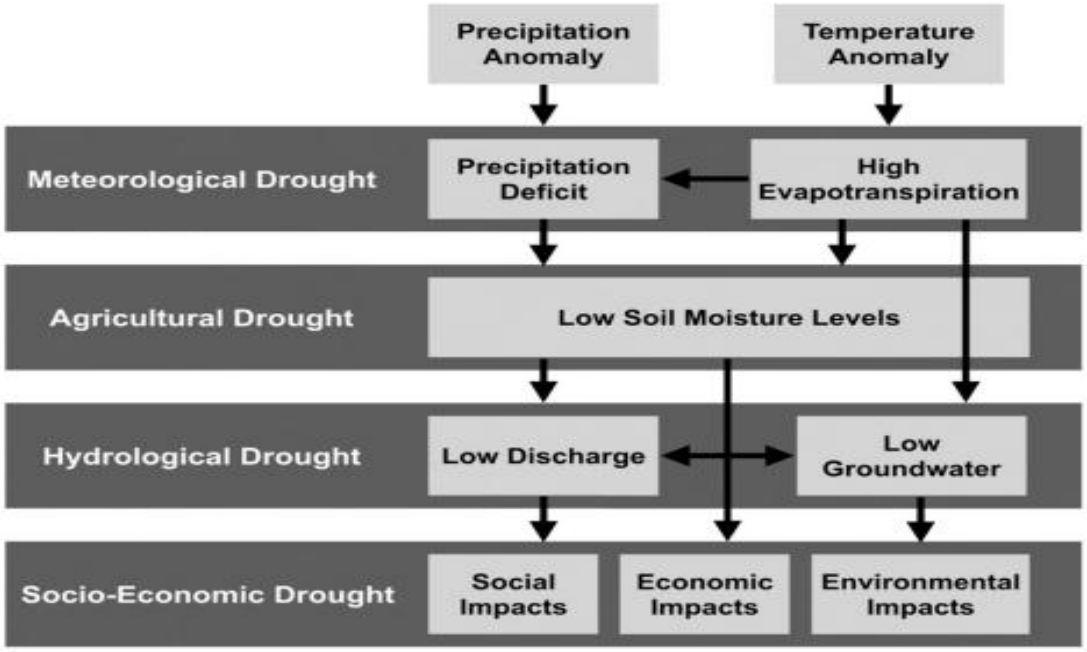

Figure 15: Different types of drought, their interactions and associated impacts. Source: Adapted from **(Van Loon, 2015).**

Since agricultural drought is closely connected to soil moisture and crop water deficit, it is safe to say that by applying remote sensing to monitor water inversion in soil and vegetation you are monitoring drought. Data assimilation methods are generally used to estimate soil moisture **(Kumar *&* *al.*, 2014)**. Among these methods, thermal inertia models of different soil textures, established by (**Chen, 1999)**, improved the accuracy of water inversion by introducing parameters of topography and wind field. However, the parameters are difficult to determine in practice. Then, **(Zhang, 2001)** integrated the thermal inertia model, heat balance model, and temperature difference model by using temperature differences of the soil and leaves facing the sun and away from the sun, developing a new method of soil moisture inversion on the basis of multi-angled remote sensing data. In addition, by applying the improved IEM model, **(Bindlish, 2006)** obtained an inversion result whose correlation with actual soil moisture was 0.95. Although microwave remote sensing can work continuously without being influenced by clouds, it is only capable of inverting the soil moisture of the surface (2–5 cm), while crop roots are usually 10–20 cm under the surface. Hence, water stress in crops cannot be examined accurately, and the result is highly uncertain **(Chen *&* *al.*, 2012)**. However, accurate estimation of soil moisture at different depths is very important, since it is a key parameter for agricultural drought monitoring. Therefore, despite the limitations of the applying remote sensing method

to agricultural monitoring, further studies are still required; the microwave inversion results should be coupled with the terrestrial surface model, and field survey data should be collected to increase inversion accuracy and depth **(AghaKouchak *&* *al.*, 2015)**. With respect to crop water deficit, crop water stress index (CWSI was developed by analyzing the empirical relationship between air vapor and temperature differences of the canopy and air **(Idso *&* *al.*, 1981)**. Later, **(Moran, 1994)** developed the water deficit index (WDI) on the basis of the two-layer model of the energy balance model, while **(Gao, 1996)** proposed the normalized difference of water index (NDWI). To eliminate the influence of both Normalized Difference Vegetation Index (NDVI) spatial variation and other parameters of geography and ecosystem, **(Kogan, 1995)** proposed the vegetation condition index (VCI) for drought monitoring, and then **(Wang, 2003)** developed the vegetation temperature condition index (VTCI) in 2003. On basis of this, Kogan proposed the vegetation health index (VHI) by linear integration of TCI and VCI **(Boken *&* *al.*, 2004; Kogan *&* *al.*, 2013)**, which was proven to be effective in reflecting the drought situation of crops **(Mu *&* *al.*, 2007)**. In 2004, Haboudane proposed the vegetation supply water index (VSWI), which is a relatively simple synthesis index for vegetation and temperature **(Haboudane *&* *al.*, 2004).** Previous studies have shown that VSWI is appropriate for regions with high vegetation coverage, and it is widely applied in practice **(Liu *&* *al.*, 1998)**. **(Sandholt, 2002)** proposed the temperature vegetation drought index (TVDI) to estimate soil moisture on the basis of the relationship between land surface temperature (LST) and vegetation index (VI), which is an important method to reflect agricultural drought conditions through soil moisture monitoring. A hypothesis of TVDI is that NDVI is negatively correlated with LST **(Karnieli *&* *al.*, 2010)**. However, NDVI is negatively correlated with LST when water is the limitation factor of vegetation growth, whereas NDVI is positively correlated with LST when energy is the limiting factor of vegetation growth. Moreover, TVDI can well explain regions with drought episodes, but failure in performance of agricultural monitoring and earlier warning.

4.3 Crop mapping and crop management:

For agricultural management and land-use planning, the process of identifying and mapping the various crops in a region is known as crop mapping. The use of remote sensing technologies to map crops has become increasingly practical since they deliver precise and timely data on crop distribution, health, and yield. The various remote sensing techniques and their applications for crop mapping will be covered in this article.

One of the most used remote sensing techniques for crop mapping is satellite remote sensing. It involves taking pictures of various crop fields using satellites that are orbiting the planet. Remote sensing software is used to analyse these photos in order to map and identify various crops based on their spectral properties. Wide coverage and regular updates from satellite remote sensing make it an effective tool for extensive crop mapping. **(Thenkabail *& al.*, 2011)**.

Another remote sensing technique used in crop mapping is aerial remote sensing. It entails the use of drones or airplanes to take high-resolution pictures of crop fields. Remote sensing software is used to analyze these photographs in order to map and identify various crops. Since aerial remote sensing has a higher spatial resolution than satellite remote sensing, it is possible to map individual crop fields in greater detail. **(Yang *& al.*, 2018)**.

A sort of remote sensing technology called hyperspectral remote sensing is used to recognize crops based on their spectral signature. Crop images are captured by hyperspectral sensors at hundreds of fine spectral bands, enabling in-depth study of crop health and stress. Early symptoms of crop illnesses and nutritional deficits can be found using hyperspectral remote sensing, allowing farmers to take prompt corrective action. **(Daughtry *& al.*, 2000)**

Another remote sensing technique for crop mapping is radar remote sensing. In order to take pictures of crops, radar sensors are used. Radar remote sensing can see through plants and clouds, providing information on crop growth and moisture levels. Radar remote sensing is particularly helpful for mapping crops in areas with regular cloud cover or extensive vegetation. **(Chen *& al.*, 2014)**

remote sensing technologies have emerged as powerful tools for crop mapping, providing accurate and timely information on crop distribution, health, and yield. Satellite remote sensing provides wide coverage and frequent updates, while aerial remote sensing provides higher spatial resolution. **(figure 16).**

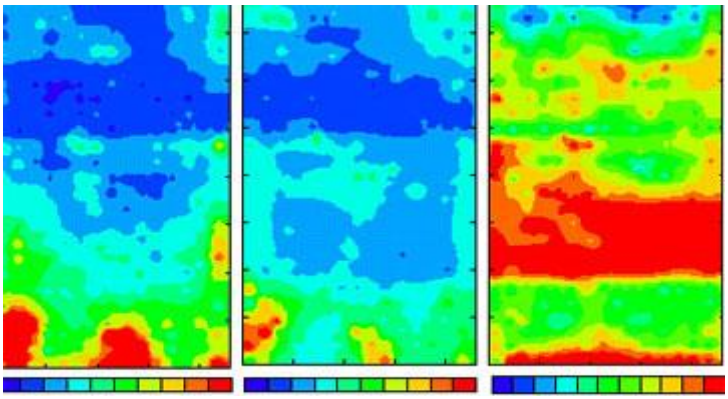

Figure 16: soil test of phosphorus, potassium and pH for a central Missouri (USA) farm. (Blue to red is low to high for the concentrations and acidic to alkaline for the acidity) source: **(Davis *&* *al.*, 1998)**

4.4 Yield estimation

Given that it provides a non-destructive method of acquiring information on crop growth and development, remote sensing is an important tool in yield estimation. Data gathering from a distance is referred to as remote sensing, and it often involves the use of sensors that are mounted on planes or satellites. Through the analysis of various vegetation indices and spectral reflectance patterns, the data gathered can be used to estimate crop yield. By providing more precise and effective yield prediction, which is essential for the optimization of farming operations and food security, this technology has completely transformed the agricultural sector.

The detection and monitoring of crop stress are one of the main applications of remote sensing in yield estimate. Crop stress can be caused by a number of things, including a lack of water and nutrients, an infestation of pests and diseases, or environmental stresses like extreme weather events. By examining spectral reflectance patterns, which are sensitive to changes in vegetation health, remote sensing can identify and measure this stress. Using this data, crop management techniques can be improved in order to reduce stress and increase yield. (**Peng *&* *al.*, 2019)**.

The identification and mapping of crop variability across fields is another use of remote sensing in yield estimate. Due to variations in terrain, soil quality, and other environmental conditions, crop growth and production might vary. Farmers can recognize and control variability within a field by using high-resolution spatial data on crop growth and development provided by remote

sensing. In order to increase agricultural output and quality, planting density, fertilizer, and irrigation procedures can be optimized using this information **(Zhang *&* *al.*, 2019)**.

By examining vegetation indices like the Normalized Difference Vegetation Index (NDVI) or the Enhanced Vegetation Index (EVI), remote sensing can also be used to estimate crop yield at a regional level. These indexes quantify the density and health of the vegetation and can be used to calculate yield and biomass. At the regional or national level, this information is essential for management and crop forecasting decisions **(Xu *&* *al.*, 2019)**.

The capacity to track crop growth and yield in real-time is another advantage of using remote sensing to estimate yield. Manual sampling and field measurements are labor- and time-intensive traditional yield estimating techniques. In order to help farmers manage crop stress or unpredictability, remote sensing technology can often and reliably offer data on crop growth and yield **(Huete *&* *al.*, 2019)**.

remote sensing is a powerful yield estimating technology that gives farmers the ability to optimize crop management techniques and enhance food security. Remote sensing offers essential information for agricultural decision-making by identifying and measuring crop stress, mapping crop variability, calculating yield at a regional level, and tracking crop growth in real-time.

Figure 17 represent a color-scaled image of the final corn yield data for the three studied seasons in Ferrara North Italy. It shows how remote sensing technologies (satellite sentinel 2) can provide exact information and help track yield.

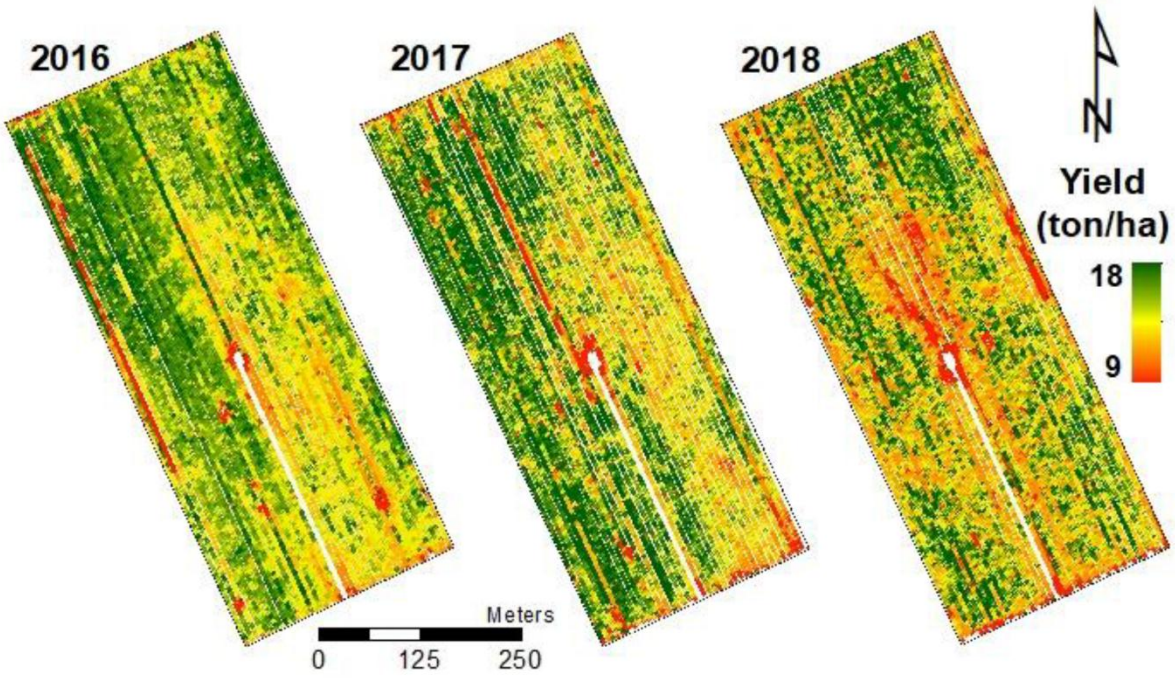

Figure 17: Corn grain yield data for the 2016, 2017, and 2018 growing seasons study field in Ferrara North Italy. Source: **(Ahmed K. *&* *al.*, 2019)**

4.5 Detecting pests and diseases:

For identifying and keeping track of diseases and pests in agricultural crops, remote sensing is an effective tool. Farmers can promptly detect the presence of pests or illnesses, determine their severity, and take the necessary precautions to minimize the harm they cause by using remote sensing. Farmers' yields and losses may be reduced as a result, improving economic results.

The application of aerial images is one of the most used remote sensing techniques for detecting pests and diseases. Aerial photographs with high resolution can provide specific details about crop health, including the presence of pests and diseases. For instance, it is feasible to determine the precise wavelengths of light that are being absorbed or reflected by plants affected by pests or diseases by examining the spectral signatures of plants in aerial pictures. Maps of the impacted areas may then be made using this data, which will aid farmers in more precisely focusing their pest and disease control efforts. **(Zhang *&* *al.*, 2021)**.

Using satellite imagery is another way that remote sensing is used in the detection of pests and diseases **(Figure 18).** It is possible to spot changes in crop health over time by examining satellite photos, which may indicate the presence of pests or diseases. For instance, a dramatic

drop in the amount of vegetation in a particular location may be a sign of an infestation. Additionally, farmers can quickly spot areas that need attention by using satellite imagery to monitor crop health on a large scale. **(Lobell *& al.*, 2002)**.

Figure 18: A represent a map of wheat field highlighting the areas touched by disease of powdery mildew

B represent a map of a corn field classifying the health of vegetation and mapping the areas touched by pests

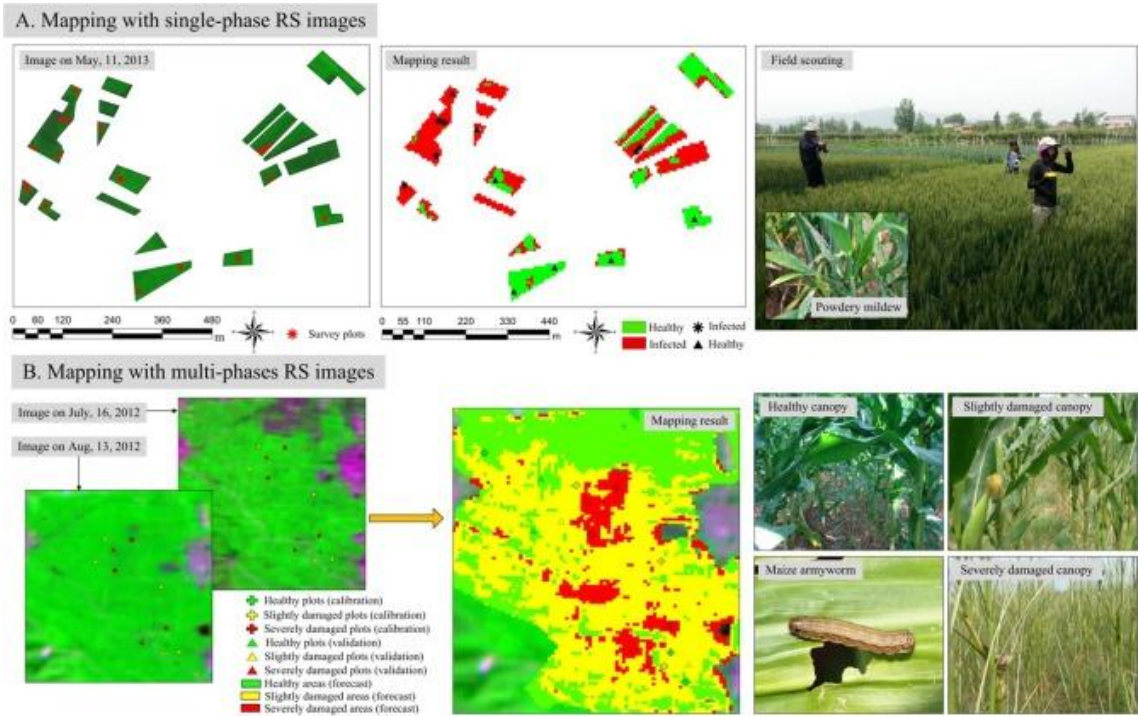

Figure 18: Mapping plant disease and pest with single-phase RS image (A, mapping powdery mildew in wheat, Source: **(Yuan *& al.*, 2015)** and multi-phases images (B, mapping armyworm in maize, Source: **(Zhang *& al.*, 2015)**.

Other remote sensing technologies can be used for pest and disease detection in addition to aerial and satellite imagery. For instance, minor changes in plant health that would not be evident to the naked eye can be found via hyperspectral imaging. By examining the reflectance of light from plants at a variety of wavelengths, this technique can detect subtle changes in plant health that may be signs of pests or diseases. **(Vigneau *& al.*, 2014)**

Remote sensing has generally shown to be a useful tool for spotting and keeping track of pests and illnesses in agricultural crops. Remote sensing can help farmers raise yields and decrease losses by giving them accurate information on the health of their crops, improving economic outcomes. It is expected that as remote sensing technologies advance, they will become even more successful at spotting and tracking pests and illnesses, thus increasing their value to farmers. **(Huang *&* *al.,* 2021)**.

4.6 Soil health monitoring

Remote sensing technology has emerged as a powerful tool for monitoring and assessing various aspects of soil health. By capturing and analyzing data from different regions of the electromagnetic spectrum, remote sensing provides valuable information on soil properties and processes.

Identification of Soil Properties: Remote sensing techniques allow for the mapping and identification of a variety of soil characteristics. To determine the soil's moisture content, organic matter content, texture, compaction, and nutrient levels, spectral reflectance data from aerial or satellite sensors can be evaluated. Effective soil management strategies depend on an understanding of spatial patterns of soil attributes, which is facilitated by these data **(Jackson *& al.,* 2019)**.

Detecting Soil Erosion: Agriculture productivity and soil health are both seriously threatened by soil erosion. By collecting high-resolution photos over time, remote sensing makes it easier to identify and keep track of soil erosion. It is possible to spot places prone to erosion by observing changes in the land cover, the amount of vegetation, and the color of the soil. This information facilitates the implementation of erosion control strategies and stops future deterioration **(Hanqiu Xu *&* *al.,* 2019)**.

Evaluation of Soil Moisture: For effective irrigation management and crop output, accurate soil moisture monitoring is essential. Large-scale soil moisture content estimation via remote sensing is non-intrusive. Synthetic aperture radar (SAR), for example, can detect the backscattered microwave radiation and analyze soil moisture levels and fluctuations, allowing for timely irrigation decisions and minimizing water waste **(Tian *&* *al.,* 2022)**.

Evaluation of Soil Salinity: Agricultural systems are severely hampered by salinity in the soil. By obtaining electromagnetic radiation that is reflected or emitted by the soil surface, remote sensing provides a useful method for determining the salinity levels of the soil. Remote sensing

algorithms can predict soil salinity levels by examining the spectral properties of the reflected radiation, assisting farmers and land managers in successfully identifying and managing saline areas **(Sh Kholdorov, *& al.*, 2022)**.

Monitoring Soil Nutrient Status: By examining vegetation indices produced from satellite data, remote sensing techniques can help in the assessment of soil nutrient status. According to soil nutrient levels, vegetation indices like the normalized difference vegetation index (NDVI) can be used to determine the health plants. this information helps to optimize fertilizer application, decrease nutrient loss, and increase crop yields. **(Bouman *& al.*, 2017)**

Remote sensing technologies have revolutionized soil health monitoring by providing spatially explicit information on various soil parameters.

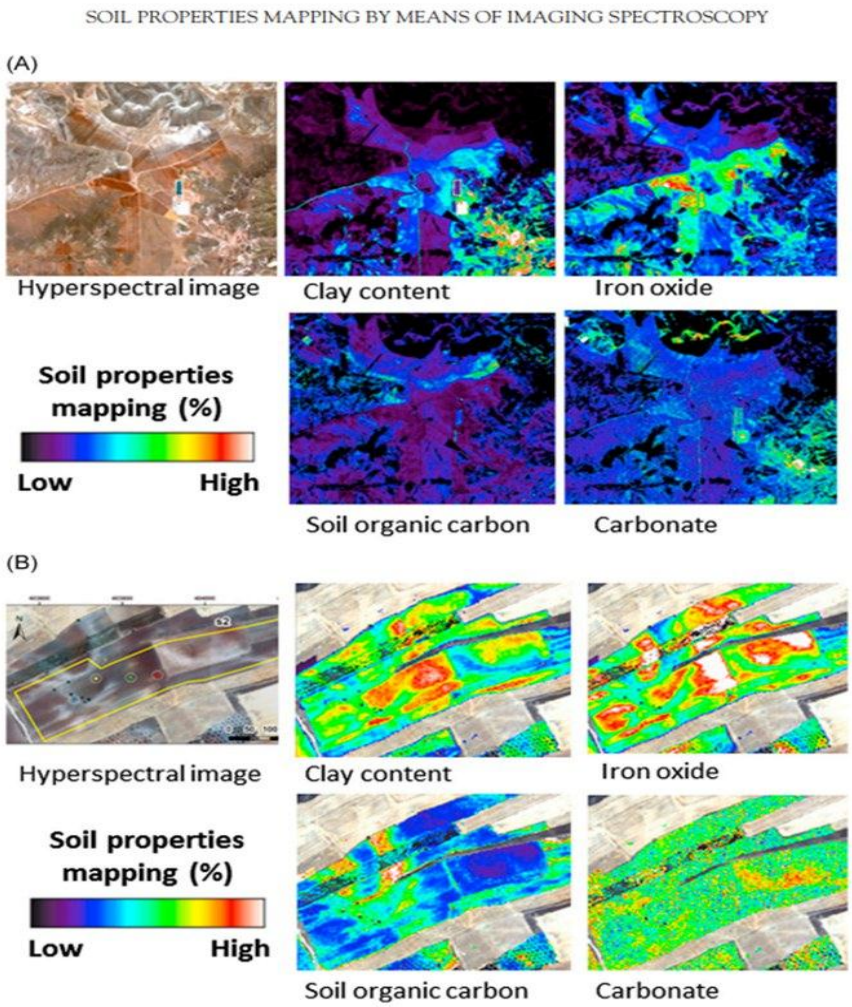

Figure 19 : Mapping of common soil surface properties with airborne imaging spectroscopy data using HYSOMA software automatic outputs (A) Cabo de Gata-Níjar Natural Park,

region of Cortijo del Fraile, (B) Camarena agricultural fields. Source: **(Chabrillat, S *&* *al.*, 2016)**

Chapter V: Study area description

5.1 General context

The City of Tiaret, located in the North-West of Algeria (220 km) west of the capital Algiers, (182 km) east of Oran. It presents on the physical level three large distinct zones:

- the north: a mountainous area of the Tell Atlas (such as Djbel Gezoul);
- the center: the highlands;
- the south: semi-arid spaces (the steppe).

The city of Tiaret covers an area of (20112.52 km²). It is bounded to the north by the Cities of Tissemsilet and Relizane; to the south by the two Cities El-Bayadh and Laghouat; Djelfa in the East; and Mascara and Saida in the West.

The city has significant natural potential and in particular (745,605.62 Ha) of agricultural land, (1007,303.57 Ha) of steppe areas (steppe/Alfa courses) and a forest area of (154,200.09 Ha forest/reforestation/maquis), and on the other (104,136.74 Ha) urban routes and bodies of water. It is dominated by the "cereal-livestock" system which plays an essential role in agricultural production and economic growth in this region.

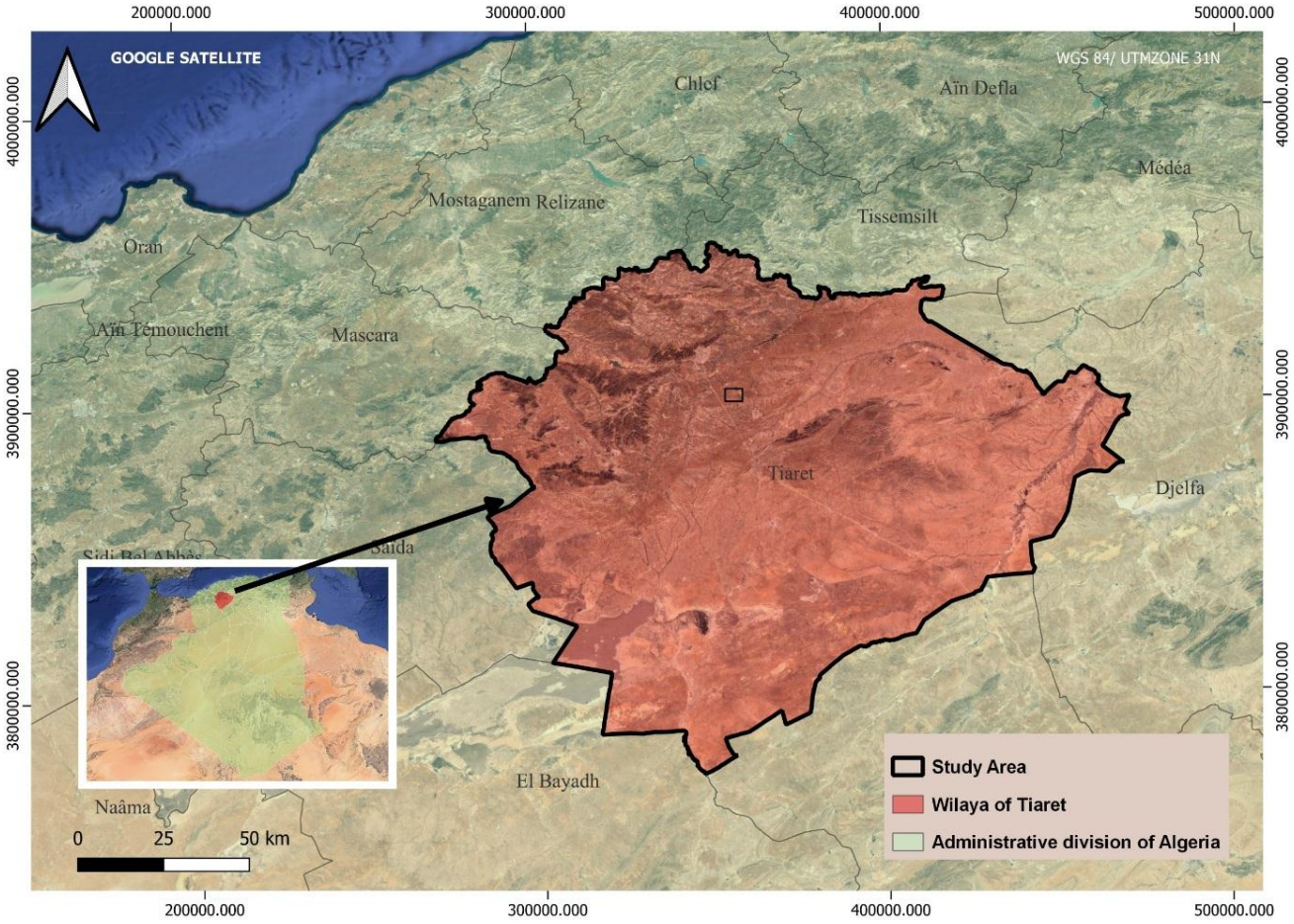

Figure 20: location map for the study area

5.2 Climate

Climatic phenomena are currently the major concern of scientists in all countries. The search for the slightest variation makes it possible to predict the future of any studied area with respect to climate change **(Boulenouar, 2016).**

Due to its extent space Tiaret has a heterogeneous character underpinned by:

A mountainous area to the north.

high plains in the center.

semi-arid to arid spaces in the south of the city.

This denotes the variety of landscapes and relief (ANRH) (Agence Nationale des ressources Hydriques)

In the classification of climates, the essential factors considered are: temperature, precipitation, number of rainy days, hygrometric state, fog and dew. These meteorological data are not always used in isolation. They are combined together so as to show the periods having an influence on the vegetation, that is to say: hot periods, cold periods, dry periods, wet periods. **(Achir, 2016)**

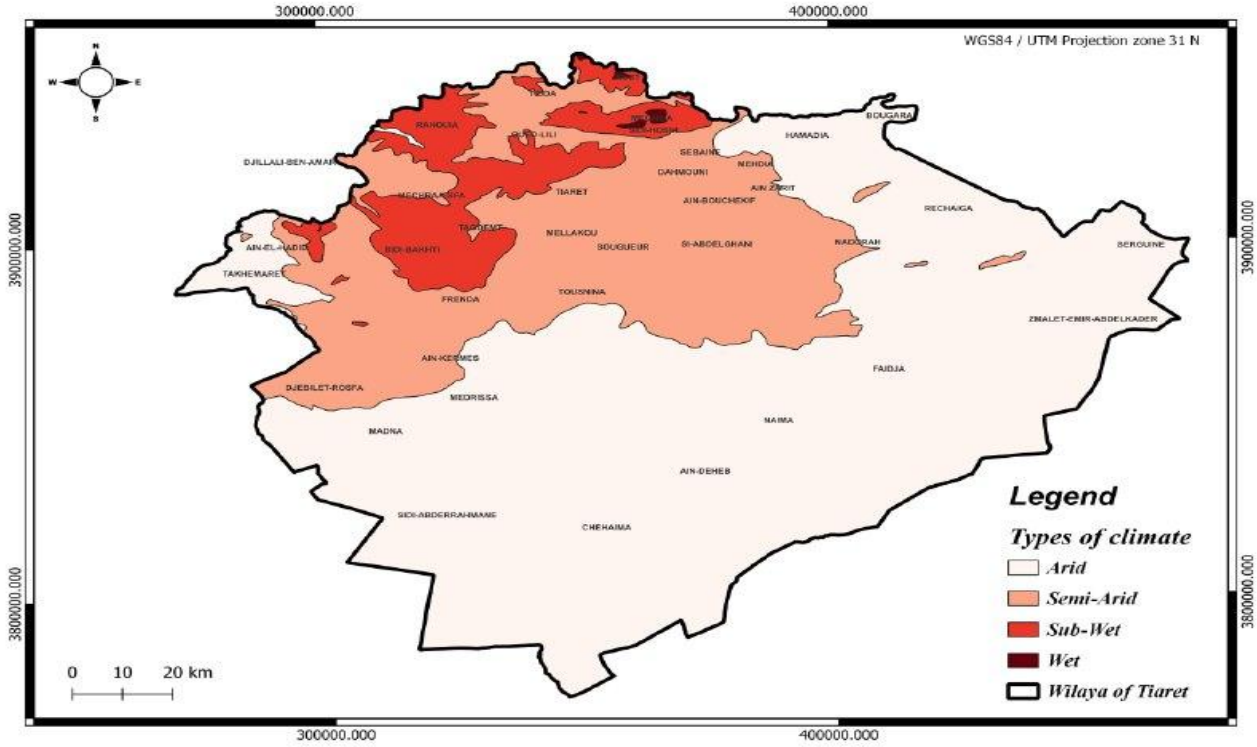

Figure 21: climate types in Tiaret **(Bouacha, 2013)**

5.2.1 Temperature

5.2.1.1 Monthly mean temperature (MMT)

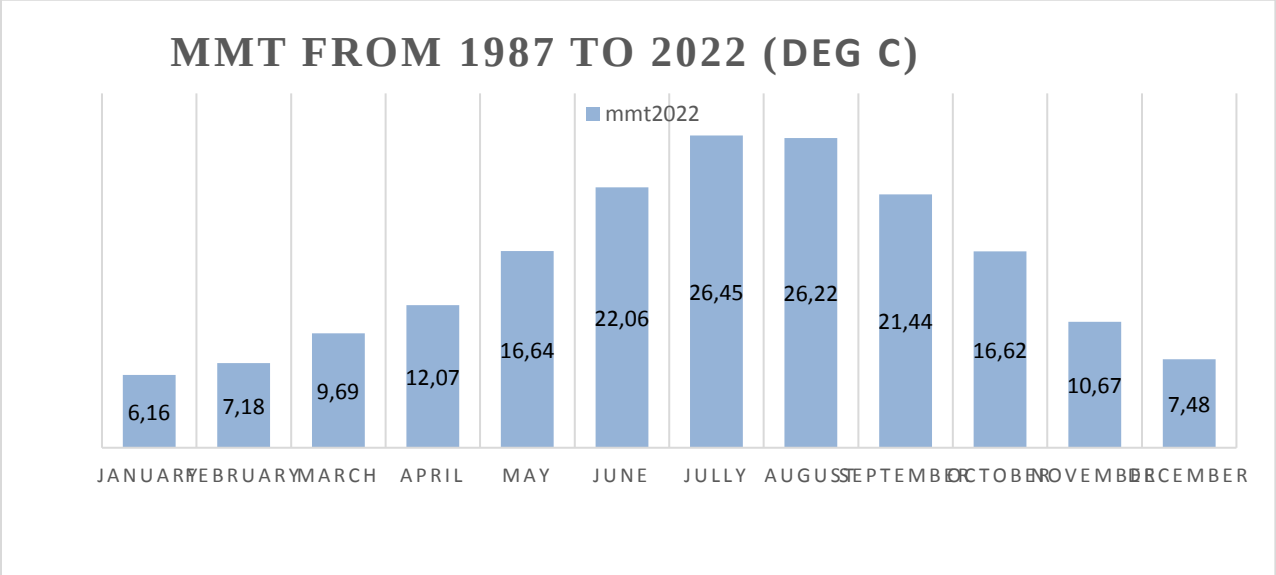

Figure 22: Monthly mean temperature in Tiaret region from 1987 to 2022

The graph displays the monthly mean temperatures in degrees Celsius (°C) for the region of Tiaret from 1987 to 2022. The x-axis of the graph represents the months of the year, while the y-axis represents the temperature values in degrees Celsius.

We can see a gradual increase in temperature from January to July, with the warmest months being July and August. The temperatures then gradually decrease from September to December, with the coldest months being December and January.

The graph also shows some variation in temperature within each season, with slightly cooler temperatures at the beginning and end of each season. For example, there is gradual increase in temperature from March to May, with temperatures peaking in June, before gradually decreasing again from September to November.

Overall, the graph shows the seasonal changes in temperature in the region of Tiaret throughout the year, with colder temperatures in the winter months and warmer temperatures in the summer months. The graph also shows some variation within each season, reflecting the region's climate and weather patterns.

5.2.1.2 Mean annual temperature (MAT):

Temperature is an essential climatic factor that enters into the calculation of evapotranspiration. The latter is also an essential parameter for estimating the water balance.

Tiaret region has a semi-arid climate type the mean temperature of this region from 1987 to 2020 is 15.22°C. with an irregular precipitation schedule. The climate in Tiaret is classified as semi-arid

(figure 23) shows the mean temperature in the region of Tiaret from 1979 to 2022

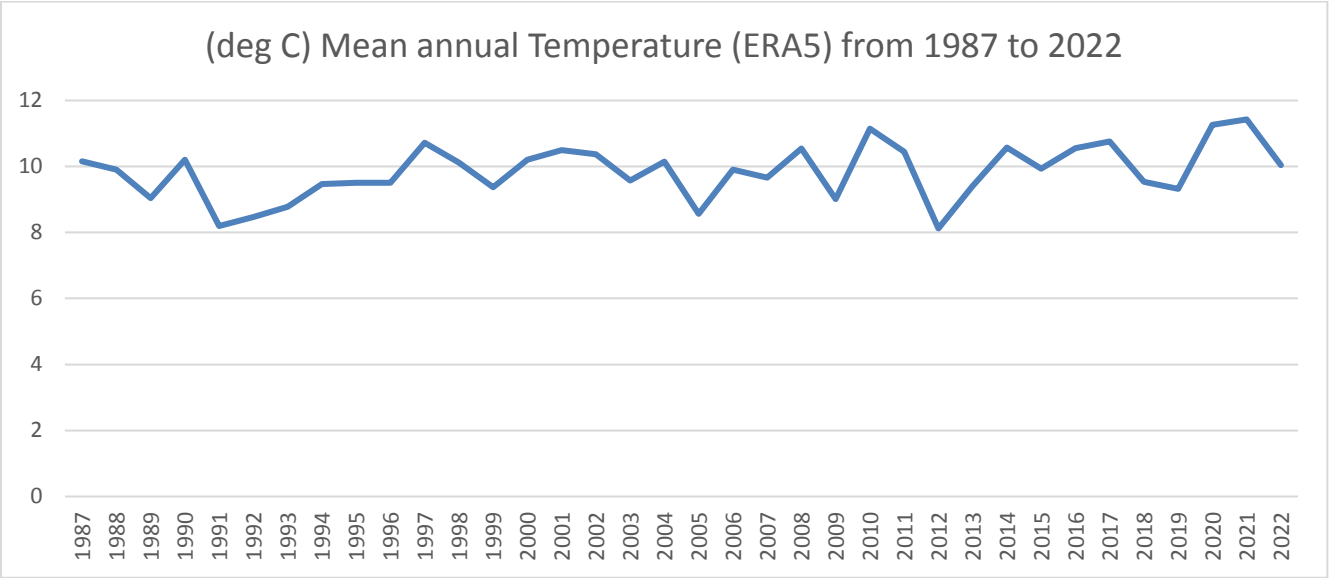

Figure 23: mean annual temperature in Tiaret region from 1987 to 2022

The graph shows the mean annual temperature in degrees Celsius (°C) for each year from 1987 to 2022. Based on the information in the table, the mean annual temperature in the region of Tiaret ranges from 8.1231 °C in 2012 to 11.4259 °C in 2021, with an overall average of approximately 9.9468 °C over the 36-year period.

It also shows some variation in mean annual temperature over time. For example, the mean annual temperature appears to have fluctuated between 8.1231 °C and 11.4259 °C. over the 36-year period, with some years being warmer than others.

Overall, the table shows the mean annual temperature trends in the region of Tiaret over the past 36 years. It may be possible to analyze these trends to identify patterns, such as whether temperatures are generally increasing or decreasing over time, and to understand how the region's climate and weather patterns are changing over time.

5.2.2 Precipitation

Rainfall was identified by Djeballi 1978 as the key determinant of climate type. In fact, it influences both the distribution and upkeep of the vegetative cover and the erosion phenomenon's destruction of the natural environment.

5.2.2.1 Monthly mean precipitation (MMP)

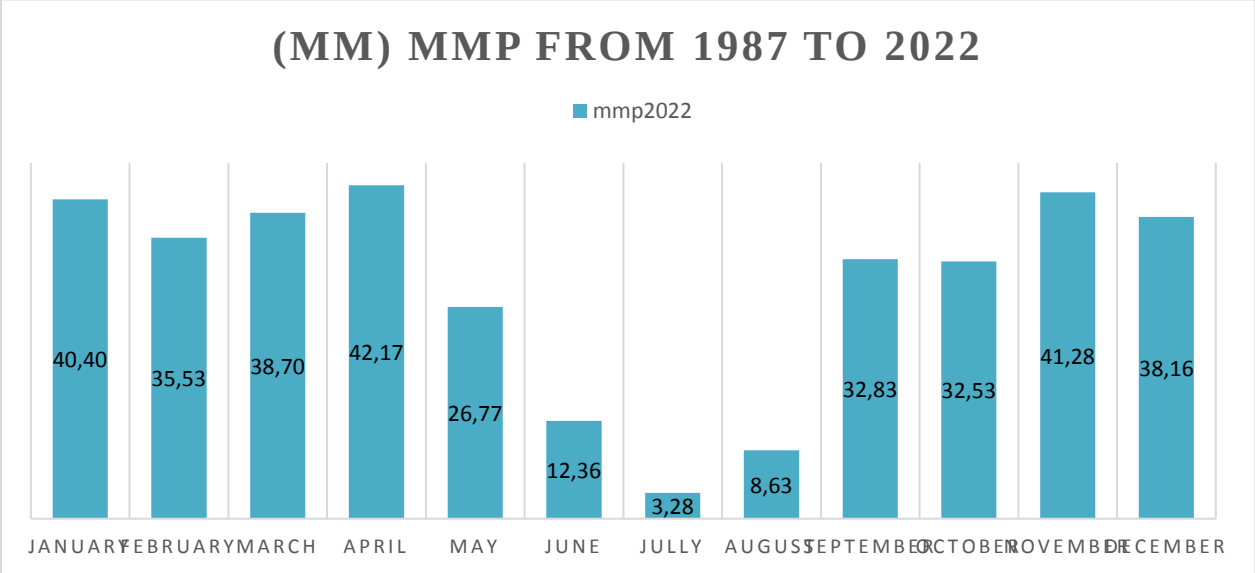

Figure 24: Monthly mean precipitations in Tiaret region from 1987 to 2022

The graph likely displays the monthly mean precipitation in millimeters (mm) for the region of Tiaret from 1987 to 2022. The x-axis of the graph represents the months of the year, while the y-axis represents the precipitation values in millimeters.

the graph shows a seasonal pattern in precipitation in the region of Tiaret. The region experiences a wet season from October to April and a dry season from May to September.

The graph shows the highest levels of precipitation in the months of November, April, and January, with mean values of 41.28 mm, 42.17 mm, and 40.40 mm, respectively. These months are likely to be part of the wet season and experience more rainfall.

On the other hand, the graph shows the lowest levels of precipitation in the months of June, July, and August, with mean values of 12.36 mm, 3.28 mm, and 8.63 mm, respectively. These months are likely to be part of the dry season and experience less rainfall.

Overall, the graph shows the seasonal variation in precipitation in the region of Tiaret, with wetter months in the wet season and drier months in the dry season. The graph also shows some variation within each season, reflecting the region's climate and weather patterns.

5.2.2.2 Mean annual precipitation (MAP):

The rainfall data series covers the years 1987 through 2022. We have made it feasible to confirm that the region's rainfall is extremely feeble and unevenly distributed.

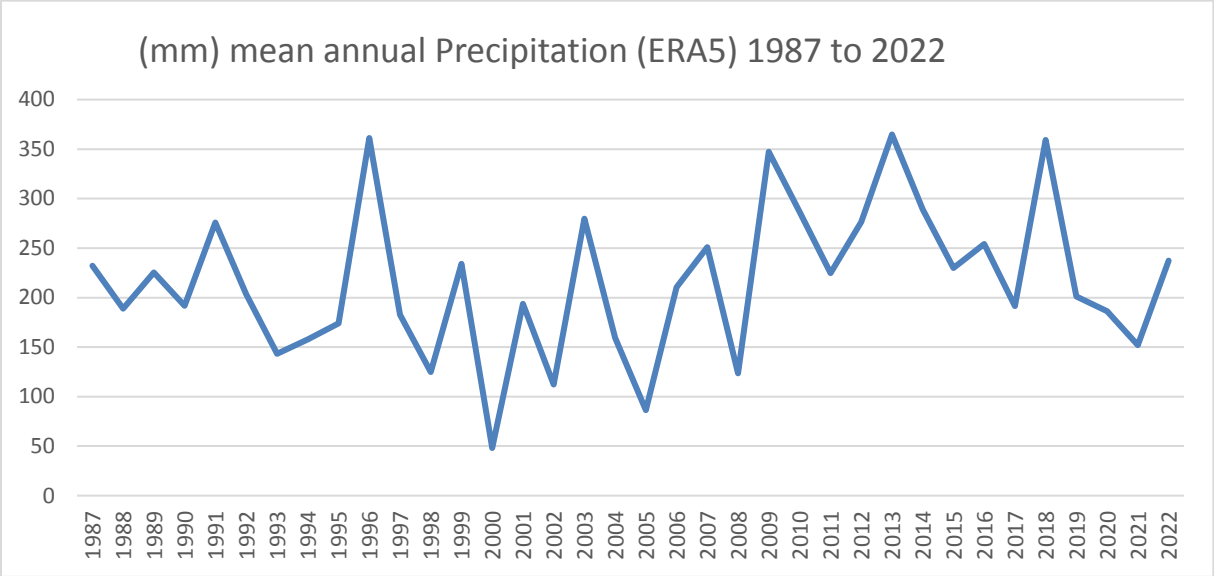

Figure 25: mean annual precipitations in Tiaret region from 1987 to 2022

The graph shows that the mean annual precipitation in the region of Tiaret varies significantly from year to year, ranging from 48.133 mm in 2000 to 364.766 mm in 2013, with an overall average of approximately 215.208 mm over the 36-year period. This suggests that the region experiences both droughts and periods of heavy rainfall, which can have significant impacts on agriculture, water supply, and other sectors.

5.3 Description of the physical environment

5.3.1 Land use

The city consists mainly of dominant vegetation. The dominant species are: (CFT 2018)

- Aleppo Pine: A forest tree that accepts poor terrain
- Holm Oak: Relatively slow growing tree
- Berber Cedar is a low elevation warm softwood
- Red Juniper - medium-sized tree in dry areas
- Oleasters: synonymous with the wild olive tree: centenary tree from 8 to 10 m
- Green Cypress: A fugal species of plains and mountains
- The lentic pistachio is very abundant everywhere, it can form clumps reaching very large dimensions.

The city of Tiaret has an estimated useful agricultural area of 688 725 ha **(MADR, 2019)**. Distributed in this way:

- Herbaceous crops: 405 690 ha
- Land at rest: 269 257 ha
- Natural meadows: 50 ha
- Vines: 563 ha
- Fruit tree plantations: 13 166 ha

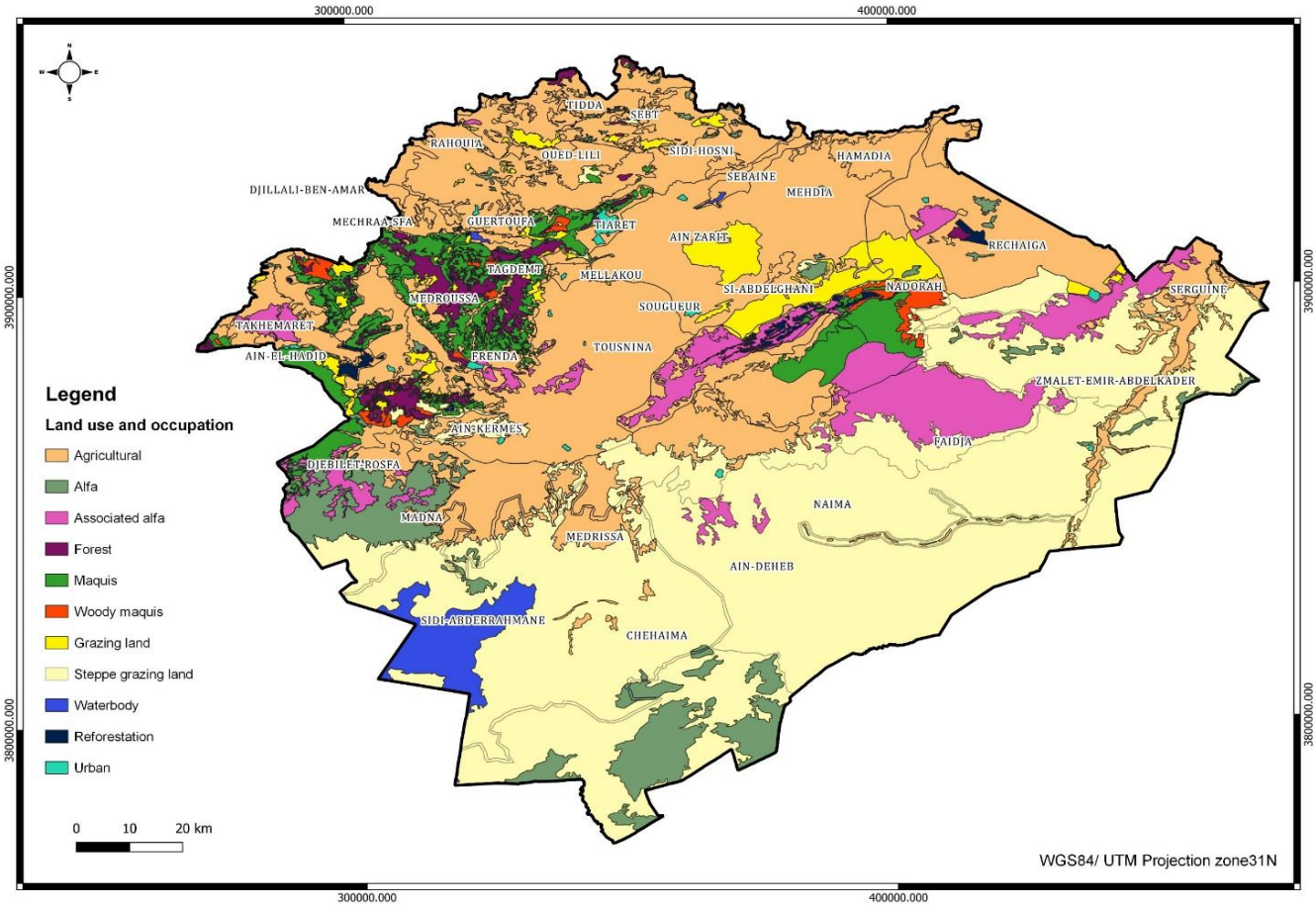

Figure 26: land use and occupation in Tiaret region **(source Bouacha 2013)**

5.3.2 Lithology

Given the agricultural identity of the study area, the various soil types encountered show certain similarities in this sense; the lithology of the land is characterized by skeletal soils poor in organic matter, among others these are of limestone type, such as the halo soils towards the sebkhas, (region of chott chergui) or towards the region of Ksar Chellala. Also, other types of soils, with sandy texture are identified.

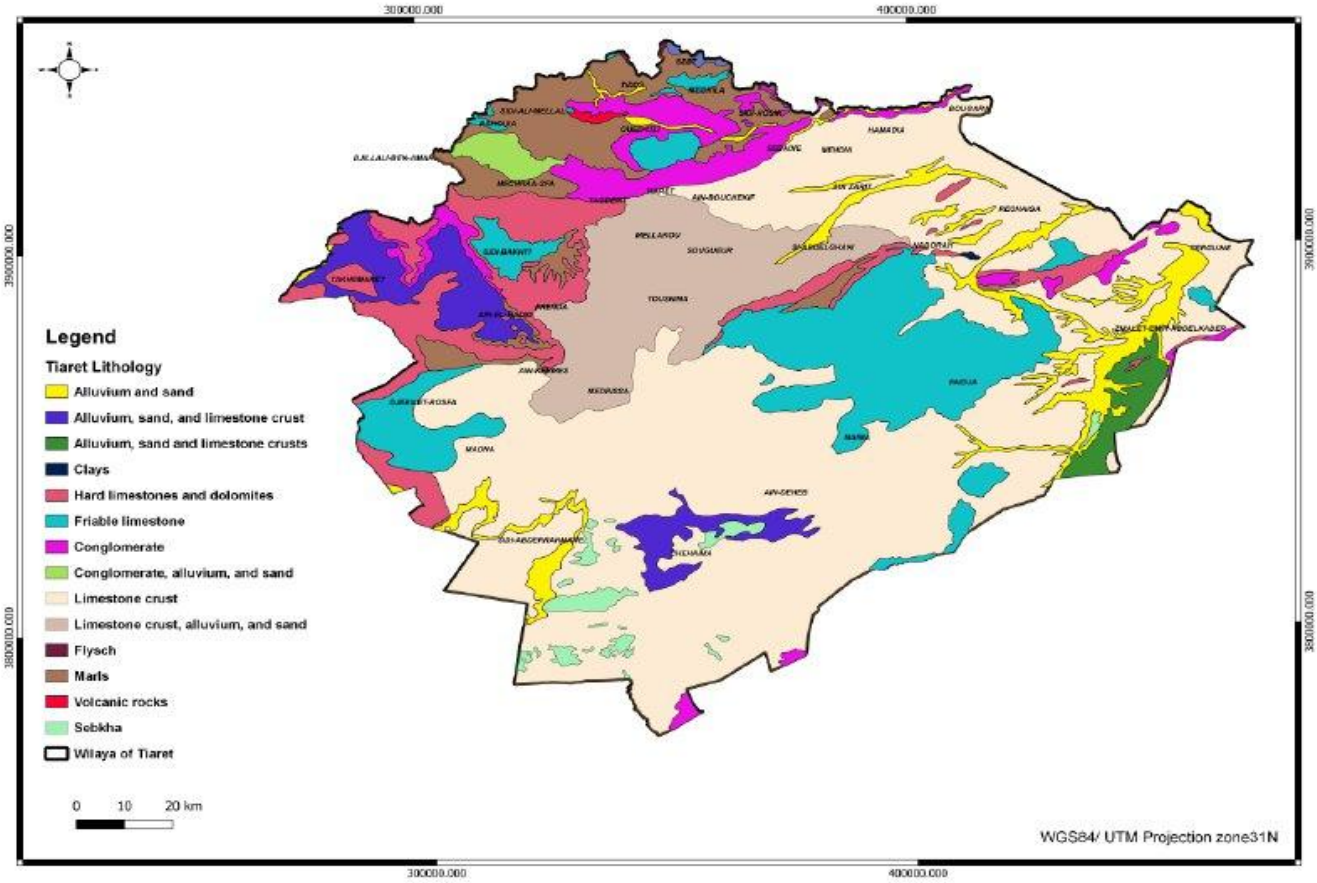

Figure 27: Lithology in Tiaret region **(source Bouacha 2013)**

5.3.3 Hydrography and water resources

The city has 03 dams with an overall capacity: 100 HM3.

- **Bekhadda** Dam: Located west of the city in the commune of MechraaSfa at an altitude of 665 meters, their Destination: drinking water supply of the localities of Tiaret, Rahouia, MechraaSfa, Djillali Ben Ammar, Kharouba, Guertoufa and Temda.

- Dam of **Dahmouni**: Located in the North of the city in the municipality of Sebaine at an altitude of 925 meters, their Destination: irrigation of the perimeter of Dahmouni for an area of 4000ha.

- **Bougara** Dam: Located to the east of the city in the commune of Bougara at an altitude of 809.50 meters, their Destination: irrigation of the perimeter of Bougara with an area of 1000Ha

Table 4: The characteristics of dams in the city of Tiaret (DHW, 2017)

Dams characteristics	Bekhadda dam	Barrage dam	Bougara dam
Date of commissioning	1936	1987	1989
Catchment area	1300 km2	530 Km2	454 Km2
Average interannual contribution of the catchment area	72Hm3	13.30Hm3	14.43Hm3
The initial capacity of the dam	45Hm3	42Hm3	13Hm3
The current reserve	39.9Hm3	26.60Hm3	11.00Hm3
Regulated volume	44.40Hm3/year	9Hm3/year	5.50Hm3/year

The territory of our city is interested hydrographically by 01 large watershed namely: The Watershed of Cheliff Zahrez I.4.1. Watershed of Cheliff: Its total area is 43750km2 grouping 08 citys, the city of Tiaret occupies only 14344km2 i.e. 33% of its total area. This watershed is articulated and is currency at our level in 13 sub-watersheds: Oued Mina upstream, Oued Mina - middle, Oued Mina - Downstream, Oued Touil - Upstream, Oued Touil - Middle, Oued Touil - Downstream, Oued Sakni , Oued Sousselem , Oued Mechti , Oued Abd, Oued Nahr Ouassel (DRE, 2018).

The length of the hydrographic network of the city is 1,938 km, including 889 km fo permanent wadis and 1,049 km for intermittent wadis, the main wadis are:

- OUED TOUIL
- OUED EL ABED
- OUED MINA
- NAHR OUASSEL

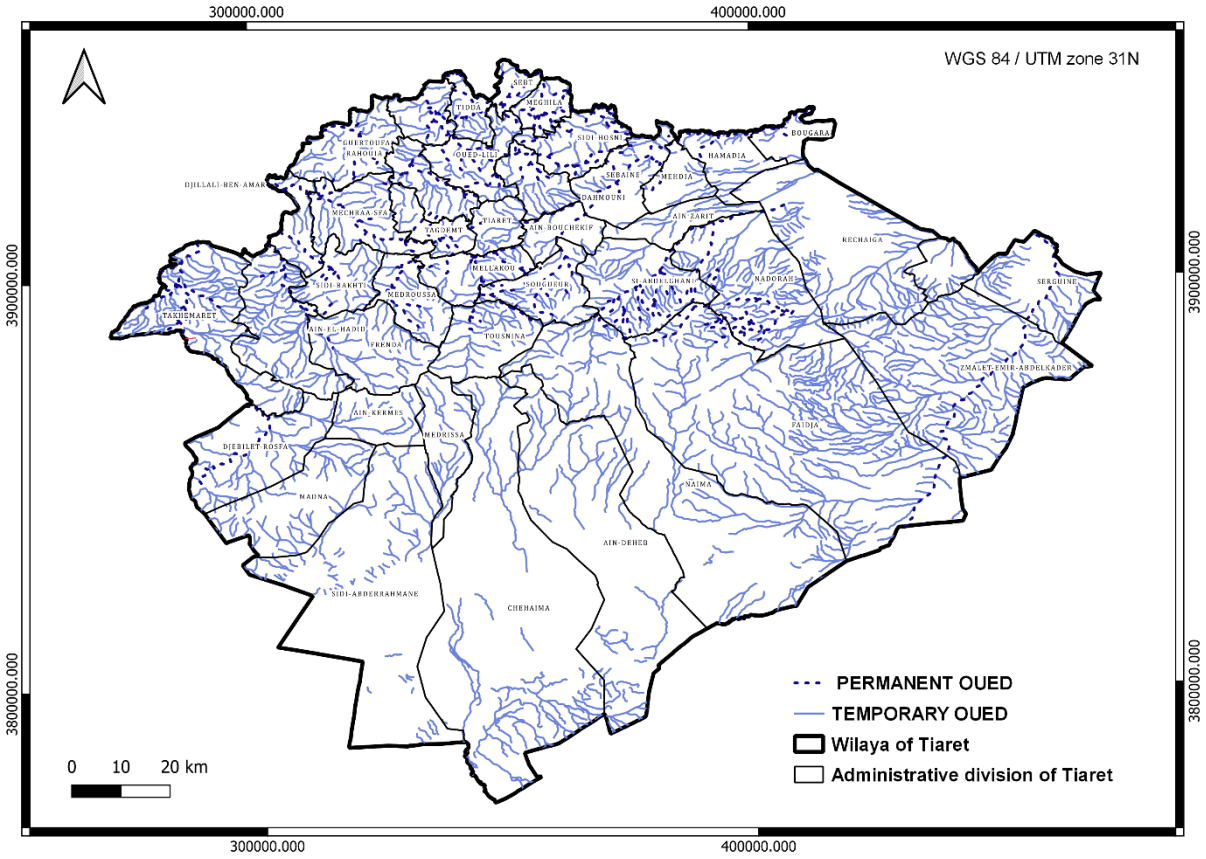

Figure 28: hydrographic network map of the study area **(Bouacha, 2013)**

5.4 Varieties and production

The city of Tiaret ranks second nationally in cereal production, which in this season reached more than 3.6 million quintals of all species (durum wheat, barley, oats). According to "The Department of Information Systems, Statistics and Statistics and Forecasting D.S.I.S.P" the total production of durum wheat in Tiaret is 1987900 qx in a surface area of 128223 ha with an approximate yield of 15.5 qx/ha. and for tender wheat in a surface area of 49638 ha the production has reached an amount of 471600 qx that result a yield of 9.5 qx/ha.(Table 5).

Table 5: the production of winter cereals in Tiaret for 2019. Source : (D.S.I.S.P Serie B 2019)

		Surface area (ha)	Surface area (ha)	Production (qx)	Yield (qx/ha)
Winter cereals	Durum wheat	136 000	128 223	1 987 900	15.5
	Tender wheat	63 000	49 638	471 600	9.5
	Barley	157 260	114 483	1 136 000	9.9
	Oatmeal	8 000	7 492	76 200	10.2
	Triticale	10	10	336	33.6
	Total	364 270	299 846	3 672 036	12.2

Chapter VI: Materials and Methods

6.1 Objective

In Our study we aim to estimate water consumption for tender wheat using models that estimate evapotranspiration using remote sensing methods. Such as The Surface Energy Balance Algorithm for Land (SEBAL) to prevent water waste in irrigation and maximize yield by determine and provide the actual needs that plant thrives in.

The data and the samples were taken from the pilot farm of CHRIF EDDINE in SOUGUEUR and the analysis and the studies were done in the Science of life and nature IBN-KHALDOUN University laboratory.

6.2 Sampling

6.2.1 Soil

Before starting the sampling, we need to examine the land in terms of its uniformity (e.g. uniformity of its level, type of soil, vegetation, applied amendments, etc.). They should be collected under the same physical conditions (T°, Humidity) and always on the same day **(Dari, 2013)**.

The sample should represent the soil of the plot as closely as possible. This is not easy but necessary for the results to be correct. And for the type of sampling we have to choose the subjective sampling.

The sample was taken from a 70ha field in Chrif Eddine pilot farm that is located in SOUGUEUR about 25 km South of the capital TIARET. We took 41 points in the Tender wheat plot, sampling was carried out to a depth of (30cm) by an auger. Each sample was clearly identified by a reference written on a label attached to the bag itself.

6.2.2 Plants

To take plant samples we followed the same method as for taking soil samples, that is, a subjective sampling method, we took a soil sample and a plant sample from the same point. The plant was at the tillering stage at the time of sampling, and after we put it in plastic bags to preserve it. We then immediately took it to the laboratory to take measurements and photos.

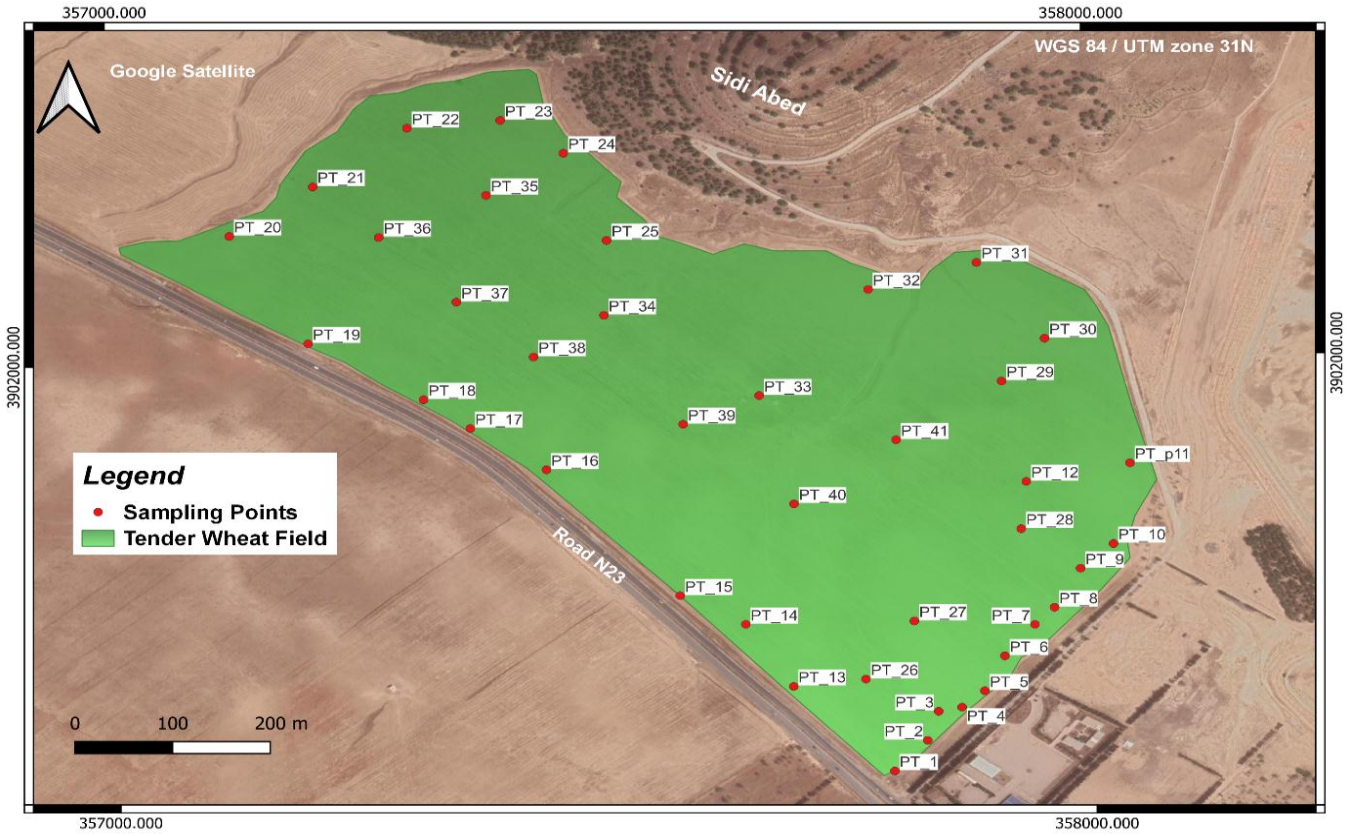

Figure 29: soil and plant sampling points (Tender Wheat)

6.3 Soil sample preparation

6.3.1 Drying

The soil sample is placed in a tray and left to dry overnight in the open air.

6.3.2 Grinding and sieving

The samples were crushed using a pestle and mortar and then passed through a 2mm diameter sieve. The fine soil samples were stored in bags for use in the various soil analyses.

Photo 1: Grinding and sieving of samples **(Cliche Tlidji).**

6.4 Physicochemical analysis

6.4.1 Moisture content

Soil moisture is the most important factor in yield. The first improvement to be made is therefore irrigation or drainage, or sometimes both **(Guet, 2003).**

Soil moisture is an essential factor in the infiltration regime, as suction forces are also a function of soil moisture content **(Musy and Higy, 2004).**

6.4.1.1 Principle

This is the weight loss after drying at 105°C expressed as a percentage (or per thousand) compared to air-dried soil **% (Dari, 2013).**

Photo 2: Weighed and oven-dried soil samples **(Cliche Benouadah).**

6.4.2 Granulometric analysis

This analysis was carried out to understand the texture of the soil in the study area.

6.4.2.1 Principle

The texture of a soil is revealed by its granulometric analysis, the principle of which is based on the sedimentation rate of the particles separated and dispersed by destruction of the organic matter by an attack with hydrogen peroxide. The fractionation of these particles is done by means of the Robinson pipette, which allows the determination of the fine clay and silt fractions. Then, fine and coarse sands are measured by sieving **(Benfardia and Chenine, 2014).**

Photo 3: Granulometric analysis using the Robinson pipette method **(cliche Benouadah).**

6.4.3 pH

Generally, to measure the pH, water is added to the substrate in a given volume ratio, thus defining the pH (H_2O). In practice, KCl or $CaCl_2$ solutions can also be used for the extraction and measurement of pH (KCl) or pH ($CaCl_2$). As exchange reactions take place between the supplied K+ or Ca+ cations and the H+ ions present on the exchange capacity of the substrate, there will be a larger amount of H+ ions in the solution at equilibrium and thus the pH will be lower. The difference between the pH (H_2O) and pH (KCl) values is in the order of 0.5 to unit. It is therefore necessary to follow the pH indication by H_2O or KCl. The knowledge of the pH is interesting for the management of fertilisation and the satisfaction of plant requirements **(Lemaire *&* *al*., 2003).**

6.4.3.1 Principle

The pH of the soil is measured in a soil/solution ratio = 1/2.5. A first measurement is made with demineralized water. The second is carried out with a molar solution of potassium chloride **(Petard, 1993).**

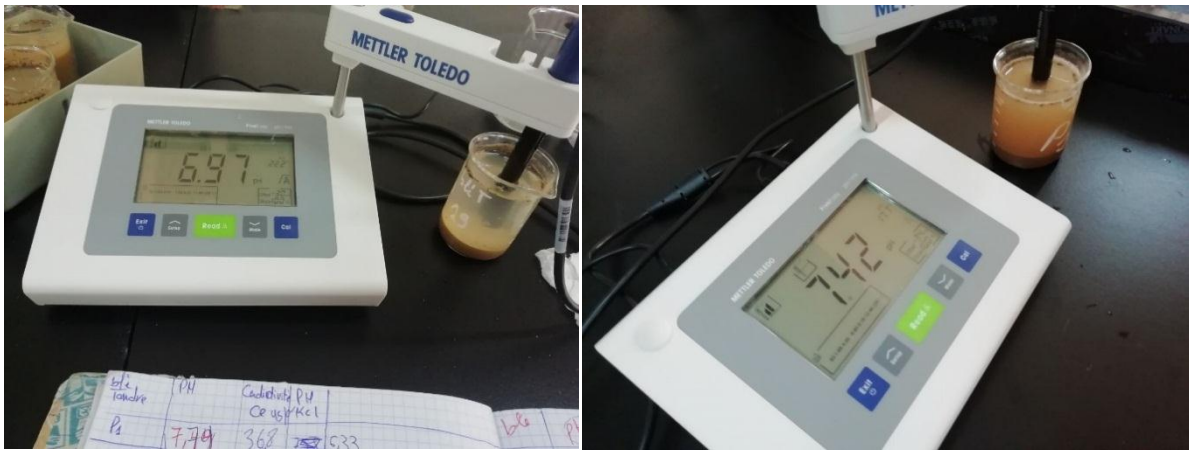

Photo 4: Measuring the pH of a soil sample using a pH meter **(Cliche Benouadah).**

6.4.4 Electrical conductivity

The liquid phase of the soil is a solution containing various ions that give the soil a certain electrical conductivity. It also depends on the minerals and organic constituents that have more insulating properties. Generally speaking, the electrical conductivity of a soil material depends on its composition, structure and water content **(Calvet, 2003).**

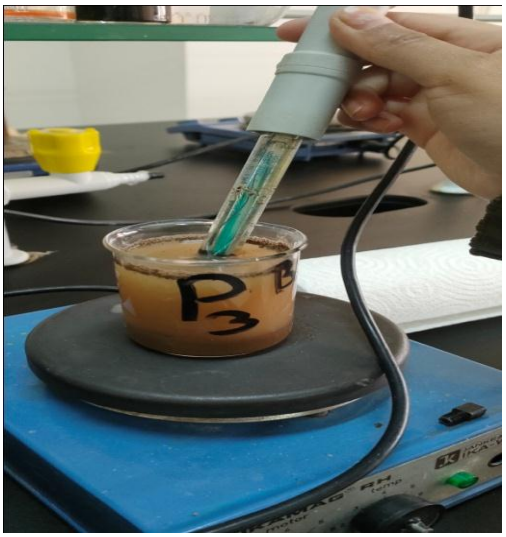

Photo 5: Measurement of soil electrical conductivity using a conductivity meter. **(Cliche Tlidji).**

6.4.4.1 Principle

The determination of soil salinity is based on the principle of extracting an electrolyte and measuring its concentration of dissolved elements. In the laboratory, the electrolyte is extracted under vacuum from a soil sample that has been air-dried, sieved to 2 mm and brought to a given water content, which varies according to the method used to prepare the extract. One of the extraction techniques commonly used is the diluted extract: the ratio between the quantity of soil and the quantity of water can vary according to the laboratories, but it is generally 1/5: the mass of water added is equal to 5 times the mass of soil (10g), i.e. a volume of water of about 50ml **(Montoroi, 1997).**

6.4.5 NPK

6.4.5.1 Principle

The NPK value of soil indicates how much Nitrogen, Phosphorus and potassium are present in your soil or substrate. All plants need these three essential macronutrients. It is important to know the NPK values of the soil or substrates, as you can provide your plants with right amount of external NPK fertilizers according to their needs.

The soil NPK sensor is suitable for detecting the content of nitrogen, phosphorus, and potassium in the soil. It helps in determining the fertility of the soil thereby facilitating the systematic assessment of the soil condition. The sensor can be dipped in the

solution that contain 20g of soil and 100 ml of distilled water after a brief moment the amount of NPK display in the screen (readings mg/kg).

Photo 6: NPK sensors **(cliche Tlidji).**

6.4.6 Total limestone

6.4.6.1 Principle

Limestone is calcium carbonate; it is present in the form of larger or smaller particles; from a purely granulometric point of view these particles are 32

$$CaCo_3 + 2\ HCl = CaCl_2 + H_2O + CO_2$$

similar to other grains of sand, but from a chemical point of view they are different. Indeed, the finest and most porous of them can release calcium which tends to neutralise acids and thus make the soil more basic **(Pousset, 2002).**

Total limestone was determined by the volumetric method using the Bernard Calcimeter. The sample is etched with 37% HCl, the volume of CO_2 released is measured; one mole of CO_2 corresponding to one mole of $CaCo_3$. The CO_2 released is compared to that obtained by the known weight of pure calcium carbonate **(Bedjadj, 2011).**

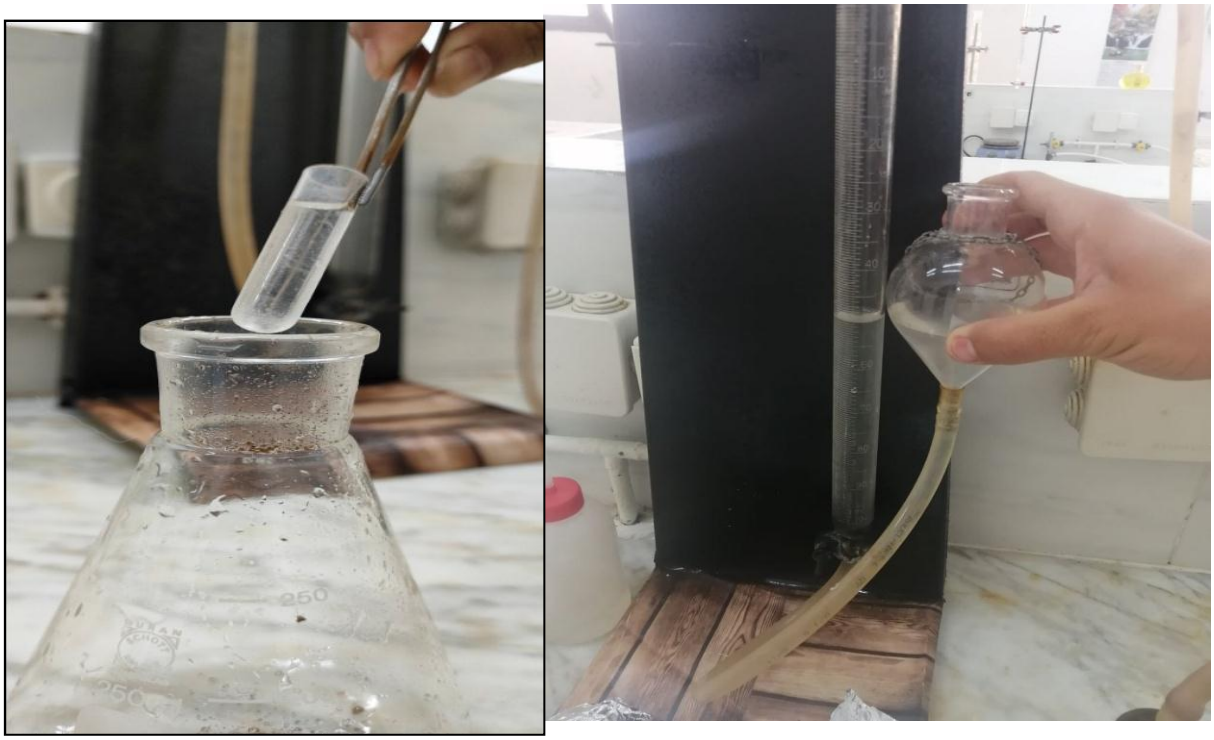

Photo 7: Measurement of total limestone by the Bernard calcimeter **(cliche Benouadah).**

6.4.7 Active limestone:

The fraction of limestone in a soil that can release calcium relatively easily is called active limestone. Note that the link between total limestone and active limestone is not automatic: a soil can be rich in total limestone and relatively poor in active limestone. Excessive active limestone is detrimental to some plants (e.g. fruit trees), but a moderate presence of active limestone improves the strength of the clay-humus complex and thus the stability of the structure **(Pousset, 2002).**

6.4.7.1 Principle

The active $CaCo_3$ (%) is determined by the Drouineau-Gallet method using ammonium oxalate, which combines with the calcium in the easily dissolved limestone (active limestone) to form insoluble calcium oxalates. The excess ammonium oxalate is then measured with a potassium permanganate solution in sulphuric medium **(Benseghir, 2006).**

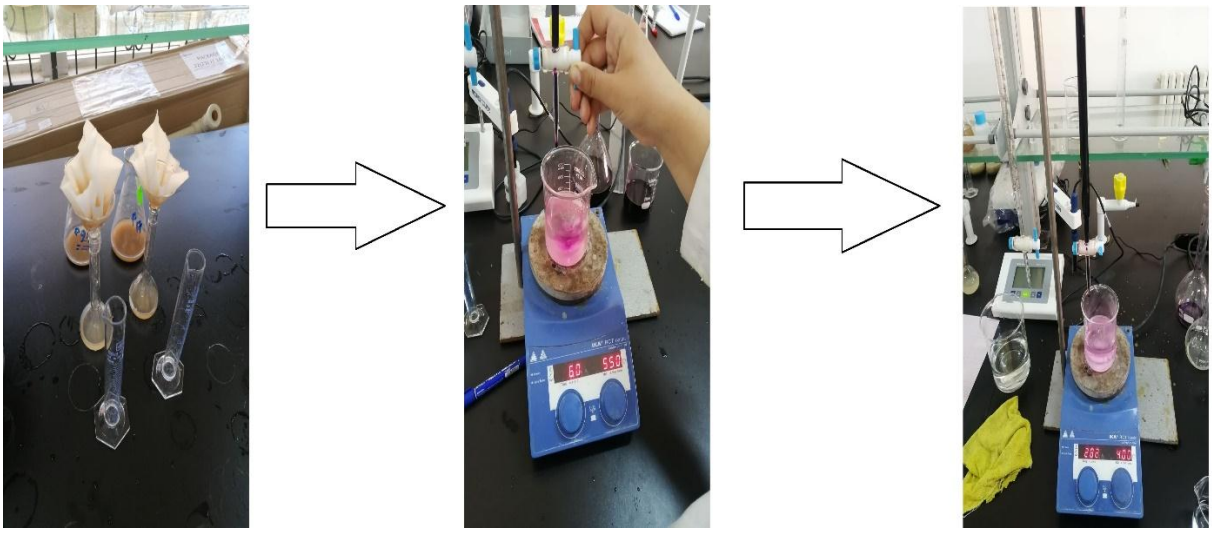

Photo 8: Dosing of active limestone **(cliche Tlidji).**

6.5 Experimental protocol

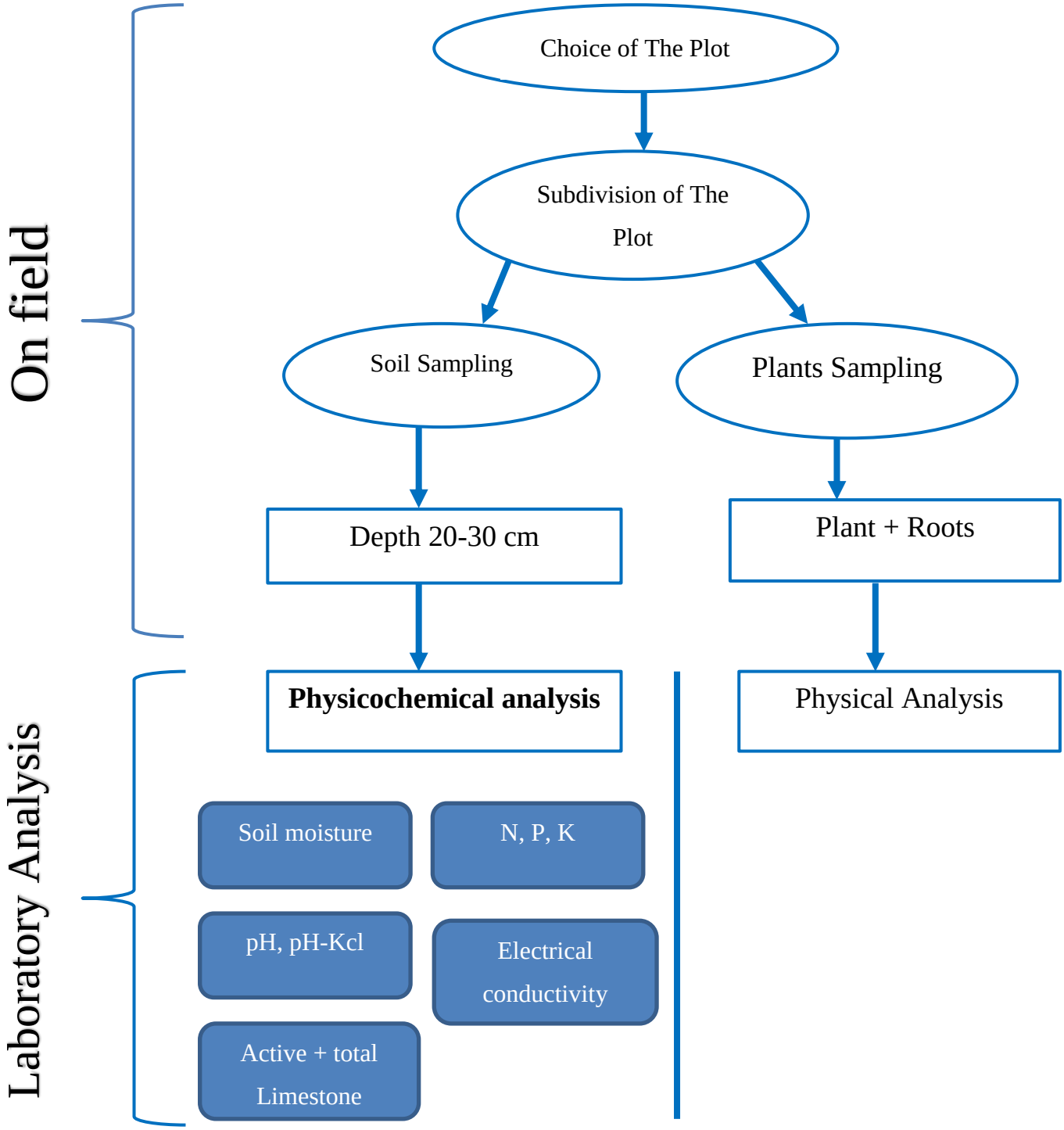

Figure 30: experimental Protocol Flow-chart

6.6 Satellite images

6.6.1 Landsat 8

Landsat 8 launched on February 11, 2013, from Vandenberg Air Force Base, California, on an Atlas-V 401 rocket, with the extended payload fairing (EPF) from United Launch Alliance, LLC. The Landsat 8 satellite payload consists of two science instruments, the Operational Land Imager (OLI) and the Thermal Infrared Sensor (TIRS). These two sensors provide seasonal coverage of the global landmass at a spatial resolution of 30 meters (visible, NIR, SWIR); 100 meters (thermal); and 15 meters (panchromatic). Landsat 8 was developed as a collaboration between NASA and the U.S. Geological Survey (USGS). NASA led the design, construction, launch, and on-orbit calibration phases, during which time the satellite was called the Landsat Data Continuity Mission (LDCM). On May 30, 2013, USGS took over routine operations and the satellite became Landsat 8. USGS leads post-launch calibration activities, satellite operations, data product generation, and data archiving at the Earth Resources Observation and Science (EROS) center. (NASA Landsat8).

6.6.1.1 Landsat 8 Instruments

Landsat 8 carries two sensors. The Operational Land Imager sensor is built by Ball Aerospace & Technologies Corporation. The Thermale Infrared Sensor is built by NASA Goddard Space Flight Center. **(USGS Landsat Missions).**

6.6.1.2 Operational Land Imager (OLI)

- **Nine spectral bands, including a pan band**
    - Band 1 Coastal Aerosol (0.43 - 0.45 µm) 30 m
    - Band 2 Blue (0.450 - 0.51 µm) 30 m
    - Band 3 Green (0.53 - 0.59 µm) 30 m
    - Band 4 Red (0.64 - 0.67 µm) 30 m
    - Band 5 Near-Infrared (0.85 - 0.88 µm) 30 m
    - Band 6 SWIR 1(1.57 - 1.65 µm) 30 m
    - Band 7 SWIR 2 (2.11 - 2.29 µm) 30 m
    - Band 8 Panchromatic (PAN) (0.50 - 0.68 µm) 15 m
    - Band 9 Cirrus (1.36 - 1.38 µm) 30 m

OLI captures data with improved radiometric precision over a 12-bit dynamic range, which improves overall signal to noise ratio. This translates into 4096 potential grey levels,

compared with only 256 grey levels in Landsat 1-7 8-bit instruments. Improved signal to noise performance enables improved characterization of land cover state and condition. **(USGS Landsat Missions).**

The 12-bit data are scaled to 16-bit integers and delivered in the Level-1 data products. Products are scaled to 55,000 grey levels, and can be rescaled to the Top of Atmosphere (TOA) reflectance and/or radiance using radiometric rescaling coefficients provided in the product metadata file (MTL file). **(USGS Landsat Missions).**

6.6.1.3 Thermal Infrared Sensor (TIRS)

- **Two spectral bands:**
    - Band 10 TIRS 1 (10.6 - 11.19 µm) 100 m
    - Band 11 TIRS 2 (11.5 - 12.51 µm) 100 m **(USGS Landsat Missions)**

6.7 Data processing

We used an analysis and processing platform developed by Google for the cloud-based geo-spatial remote sensing domain, called Google Earth Engine (GEE).

6.7.1 Google earth engine

Google Earth Engine is a cloud-based geospatial analysis platform that allows users to view and analyze satellite images of our planet. Scientists and nonprofits use Google Earth Engine for remote sensing research, epidemic prediction, natural resource management, and other activities.

Google Earth Engine brings together more than 40 years of old and current satellite images, together with the tools and computing power needed to analyze and exploit this huge data warehouse. This planetary-scale platform is dedicated to the analysis of environmental data.

Earth Engine is a public data catalog, computing infrastructure, geospatial APIs, and interactive application server. It is an extremely valuable tool for students who wish to deepen their knowledge through the availability of Earth Engine's public data archives, which include historical images and scientific datasets, updated and enriched daily in three areas :

- Climate and weather: Surface temperature, Climate, Atmospheric and Time.
- Imagery: Landsat, Sentinelle, MODIS and high resolution imagery.
- Geophysics: Terrain, Land Cover, Cropland and Other Geophysical Data including nighttime images from the Defense Weather Satellite Program Operational Line Scan System (DMSP-OLS) **(web master 4)**

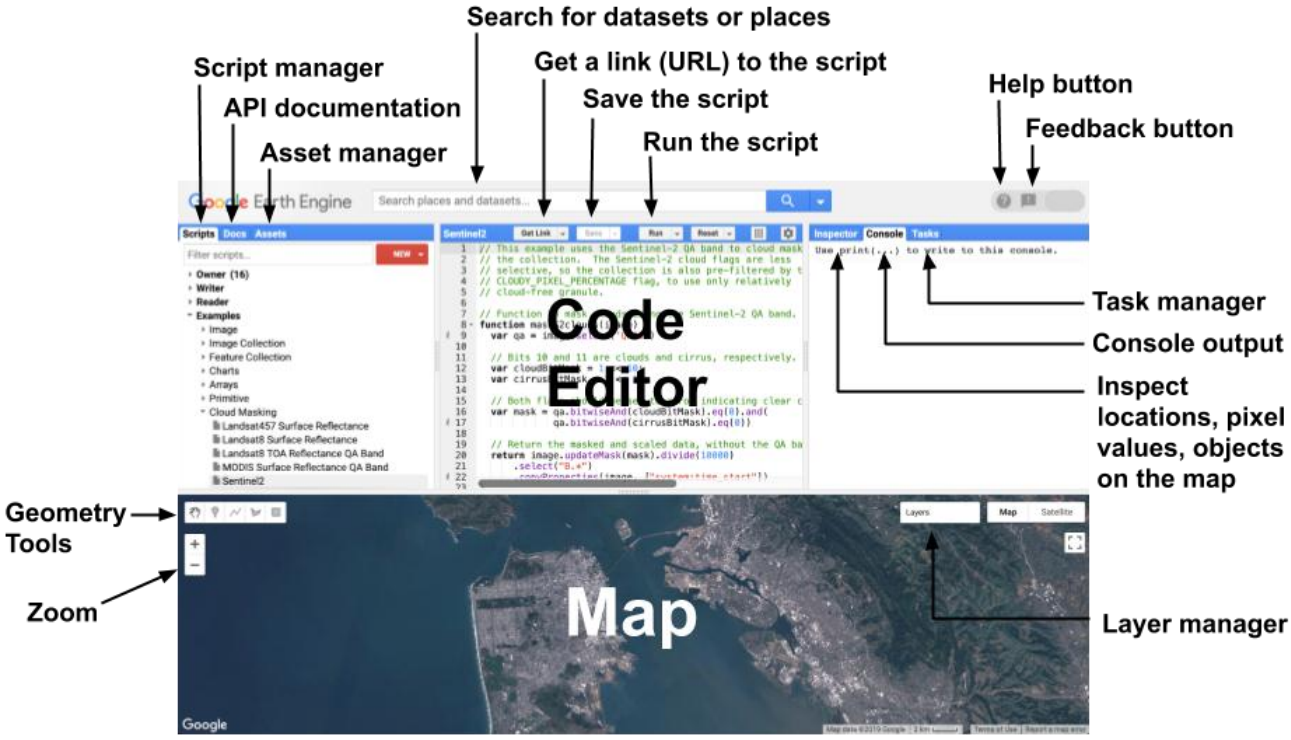

Figure 31: Google Earth Engine interface **source: (web master 4)**

6.7.2 Surface Energy Balance Algorithm for Land (SEBAL) model

Numerous models have been developed to estimate evapotranspiration using remote sensing methods. Out of all the proposed models for estimating evapotranspiration **(Allen, Tasumi, and Trezza Citation 2007),** the Surface Energy Balance Algorithm for Land (SEBAL) model has proven to be the most widely used amongst researchers in over 30 countries. This model was developed by Bastiaanssen and improved by Allen **(Bastiaanssen *& al.*, Citation1998).**

6.7.2.1 Overview how SEBAL computes evapotranspiration (ET)

In the SEBAL model, ET is computed from satellite images and weather data using the surface energy balance as illustrated in Figure 1. Since the satellite image provides information for the overpass time only, SEBAL computes an instantaneous ET flux for the image time. The ET flux is calculated for each pixel of the image as a "residual" of the surface energy budget equation:

$$\lambda ET = Rn - G - H \qquad (1)$$

Where: λET is the latent heat flux (W/m2), Rn is the net radiation flux at the surface (W/m2), G is the soil heat flux (W/m2), and H is the sensible heat flux to the air (W/m2). **(Ralf Waters *& al.*, 2002).**

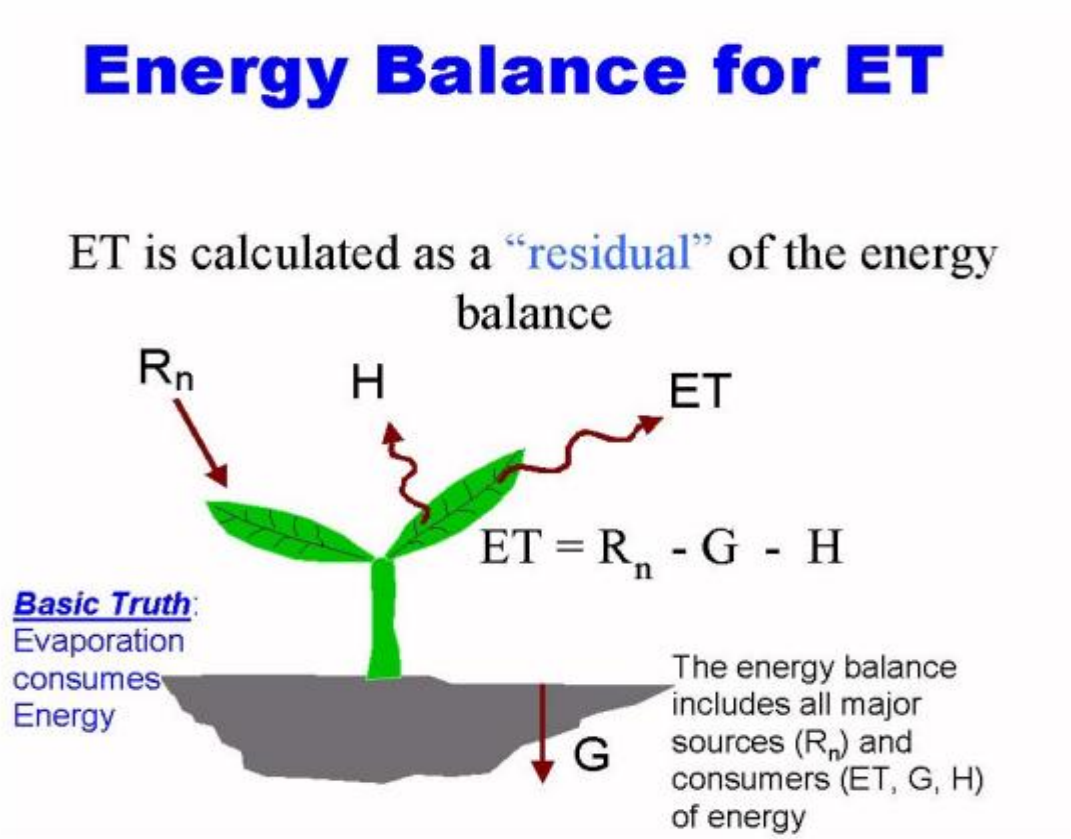

Figure 32: Surface Energy Balance. Source: **(Ralf Waters *& al.*, 2002).**

The net radiation flux at the surface (Rn) represents the actual radiant energy available at the surface. It is computed by subtracting all outgoing radiant fluxes from all incoming radiant fluxes (Figure 2). This is given in the surface radiation balance equation:

$$Rn = RS\downarrow - \alpha\, RS\downarrow + RL\downarrow - RL\uparrow - (1-\varepsilon o)RL\downarrow \qquad (2)$$

where; RS↓ is the incoming shortwave radiation (W/m2), α is the surface albedo (dimensionless), RL↓ is the incoming longwave radiation (W/m2), RL↑ is the outgoing longwave radiation (W/m2), and εo is the surface thermal emissivity (dimensionless) **(Ralf Waters *& al.*, 2002).**

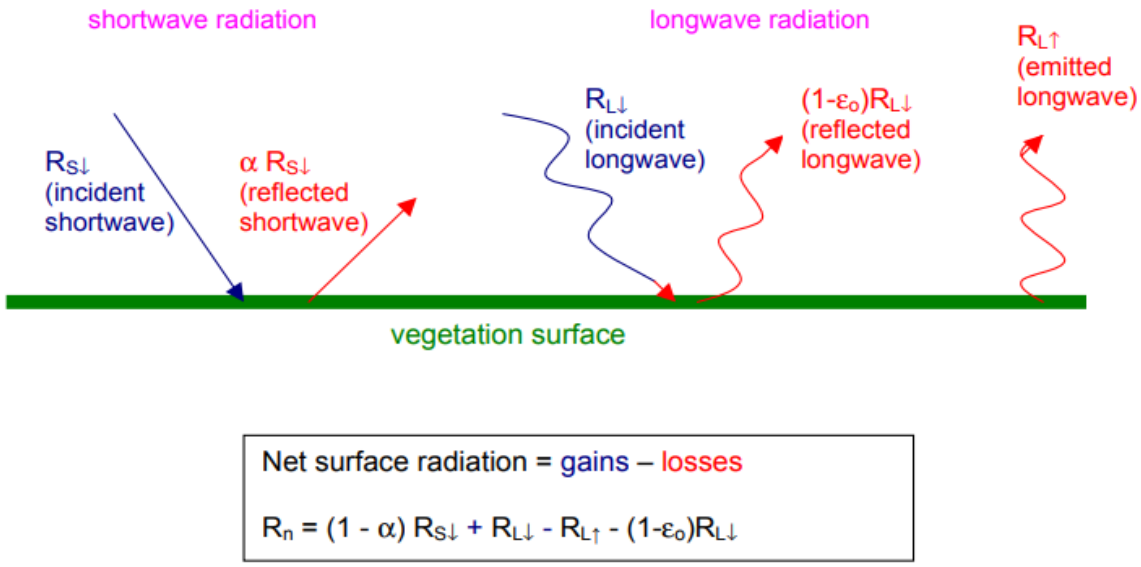

Figure 33: Surface Radiation Balance. Source: **(Ralf Waters *&* *al*., 2002).**

In Equation (2), the amount of shortwave radiation (RS↓) that remains available at the surface is a function of the surface albedo (α). Surface albedo is a reflection coefficient defined as the ratio of the reflected radiant flux to the incident radiant flux over the solar spectrum. It is calculated using satellite image information on spectral radiance for each satellite band. The incoming shortwave radiation (RS↓) is computed using the solar constant, the solar incidence angle, a relative earth-sun distance, and a computed atmospheric transmissivity. The incoming longwave radiation (RL↓) is computed using a modified Stefan-Boltzmann equation with atmospheric transmissivity and a selected surface reference temperature. Outgoing longwave radiation (RL↑) is computed using the Stefan-Boltzmann equation with a calculated surface emissivity and surface temperature. Surface temperatures are computed from satellite image information on thermal radiance. **(Ralf Waters *&* *al*., 2002).**

The surface emissivity is the ratio of the actual radiation emitted by a surface to that emitted by a black body at the same surface temperature. In SEBAL, emissivity is computed as a function of a vegetation index. The final term in Equation (2), (1-εo) RL↓, represents the fraction of incoming longwave radiation that is lost from the surface due to reflection. In Equation (1), the soil heat flux (G) and sensible heat flux (H) are subtracted from the net radiation flux at the surface (Rn) to compute the "residual" energy available for evapotranspiration (λET). Soil heat flux is empirically calculated using vegetation indices, surface temperature, and surface albedo. Sensible heat flux is computed using wind speed

observations, estimated surface roughness, and surface to air temperature differences. SEBAL uses an iterative process to correct for atmospheric instability due to the buoyancy effects of surface heating. Once the latent heat flux (λET) is computed for each pixel, an equivalent amount of instantaneous ET (mm/hr) is readily calculated by dividing by the latent heat of vaporization (λ). These values are then extrapolated using a ratio of ET to reference crop ET to obtain daily or seasonal levels of ET. Reference crop ET, termed ETr, is the ET rate expected from a well-defined surface of full-cover alfalfa or clipped grass and is computed in the SEBAL process using ground weather data. SEBAL can compute ET for flat, agricultural areas with the most accuracy and confidence. **(Ralf Waters *&* *al.*, 2002).** The flowchart of the SEBAL algorithm is illustrated in **Figure 34**

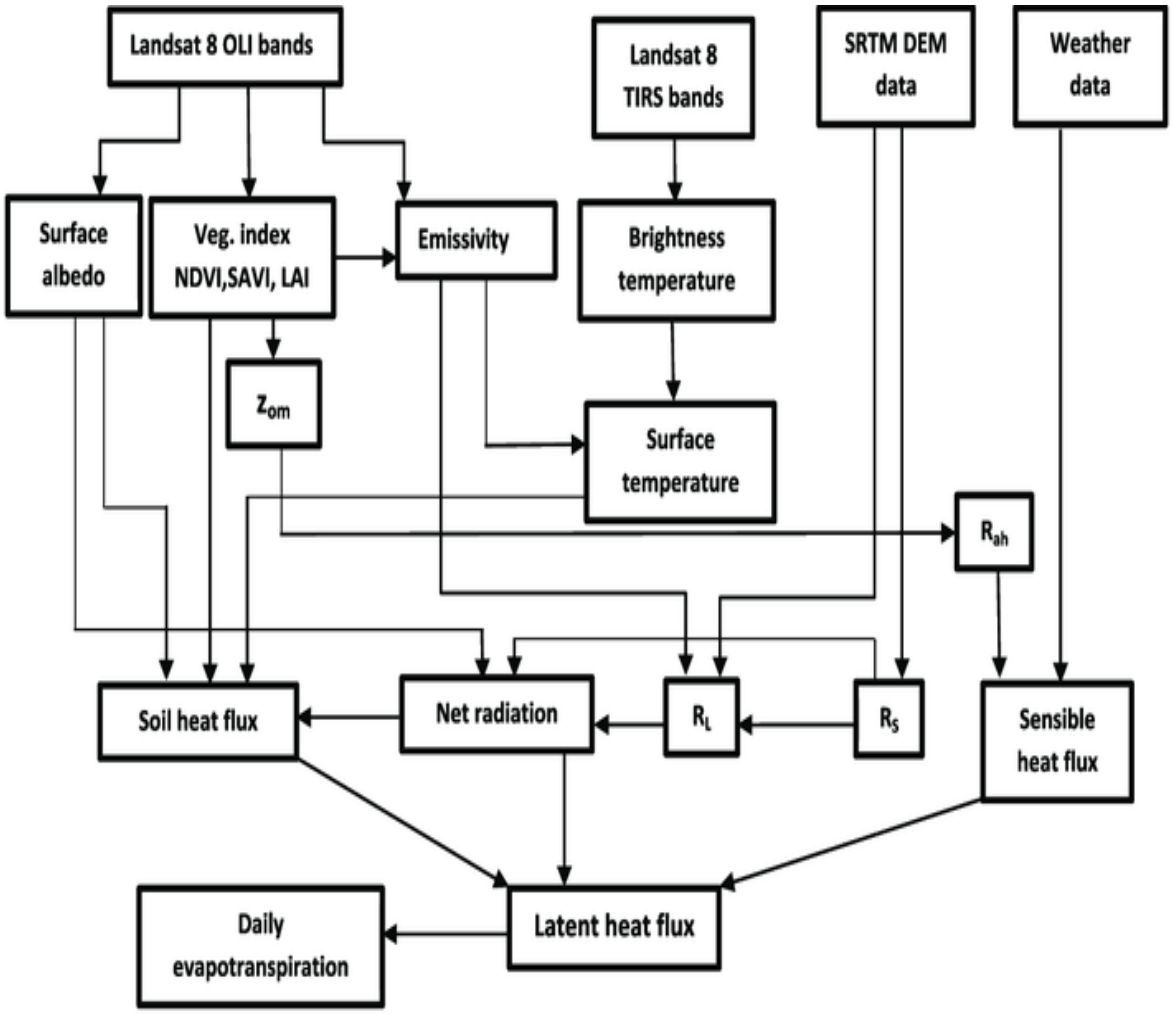

Figure 34: Flow-chart illustration for the SEBAL algorithm **(H.E.-D. Fawzy *&* *al.*, 2020)**

Chapter VII: Results and discussion

Throughout our research, we identified that the tender wheat plot predominantly consists of sandy-loam soil. Sandy-loam soil is a well-draining soil type that retains less water compared to clay soils but more water than sandy soils. It is characterized by a balanced composition of sand, silt, and clay particles, offering good aeration and nutrient retention properties. The soil's texture and structure play a significant role in determining the water-holding capacity and availability for plant uptake, which directly influences the water irrigation requirements for crops, including wheat.

7.1 Moisture

Water plays an essential role in all the physical and chemical phenomena that occur in the soil. It can compete with organic molecules for adsorption onto solid materials, leading to a drop-in pollutant adsorption when soil moisture levels increase **(Sayyad, G *&* *al.*, 2010).**

The soil moisture was calculated using this formula:

[[(The weight of empty capsule) + (the weight of soil)] - (the weight after24h)]/10] * 100

Table 6: Soil moisture values.

Value	%
Minimum value	**4.74**
Maximum value	**39.94**
Mean value	**14.32**

As mentioned in **Table 6,** the moisture content of the soil samples varied between 4.75% and 39.90%. It is necessary to take into consideration that In the region, there had been some rainfall prior to the sampling day. These values is highly dependent on the climatic conditions at the time of sampling in the spring, when not all the water had infiltrated, and on the lack of rainfall.

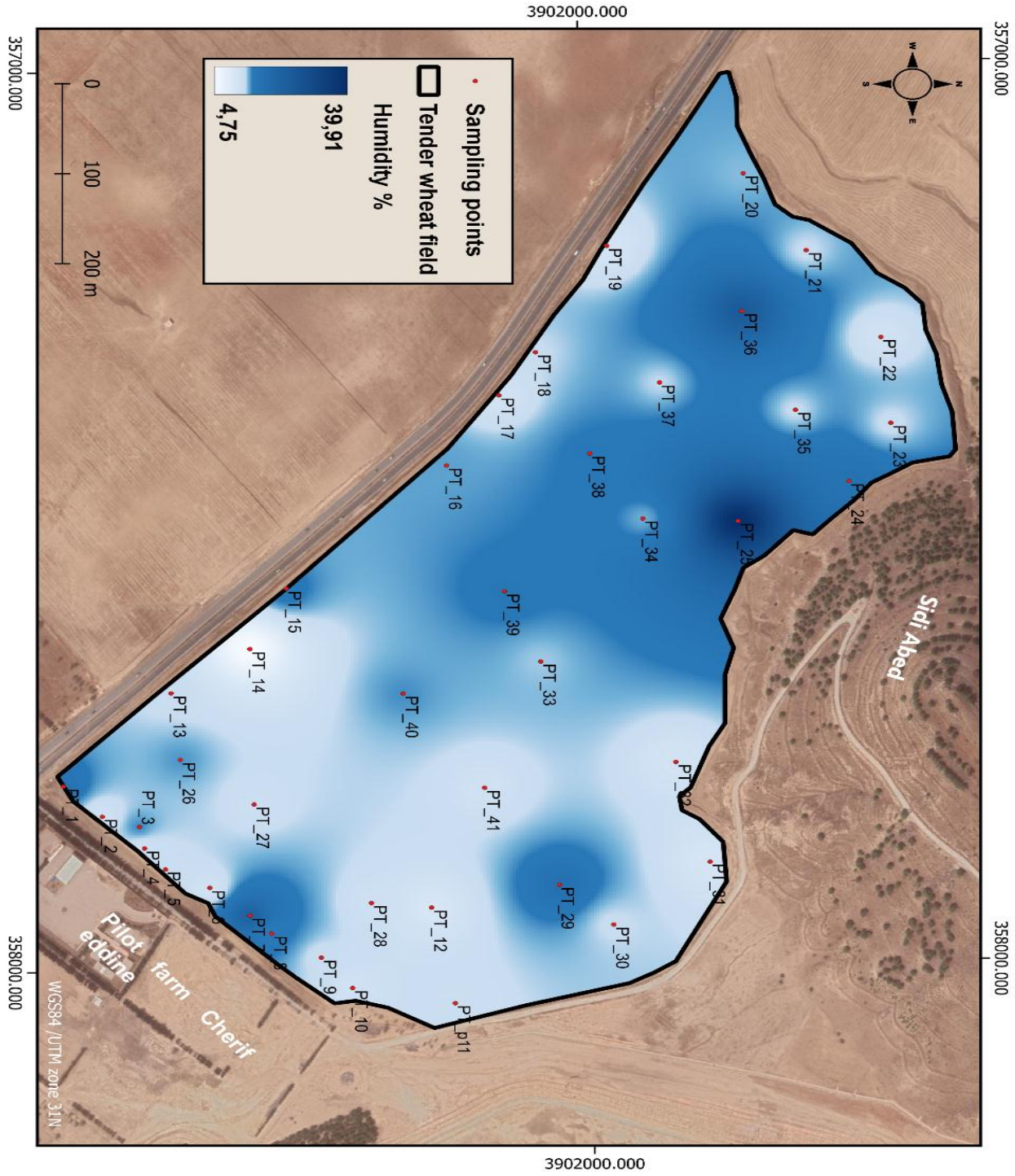

Figure 35: soil moisture map.

Approximately 24.39% of the samples (10 out of 41) have moisture levels above 15%. This samples are located in the northern area of the plot (field) **(figure 35)** near Sidi-abed forest

that provides a vegetation cover that causes these high levels of soil humidity.as we move south of the plot and due the arid climate that this area had and the lack in the precipitations. Around 75.60% of the samples (31 out of 41) exhibit moisture levels between 4.75% and 14% which considered as below optimal levels and these areas may have relatively low soil moisture content, indicating a potential risk of underdevelopment and insufficient water availability for plant growth as showed in **(figure 36).**

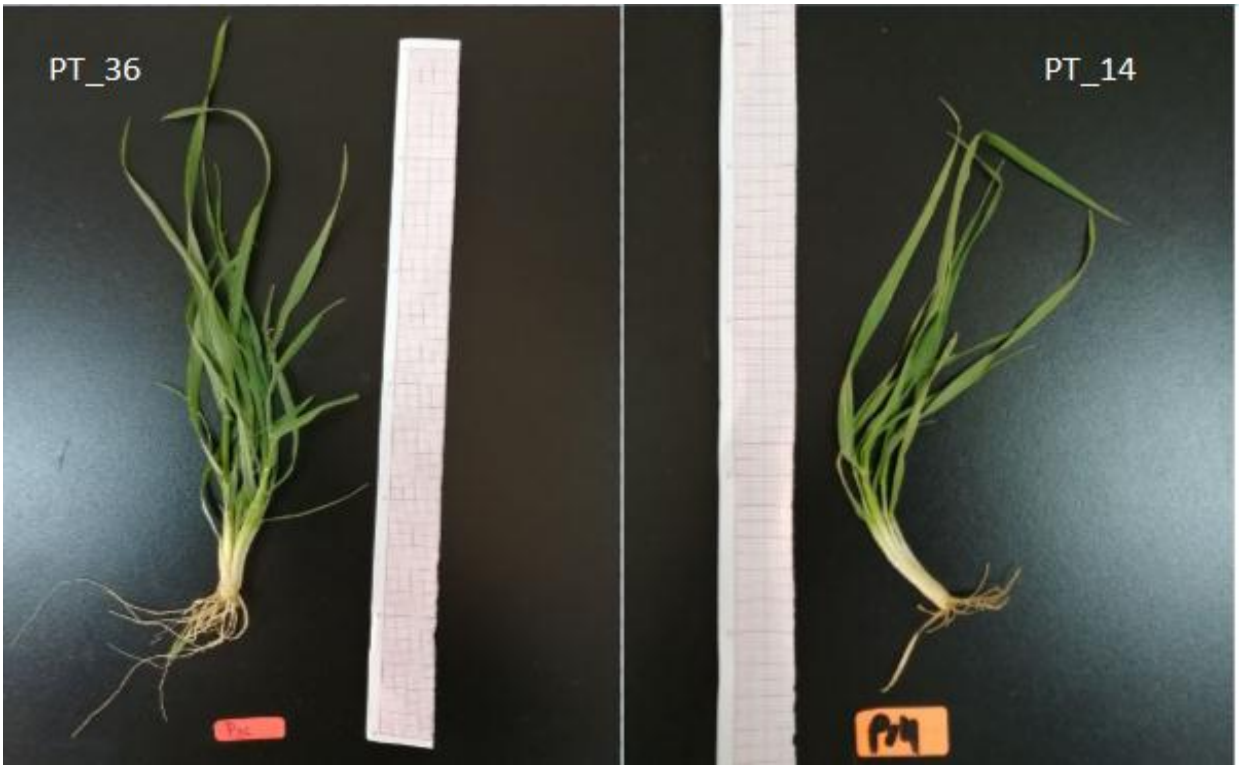

Figure 36: comparison between a plant sample from the highest moisture part (left) and the lowest moisture part (right) of the plot.

7.2 pH

pH is one of the most important physico-chemical characteristics of soils, as the speciation, mobility and availability of trace metals are linked to the pH value **(Hlavackova, P *& al.*, 2005).**

Measuring the pH (hydrogen potential) of a soil enables us to determine its acidity or alkalinity (or acid-base status). In our study soil have pH values between 7.12 and 8.37.

Table 7: pH levels of the tender wheat plot.

Minimum value	**7.12**
Maximum value	**8.37**
Mean value	**7.80**

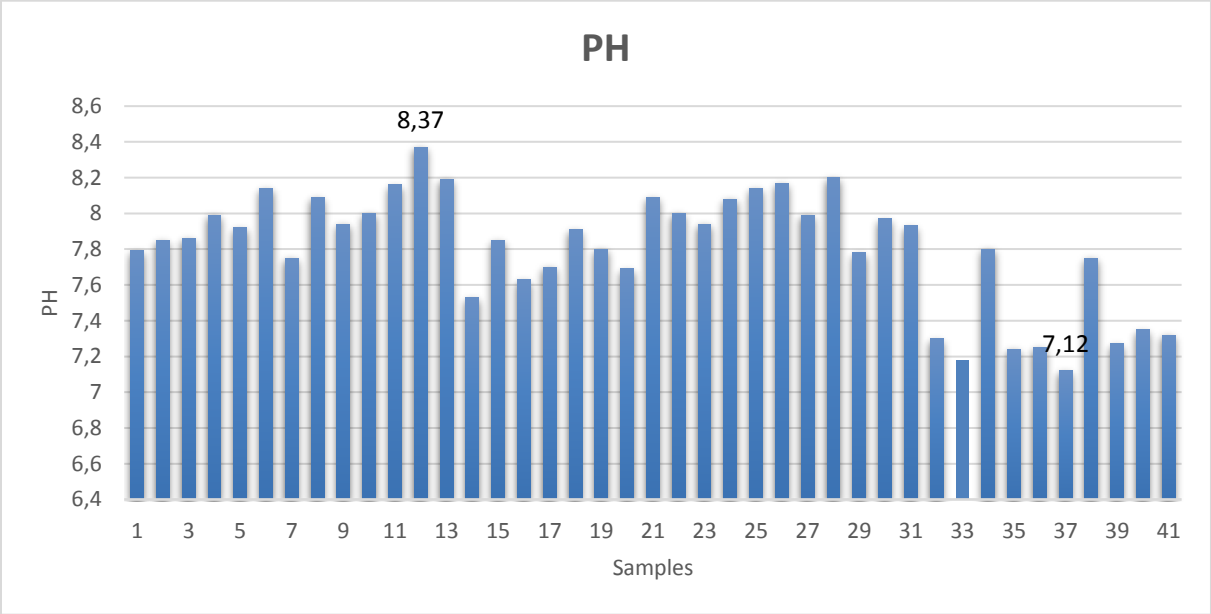

Figure 37: detailed values of the pH levels.

From the pH values recorded in **(figure 37)**, it can be seen that these values range from 7.12 to 8.37. According to Acid-base status of soils provided by FAO **(Table 8)**. The soil has a low alkaline pH, which can be attributed to the presence of carbonates.

Table 8: Acid-base status of soils according to the UNDP/FAO project.

PH	4	4.5	5	5.5	6	6.5	7	7.5	8	8.5
Degree	**Very Acidic**	**Acidic**		**Slightly Acidic**		**Neutral**		**Low Alkaline**		**Alkaline**

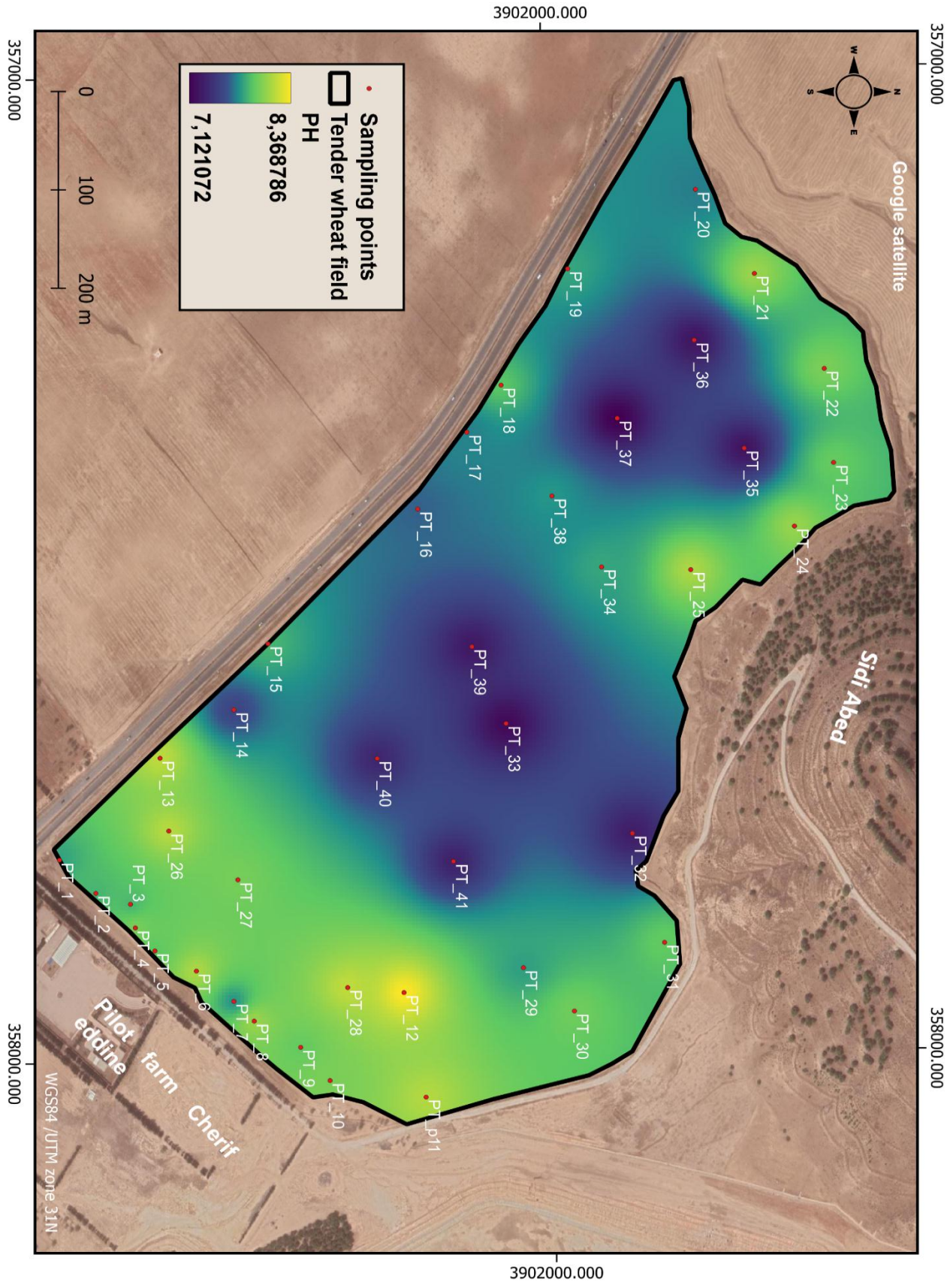

Figure 38: pH map.

None of the samples have a pH below 6.5, indicating that there are no acidic soil conditions among the provided samples. According to the map **(Figure 38)** 39.02% of the samples (16 out of 41) have ph value in the range of 7.3 these samples are located in the middle of the plot (field).As we move south of the plot the levels of ph starts to increase. the southern area have a ph values in the range of 8 as for the northern area of the field it strangely have a high levels of ph. this variation in the ph level is due to the nature of soil and the field topography and the flatness of the terrain.

7.3 pH KCl and the reserve acidity of the soil

The pH KCl represents the reserve acidity of the soil. It reports its maximum acidification limit: the lower it is, the more acidic the soil will tend to become, and the greater the need to be vigilant and make regular inputs of basic amendments.

It is measured by immersing the soil sample in a potassium chloride solution: the potassium then takes the place of the aluminum and hydrogen ions on the clay-humic complex. In a second step, the hydrogen ion concentration is evaluated to obtain the pH KCl.

As shown in **(Figure 39)** the levels of PH-kcl that range between a Minimum value of **6.06** and Maximum value of **7.49** are in the interval of optimal zone according to the scale in **(figure 40).**

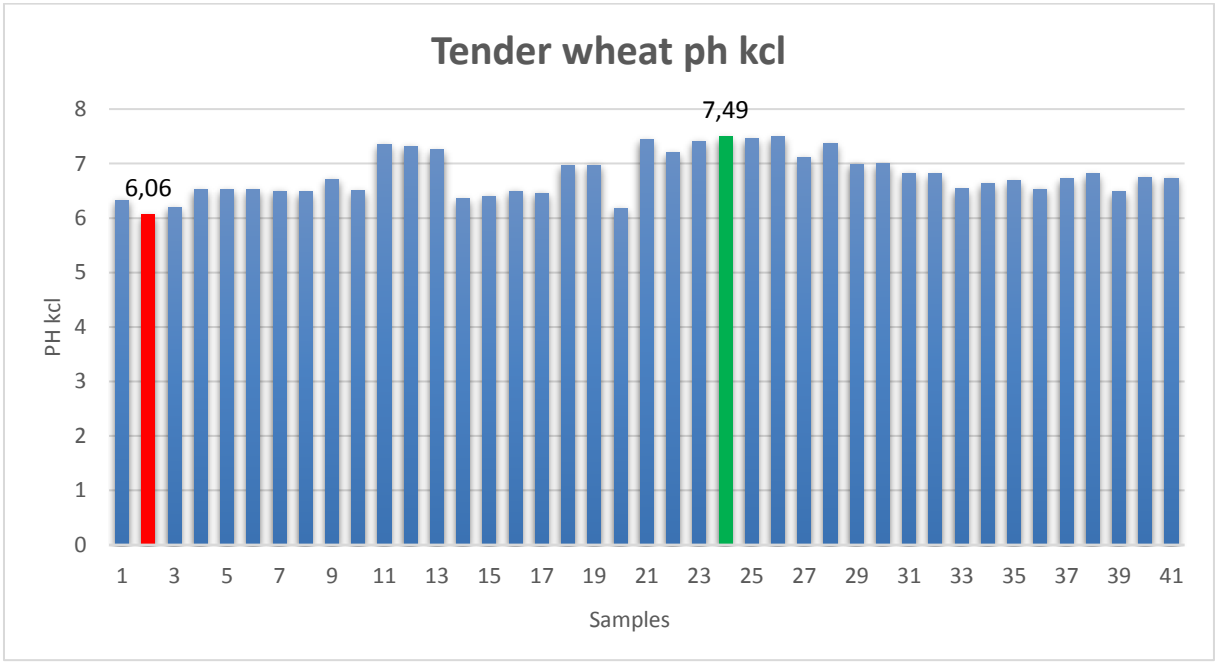

Figure 39: pH-Kcl values

Figure 40: ph-Kcl optimum values **source : web master 5**

7.4 Electrical conductivity

The electrical conductivity of soils determines their degree of salinity. This salinity is reflected in the different behavior of crops in relation to salinity classes. The Durand J.H. scale) **(table 8)** was used to indicate the salinity class of soils.

Referring to the classification of **Durand J.H.**, we have in Tender wheat soils, horizons that are not saline as a result of their low EC values, which are less than 500µS/cm. On these soils, salinity is negligible and will have no effect on crop yields.

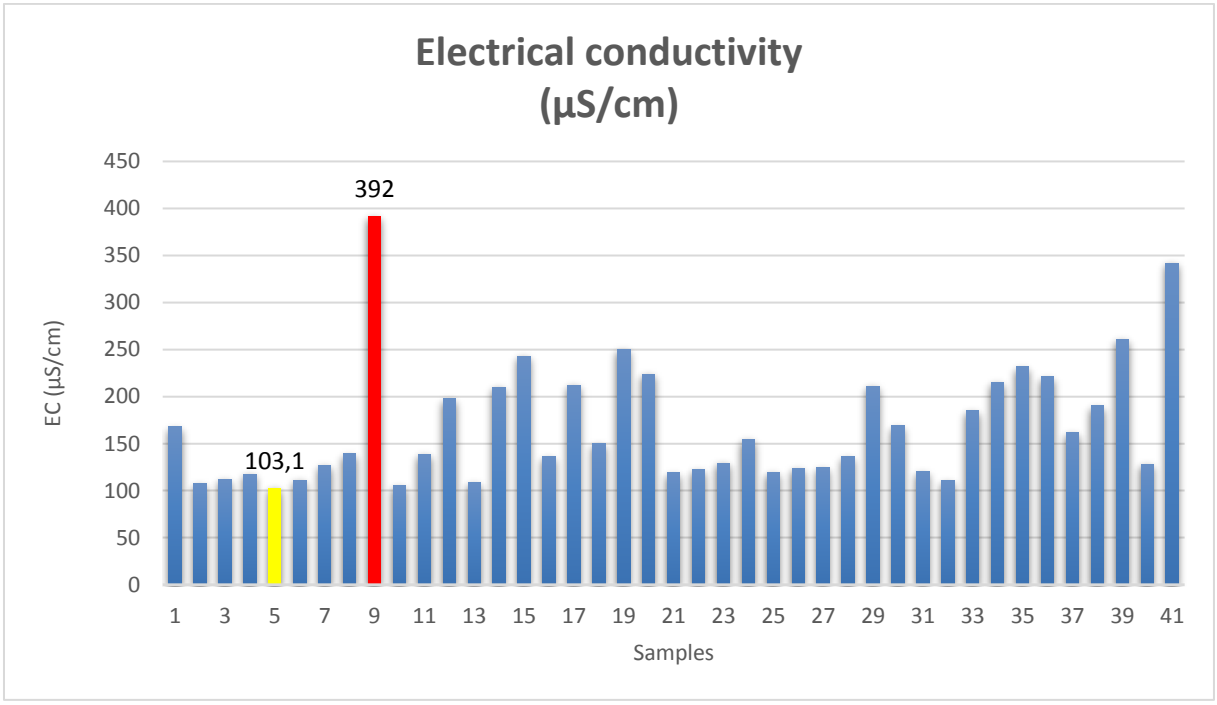

Figure 41: EC values

Table 8: EC values affect on yields **(DURAND J.H., 1983)**

Class	CE at 25 °C (µm/cm)	Soil quality	Effect on yield
Class 1	**0 to 500**	**non-saline**	**Negligible**
Class 2	**500 to 1000**	**slightly saline**	**significant decrease in yield of salt-sensitive crops**
Class 3	**1000 to 2000**	**Saline**	**Reduced yields for most corps**
Class 4	**2000 to 4000**	**highly saline**	**only resistant crops provide satisfactory yield**
Class 5	**More than 4000**	**extremely saline**	**only a few crops give a satisfactory yield**

7.5 NPK

The results were converted from (mg/kg) to (kg/ha) using this formula:

- Volume of soil layer is 10000*0.3=3000 m3
- Soil depth is 30cm (0.3m)
- Mass of soil layer is 3000m3*1.2 t/m3=3600 t or 3600000 kg
- 1.2t/m3 is the bulk density

Than we can convert by multiplication of the NPK (mg/kg) content by 3600000 giving us the content of NPK (kg/ha).

7.5.1 Phosphorus (P)

Phosphorus (P): Phosphorus is one of the macro-nutrients essential for good crop growth. It promotes root development, flowering, and grain formation. The recommended application rate of phosphorus fertilizer for tender wheat ranges from 40 to 60 kg/ha.

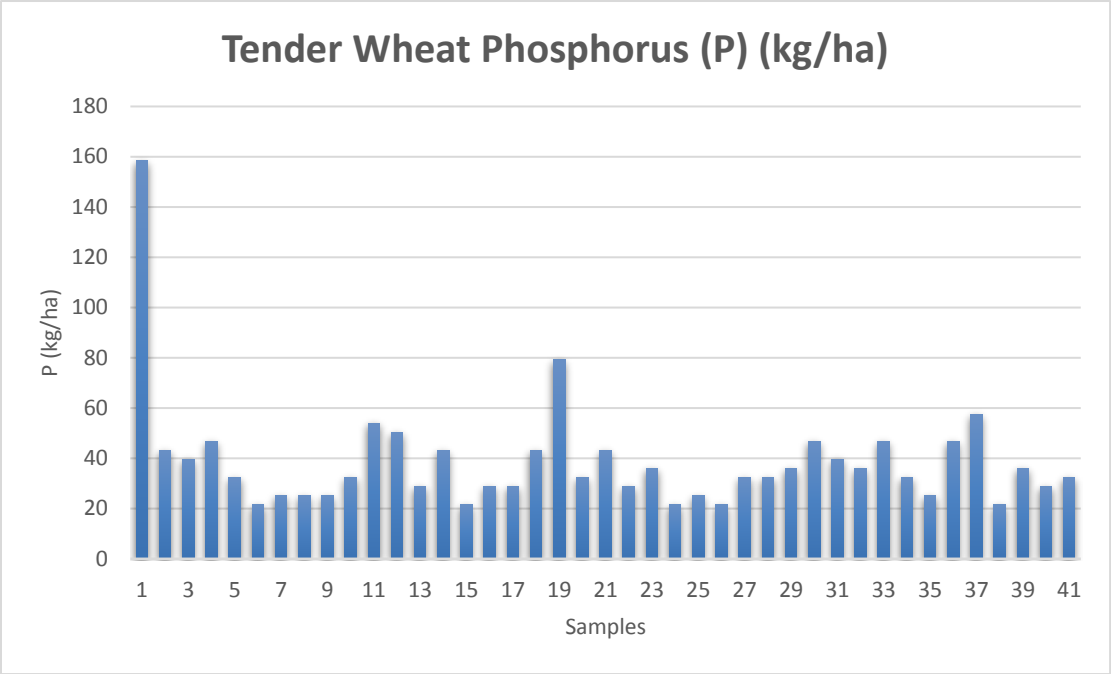

Figure 42: phosphorus values

Approximately 36.6% of the samples (15 out of 41) have phosphate levels around 40 kg/ha. These areas are located in the west zone of and the far east of the plot (field). They fall within the optimal nutrient range and have relatively average phosphate levels. Where the rest of the plot 63.4% of the samples (26 out of 41) represent a remarkable shortage in the phosphate levels less than 36 kg/ha focused in the middle area which represent a low nutrient levels and require additional phosphate supplementation to meet the optimal nutrient requirements for tender wheat growth.

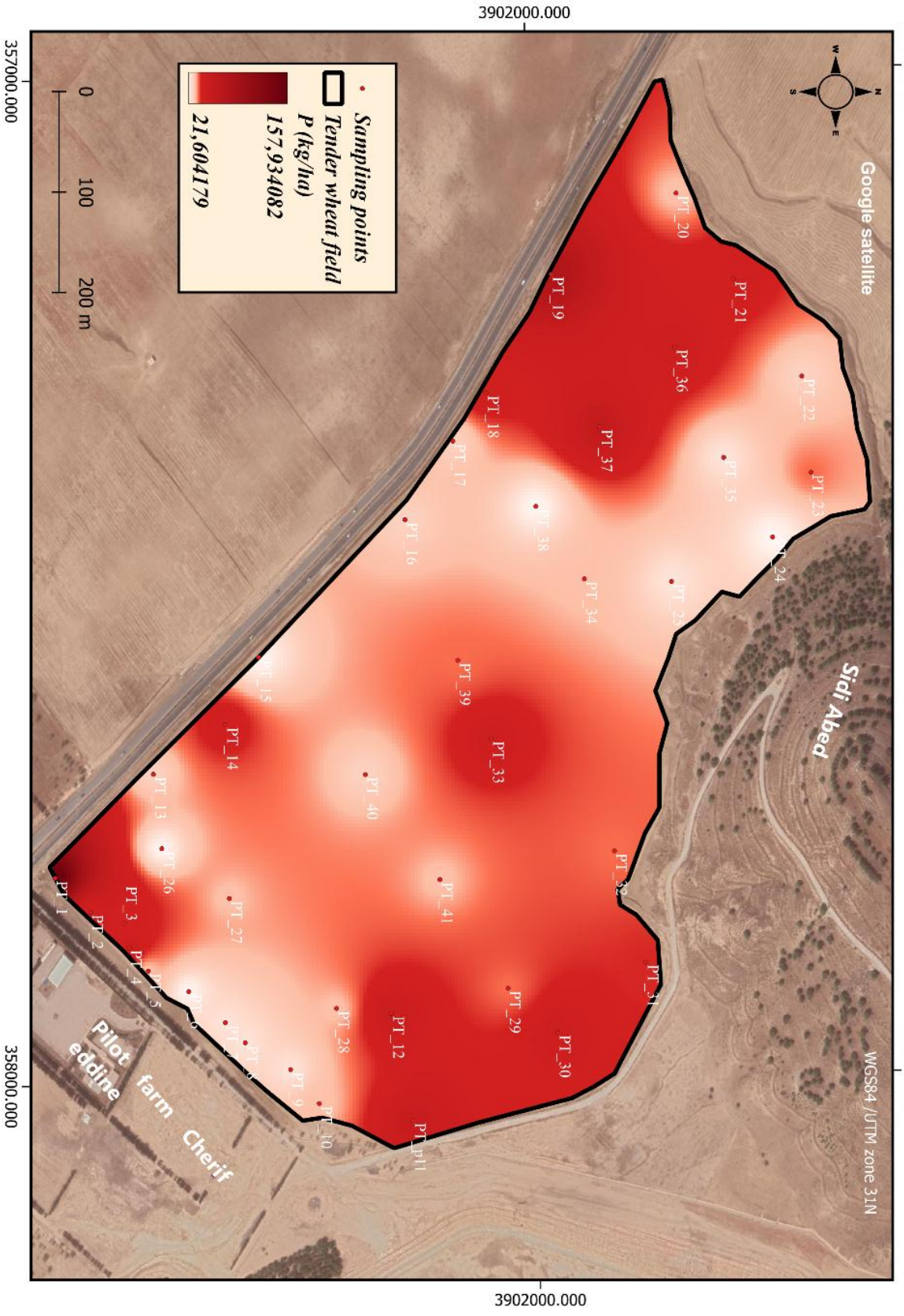

Figure 43: Phosphorus map

7.5.2 Nitrogen (N)

Nitrogen (N): Nitrogen is essential for wheat growth and is often the most critical nutrient. The recommended application rate of nitrogen fertilizer for tender wheat typically ranges from 80 to 120 kg/ha.

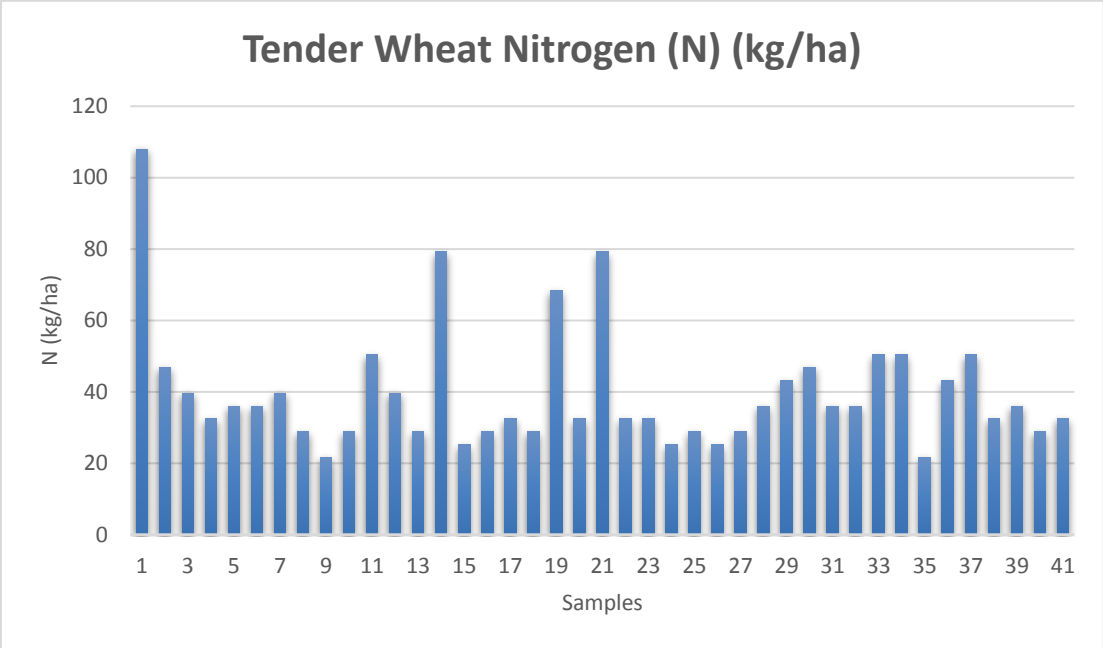

Figure 44: Nitrogen values

About 29.26% of the samples (12 out of 41) have azote levels in the optimal range higher than 40 kg/ha. Most of this samples are located in the west area of the plot (field). As for the rest of the samples (29 out of 41) exhibit, a low azote levels less than 40 kg/ha which indicate a lack in nitrogen (azote) supplementation. The distribution of these samples is scattered in the plot.

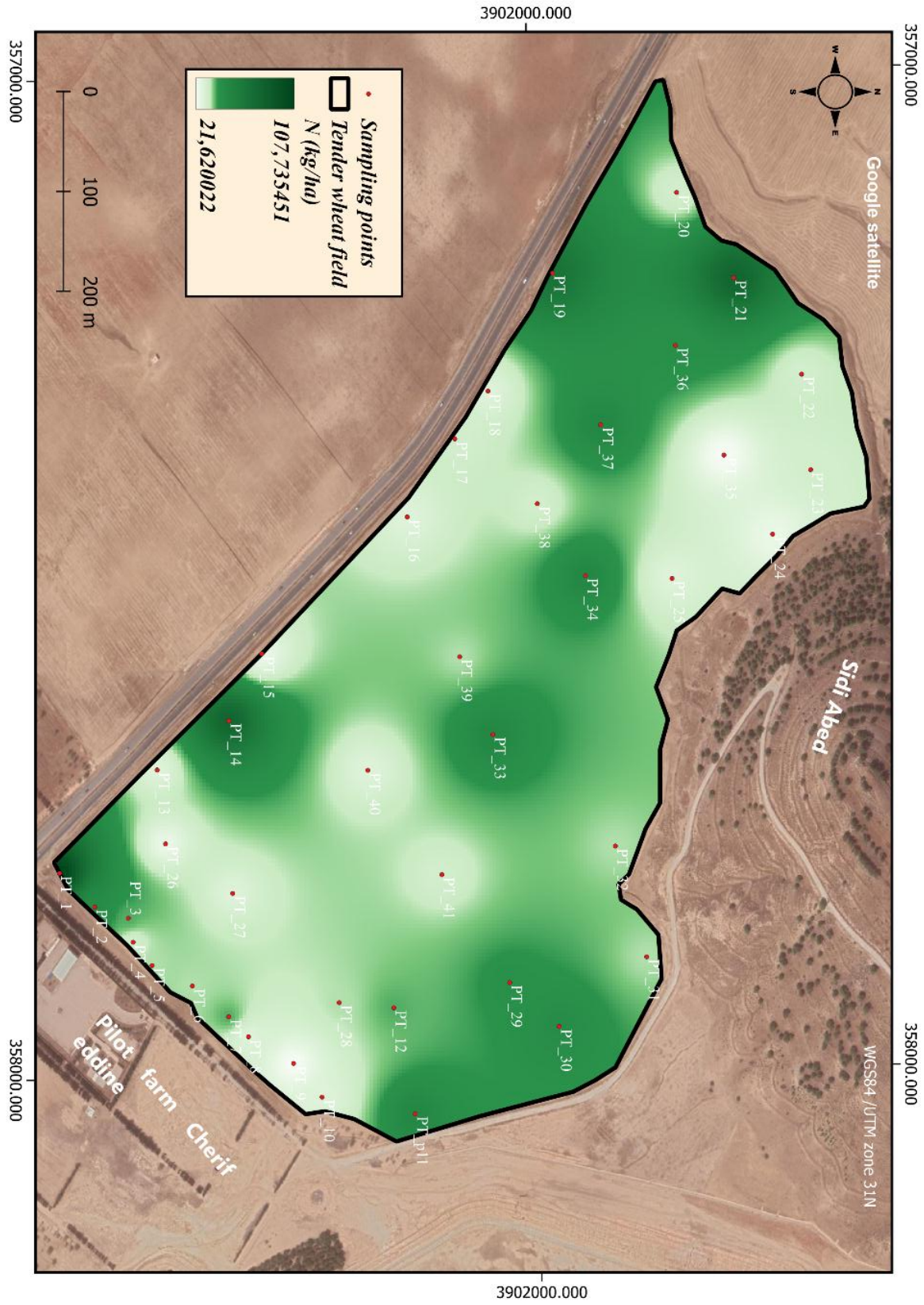

Figure 45: nitrogen map

7.5.3 Potassium (K)

Potassium (K): Potassium plays a vital role in wheat's overall health, stress tolerance, and grain quality. The recommended application rate of potassium fertilizer for tender wheat is generally around 40 to 80 kg/ha.

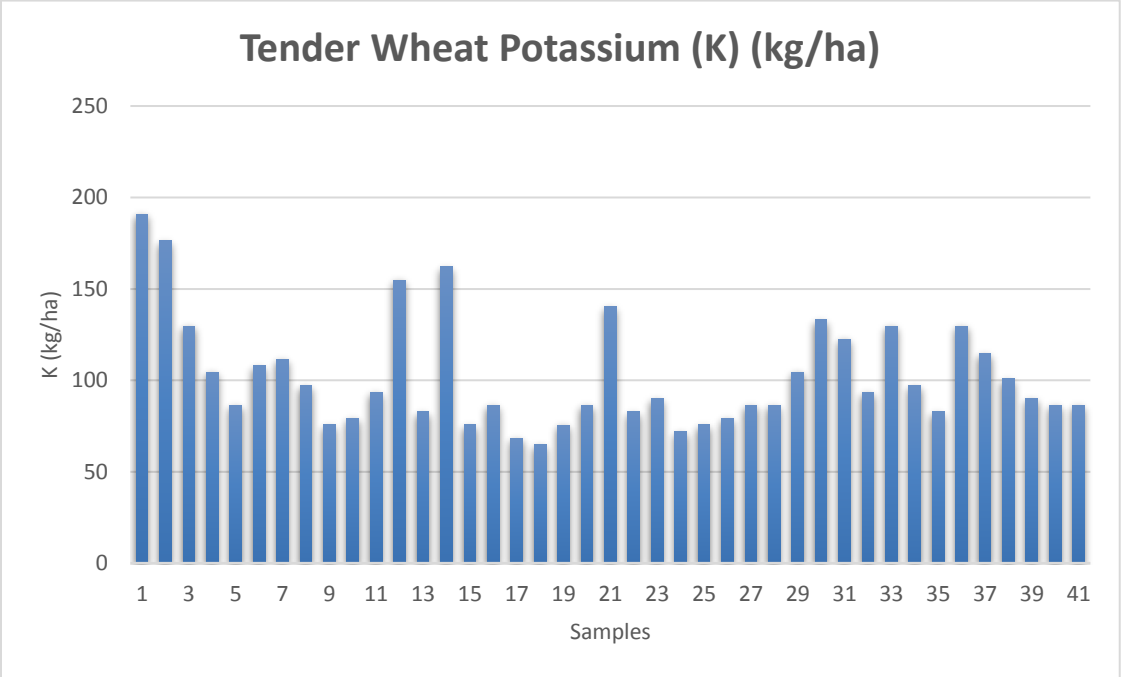

Figure 46: potassium values

The potassium levels approximately 22% (9 out of 41) of the samples have potassium levels below 80 kg/ha. Some of these samples are focused in the northern area of the plot, which represent relatively a high ground from the rest of the field. As for the rest of the samples 78% of the plot exhibit high potassium levels above 80 kg/ha these areas have relatively abundant potassium content.

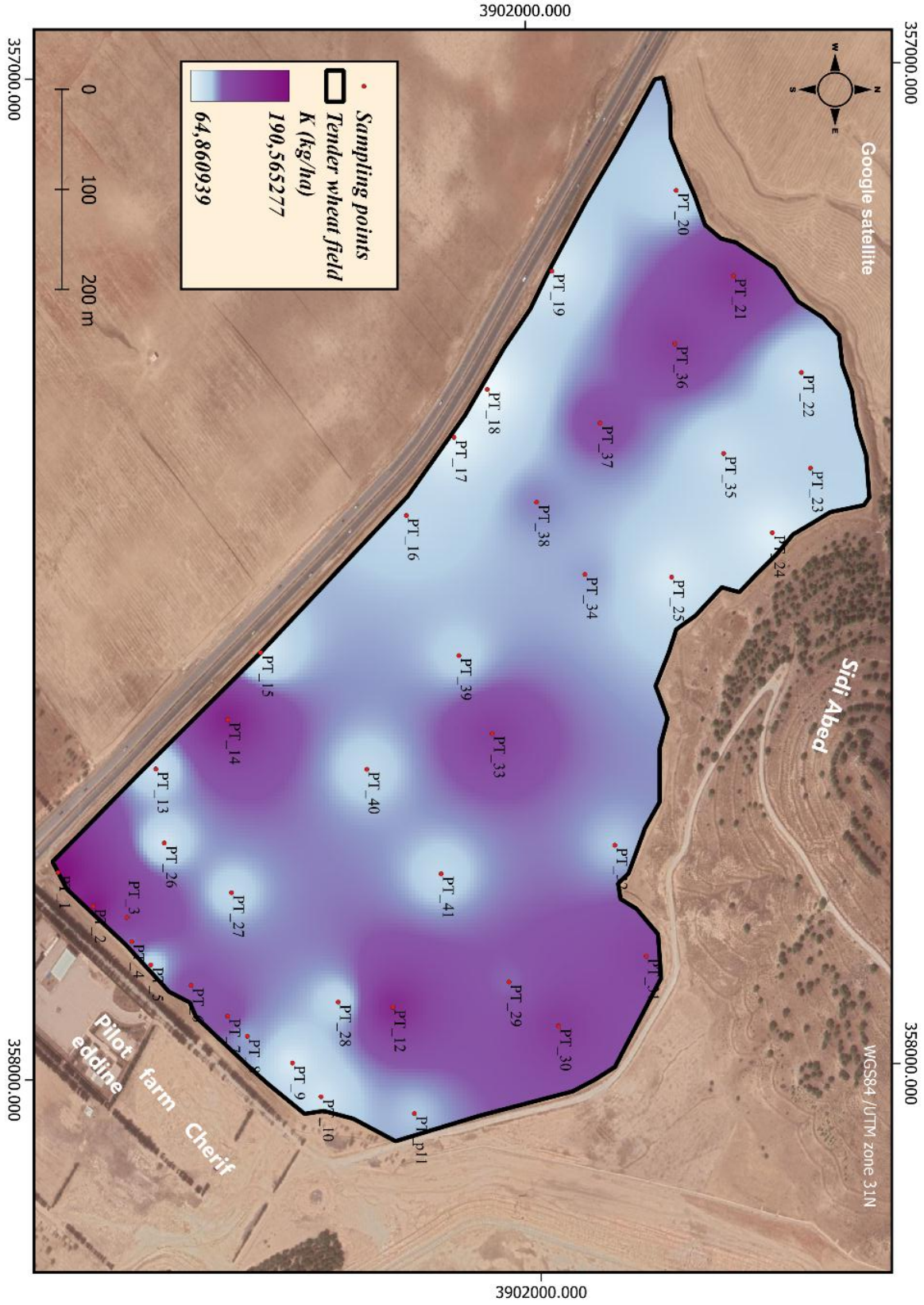

Figure 47: potassium map

Overall, the analysis of the N, P, and K values across the soil map revealed considerable variation throughout the plot. Some regions exhibited deficits in these essential nutrients. However, it is important to note that the underdevelopment of the wheat crop cannot be solely attributed to these deficits alone. Other factors such as soil composition, moisture availability, or pest pressures may have contributed significantly. Hence, while addressing the observed nutrient deficiencies is crucial for optimal crop growth, a comprehensive assessment of multiple factors is necessary to understand the underlying causes of the wheat crop's underdevelopment

7.6 Determination of total limestone and the proportion of active limestone

Analysis of total limestone gives an overall quantitative identification of the soil. As shown in **figure 48** around 66% (27 out of 41) of the samples have a percentage of total limestone Active above 10% which indicate that the soil is calcareous soil according to reference data in **Table 9**

Table 9: limestone optimum values source: **(webmaster 4)**

Total limestone		**0.5**	**5**	**10**	**25**	**50**
Soil is:	No limestone	Very low limestone	Low limestone	Limestone		
Active limestone		5		10		20
Soil is:	Low	High enough		High		Very high

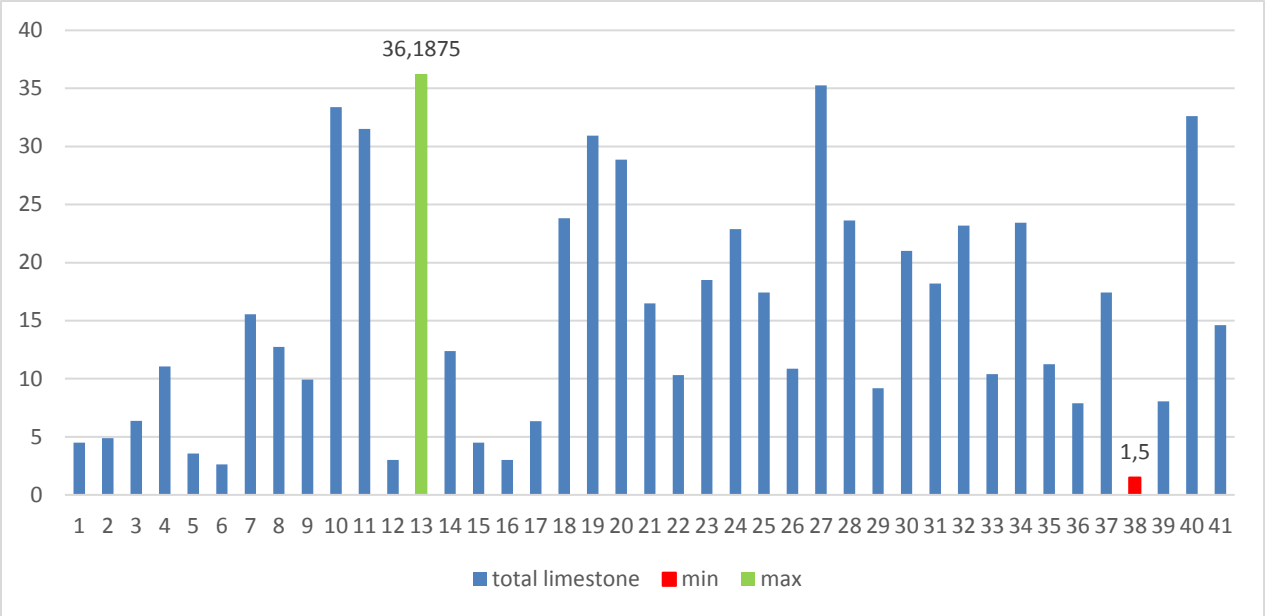

Figure 48: Total Limestone values

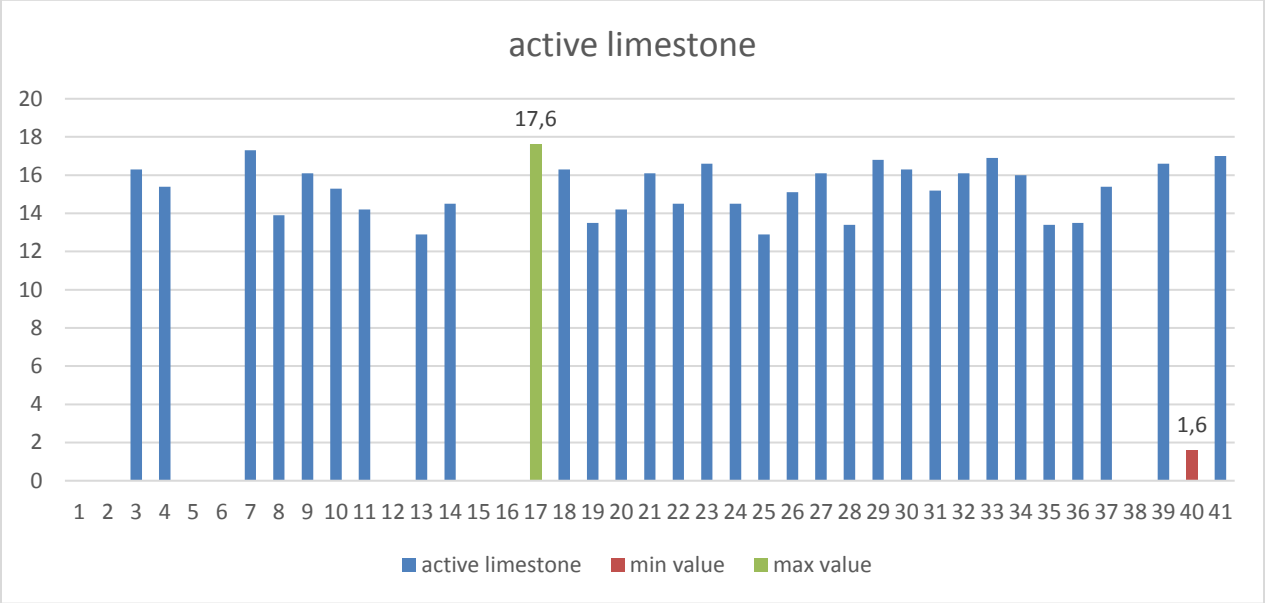

Figure 49: Active limestone values

The results from the soil samples collected in the tender wheat plot indicate varying levels of total limestone and active limestone. Total limestone refers to the overall amount of limestone present in the soil, while active limestone represents the portion of limestone that is readily available for plant uptake. The interpretation of these results reveals important insights for the wheat plot.

Most of the soil samples show a low to moderate level of total limestone, suggesting that the soil in the wheat plot has a relatively balanced composition of limestone. This is favourable

for wheat cultivation as it provides a suitable environment for root development and nutrient uptake.

The active limestone levels vary across the samples, indicating differences in the availability of limestone for plant utilization. Samples with high active limestone values indicate an adequate supply of limestone for wheat plants, which is beneficial for maintaining optimal growth and productivity. On the other hand, samples with low active limestone values may require additional limestone amendments to ensure sufficient availability of this essential nutrient for wheat crops.

These findings highlight the importance of understanding the limestone content in the soil to optimize wheat production. It underscores the need for regular soil analysis to assess the levels of total and active limestone, enabling farmers to make informed decisions regarding the application of limestone amendments. By ensuring a balanced and adequate supply of limestone, farmers can enhance the overall health and productivity of the wheat plot, leading to improved yields and quality of the harvested crop.

7.7 Evapotranspiration modelling

Table 10: The estimated evapotranspiration (ET) in the tender wheat plot using SEBAL

	ET (mm)	
Date	**Min**	**Max**
18/10/2022	4,7	10
11/03/2023	7,41	10
07/02/2023	6,08	10
06/01/2023	1,19	10
05/12/2022	2,13	10
03/11/2022	0,72	10
02/10/2022	1,15	10
28/04/2023	1,01	10

Figure 50 shows the spatiotemporal variation of the estimated evapotranspiration (ET) in the tender wheat plot using SEBAL. The distribution of ET values exhibits a fluctuating trend throughout the given period.

October 18, 2022, the ET values ranged from 4.7 to 10, with an average ET of 7.35. The eastern part of the plot shows higher ET values compared to other regions, indicating relatively higher evapotranspiration rates in that area. This suggests favorable hydrographic conditions in the eastern part, potentially influenced by factors such as higher temperature, better soil moisture, and characteristics.

October 2, 2022, the ET values ranged from 1.15 to 10, with an average ET of 5.575. The western part of the plot shows lower ET values compared to other regions, indicating relatively lower evapotranspiration rates in that area. This suggests less favorable hydrographic conditions in the western part, which could be influenced by factors such as lower temperature, reduced soil moisture, or other regional variations.

December 5, 2022, the ET values ranged from 2.13 to 10, with an average ET of 6.065. There is some heterogeneity in the distribution of ET values, with slightly lower values observed in the western region. This indicates variations in evapotranspiration rates across different parts of the plot, possibly influenced by local factors such as vegetation coverage, soil properties, or microclimatic conditions.

January 3, 2023, the ET values ranged from 1.19 to 10, with an average ET of 5.595. The lowest values of ET are observed in the center and eastern parts of the plot. The distribution of low ET values is spread throughout the plot, but there are still some higher values on the

edges. This suggests a change in the distribution pattern compared to previous dates, indicating a shift in the hydrographic conditions within the plot.

February 7, 2023 and March 11, 202, the distribution of ET values appears to be mostly stable across the plot, with a dominance of higher values. This indicates relatively high evapotranspiration rates, suggesting favorable hydrographic conditions across the entire plot during these periods.

April 28, 2023, there is a return to the lowest distribution in the western part of the plot, with a significant proportion of low ET values. This suggests less favorable hydrographic conditions in the western region, potentially influenced by factors such as lower temperatures, reduced precipitation, or other local variations.

Overall, the spatiotemporal variation in ET values in the tender wheat plot indicates fluctuating evapotranspiration rates, with some variations in hydrographic conditions throughout the given period and a clear water deficit due to the lack of precipitation and high temperature particularly in April 2023 **(ERA05)**, The vegetation are also factors in this distribution which can take us also to question the agricultural practices and specially seeding.

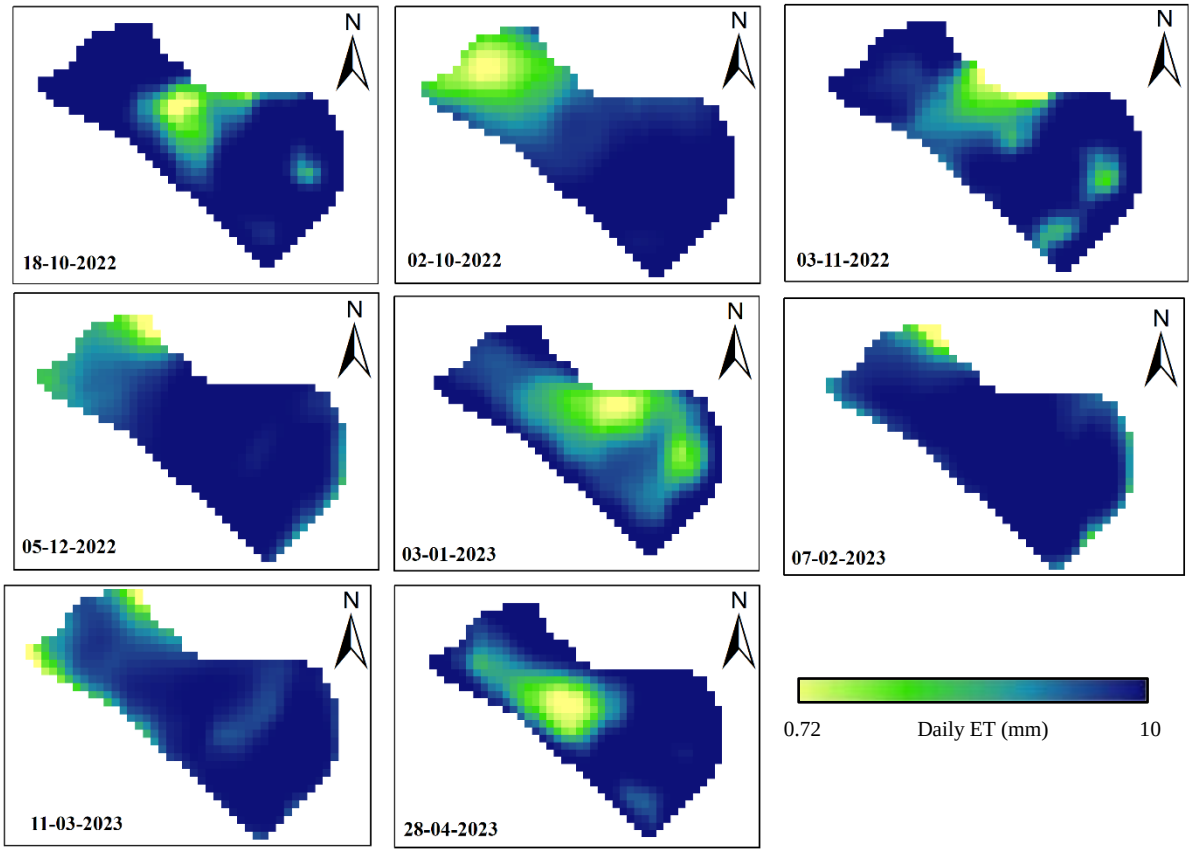

Figure 50: Spatial and temporal distribution of ET on the tender wheat plot

Several researches have been developed in the context of implicating remote sensing in the water balance field such as (**Idir Tazekrit *& al.*, 2018)** in the western region of Algeria, **(Hamimed *& al.*, 2017)** in the region of Mascara and **(Fellah *& al.*, 2020)** in the region of Oran.

These studies found out that these technologies can be a real help to understand and monitor water balance such as evapotranspiration fractions and irrigation planning.

7.8 Generation of an irrigation schedule for the tender wheat plot

To generate an irrigation, we used our meteological data provide by climate engine along with the FAO AquaCrop software **(figure 51)**. We started our simulation from the seeding of the tender wheat (December 18,2022)

Figure 51: AquaCrop software interface.

After inputting the meteological data, crop parameters, soil profile characteristics we could generate an irrigation schedule based the information and the development stage of the crop. We were able to get the irrigation events schedule **(table 10).**

The table provides the irrigation events along with the corresponding days, dates, and net application of irrigation in millimeters (mm). The net application of irrigation represents the amount of water applied to the tender wheat plot on each specific date.

The irrigation schedule seems to have a relatively consistent net application of irrigation, ranging from 58.2 mm to 60.9 mm across the events. This suggests a regular and planned irrigation approach, aiming to provide a consistent water supply to the crop.

Table 11: Irrigation events Schedule generated by AquaCrop.

Event	**Day**	**date**	**Net application(mm)**
1	103	30 march 2023	60.9
2	116	12 april 2023	60.9
3	127	23 april 2023	59.7
4	132	28 April 2023	58.2

Conclusion

Our study focused on estimating water irrigation consumption for the wheat crop in the region of Tiaret using remote sensing data. Through the integration of the SEBAL model for evapotranspiration calculation and the Aquacrop software for water needs quantification, we were able to derive valuable insights and result.

The key findings of this study include the development of an irrigation schedule based on the analysis of evapotranspiration and the data obtained through remote sensing. This irrigation schedule can guide farmers in effectively managing water resources, ensuring that crops receive adequate irrigation while minimizing water wastage.

We also aimed to address the water deficit issue and its impact on the underdevelopment of wheat crops in the region of Tiaret, through the implication of remote sensing data and the SEBAL model integrated with the Google Earth Engine platform, we were able to estimate and map evapotranspiration rates, leading to the development of an irrigation schedule that can benefit both farmers and decision-makers in the agricultural sector.

Furthermore, the study highlights the crucial role and importance of remote sensing in agriculture, particularly in the context of precision agriculture.

It is important to note that the study also discovered that while soil parameters were found to be satisfactory, the underdevelopment of crop yields was primarily attributed to factors such as precipitation, drought, and climatic conditions. This emphasizes the need for comprehensive approaches that consider both the physical and environmental aspects of crop growth.

Looking forward, the results of this study provide a perspective for other researchers and practitioners to follow. The integration of remote sensing data and models can significantly contribute to sustainable agricultural practices by optimizing water use and increasing crop resilience. By adopting similar methodologies and utilizing remote sensing technologies, it is possible to enhance crop productivity, mitigate water scarcity, and improve overall agricultural outcomes in various regions facing similar challenges.

In conclusion, the integration of remote sensing data, the development of irrigation schedules, and the adoption of precision agriculture practices are pivotal in optimizing water use and mitigating the impacts of drought. Embracing these advancements not only benefits farmers and the agricultural sector but also promotes sustainable resource management for a more resilient future.

Bibliographic References

Abolafia-Rosenzweig, R., Livneh, B., Small, E. E., & Kumar, S. V. (2019). Soil moisture data assimilation to estimate irrigation water use. Journal of Advances in Modeling Earth Systems, 11, 3670–3690.

Abuzar, M., Whitfield, D., & McAllister, A. (2017). Farm level assessment of irrigation performance for dairy pastures in the Goulburn-Murray District of Australia by combining satellite-based measures with weather and water delivery information. ISPRS International Journal of Geo-Information, 6(8), 239.

Adams, R. M., Hurd, B. H., Lenhart, S., & Leary, N. (1998). Effects of global climate change on agriculture: An interpretative review. Clim. Res., 11, 19–30.

AghaKouchak, A., Farahmand, A., Melton, F. S., *& al*. (2015). Remote sensing of drought: Progress, challenges and opportunities. Reviews of Geophysics, 53, 452–480.

Agricultural Development in Algeria: Opportunities and Challenges", International Food Policy Research Institute, https://www.ifpri.org/publication/agricultural-development-

Ahmadi, M., Dabiri, H., & Jalilvand, H. **(2021)** : Estimation of crop evapotranspiration and irrigation water requirement using remote sensing data. Journal of Applied Remote Sensing, 15(1), 014507. doi: 10.1117/1.JRS.15.014507

Ahmed Kayad, Marco Sozzi, Simone Gatto ,Francesco Marinello and Francesco. Monitoring Within-Field Variability of Corn Yield using Sentinel-2 and Machine Learning Techniques. Department TESAF, University of Padova, viale dell'Università 16, 35020 Legnaro (PD), Italy. Remote Sens. **2019**, *11*(23), 2873. https://doi.org/10.3390/rs11232873

Algeria Agriculture Market", Mordor Intelligence, https://www.mordorintelligence.com/industry-reports/algeria-agriculture-market

Anderson, M.C., Allen, R.G., Morse, A., Kustas, W.P.(2012) : Use of Landsat thermal imagery in monitoring evapotranspiration and managing water resources. Remote Sens. Environ. 122, 50–65.

Anderson, R. G., Lo, M. H., Swenson, S., Famiglietti, J. S., Tang, Q., Skaggs, T. H., Lin, Y. H., & Wu, R. J. (2015). Using satellite-based estimates of evapotranspiration and

groundwater changes to determine anthropogenic water fluxes in land surface models. Geoscientific Model Development, 8(10), 3021.

Aryal, J. P., Jat, M. L., Sapkota, T. B., Rai, M., Jat, H. S., Sharma, P. C., & Stirling, C. (2019). Learning adaptation to climate change from past climate extremes: Evidence from recent climate extremes in Haryana, India. International Journal of Climate Change Strategies and Management, 12(1), 128-146.

ASAP. (2021) : SPECIAL FOCUS, anomaly hotspots for agriculture production. P 7.

Ault, T. R., Mankin, J. S., Cook, B. I., & Smerdon, J. E. (2016). Relative impacts of mitigation temperature and precipitation on 21st-century megadrought in the American Southwest. Sci. Adv., 2(10), e1600873.

Bastiaanssen, W. G., Molden, D. J., & Makin, I. W. (2000). Remote sensing for irrigated agriculture: examples from research and possible applications. Agric. Water Manag., 46, 137–155.

Baudoin, M. A., Vogel, C., Nortje, K., & Naik, M. (2017). Living with drought in South Africa: lessons learnt from the recent El Niño drought period. International Journal of Disaster Risk Reduction, 2, 128–137.

Bedjadj S., 2011. Contribution à l'étude des caractéristiques microbiologiques des sols dans la région de Ouargla (Cas de l'exploitation de l'université de Ouargla).Mémoire de fin d'étude en vue de l'obtention du diplôme d'ingénieur d'état en sciencesagronomiquesoptionmiseenvaleurdessolssahariens.UniversitéKasdiMerbahOuargla.Pages: 06, 07,14, 37. 59P

Bencharif, S. (2018). Origins and recent transformations of pastoral livestock of the Algerian steppe. International Journal of Development Studies, 236, 55-79.

Benfardia H., Chenine A., 2014. Effet de la nature du sol sur l'efficacité d'un dispositif de bio dépollution à l'aide des bactéries hydrocarbonates. Mémoire de fin d'étude en vue de l'obtention du diplôme d'un master académique en biologie spécialité microbiologie appliquée .Université Kasdi Merbah Ouargla.Page:22. 43P.

Benseghir A., 2006. Contribution à l'étude de l'état nutritionnel par la méthodedu diagnostic foliaire de trois variétés d'abricotier (Prunus Armenia ca L.) en zone aride(Commune de Doucen, W. Biskra). Mémoire de fin d'étude en vue de l'obtention du diplôme d'ingénieur

d'état en agronomie, option cultures pérennes .Université de Biskra. Page: 22. 43P.

Bensemane, L., Bouzerzour, H., Benmahammed, A., & Mimouni, H. (2011). Assessment of the phenotypic variation within two-and six-rowed barley (Hordeum vulgare L.) breeding lines grown under semi-arid conditions. Advances in Environmental Biology, 1454-1461.

Bessaoud, O., Pellissier, J. P., Rolland, J. P., & Khechimi, W. (2019). Rapport de synthèse sur l'agriculture en Algérie. CIHEAM-IAMM. Available at: [link to document].

Bindlish, R., Jackson, T. J., Gasiewski, A. J., (2006). Soil moisture mapping and AMSR-E validation using the PSR in SMEX02. Remote Sensing of Environment, 103(2), 127–139.

Boken, V. K., Hoogenboom, G., Kogan, F. N. (2004). Potential of using NOAA-AVHRR data for estimating irrigated area to help solve an inter-state water dispute. International Journal of Remote Sensing, 25(12), 2277–2286.

Bouguerra, A, Kherici, N, & Bouaicha, R., (2019) : Droughts in Algeria: Causes and Impacts. Journal of Arid Environments, 164, 59-68.

Boulenouar. (2016) : Contribution à l'étude de l'impact des pratiques agroforestières sur le développement durable de la zone rurale d'Oued Lili (W. de Tiaret). Université Abdelhamid Ibn Badis de Mostaganem. P 35.

Bouman, B. A. M., van Ittersum, M. K., Leffelaar, P. A. (2017). Yield gaps and nutrient use efficiencies in rice production systems in the tropics. Field Crops Research, 214, 1-12.

Brocca, L., Tarpanelli, A., Filippucci, P., Dorigo, W., Zaussinger, F., Gruber, A., & Fernández-Prieto, D. (2018). How much water is used for irrigation? A new approach exploiting coarse resolution satellite soil moisture products. International Journal of Applied Earth Observation and Geoinformation, 73, 752–766.

Calvet R.,2003. Le sol Propriété set fonctions : Constitution et structure, phénomènes aux interfaces. Tome1.Vol1.Editions France agricole. Paris.457P.

Calvet R.,2003. Le sol,Propriétésetfonctions:Phénomènesphysiquesetchimiques, applications agronomiques et environnementales. Tome2. Vol2. Editions France agricole. Paris. 513P.

Campos, I., Neale, C. M. U., Suyker, A. E., Arkebauer, T. J., & Gonçalves, I. Z. (2017). Reflectance-based crop coefficients REDUX: For operational evapotranspiration estimates in the age of high producing hybrid varieties. Agricultural Water Management, 187, 140–153.

Chabrillat, S., Naumann, N., Escribano, P., Bachmann, M., Spengler, D., Holzwarth, S., et al., 2016. Cabo de Gata-Níjar Natural Park 2003-2005—A Multitemporal Hyperspectral Flight Campaign for EnMAP Science Preparatory Activities. EnMAP Flight Campaigns Technical Report, GFZ Data Services.

Chao, N., Wang, Z., Jiang, W., Chao, D. (2016). A quantitative approach for hydrological drought characterisation in Southwestern China using GRACE. Hydrogeol. J., 24(4), 892–903.

Chehbouni, Abdelghani, Hoedjes, J.C.B., Rodriquez, J.-C., Watts, C.J., Garatuza, J., Jacob, F., Kerr, Y.H.(2008). Using remotely sensed data to estimate area-averaged daily surface fluxes over a semi-arid mixed agricultural land. Agric. For. Meteorol. 148, 330–342.

Chen Huailiang, Zhang Hongwei, Liu Ronghua (2009). Agricultural drought monitoring, forecasting and loss assessment in China. Technology Review, (11), 82–92. (in Chinese)

Chen Shulin, Liu Yuanbo, Wen Zuomin (2012). Satellite retrieved of soil moisture: An overview. Advances in Earth Science, (11), 1192–1203. (in Chinese)

Chen, R., & Chen, K. S. (2014). Crop mapping using SAR data: A review. Remote Sensing of Environment, 147, 522-535.

Cook, B. I., Anchukaitis, K. J., Touchan, R., Meko, D. M., Cook, E. R. (2016). Spatiotemporal drought variability in the Mediterranean over the last 900 years. J. Geophys. Res., 121(5), 2060–2074.

D.S.I.S.P Serie B 2019: Direction des Systèmes d'Information, des Statistiques et de la Prospective. Rapport de statistique agricole superficies et production serie B 2019. Juillet 2021.

Dari R., 2013.Dénombrementdelabiomassemicrobienne des sols arides, exemple d'un sol salé sous deux types de cultures. Mémoire de fin d'étude en vue de l'obtention du diplôme d'ingénieur d'état en sciences agronomiques, option mise en valeur des sols sahariens. Université KasdiMerbahOuargla.Pages:03, 34,53. 53P.

Daughtry, C. S. T., Walthall, C. L., Kim, M. S., De Colstoun, E. B., & McMurtrey, J. E. (2000). Estimating corn leaf chlorophyll concentration from leaf and canopy reflectance. Remote Sensing of Environment, 74(2), 229-239.

Davis, G., Casady, W. and Massey, R.(1998): Precision Agriculture: An Introduction, University of Missouri

Debnath, S., Khan, M. R., & Mandal, S. **(2018)**. Economic losses due to drought in India

Deshar, R., Koirala, M. (2019). Climate Change and Gender Policy. In Global Climate Change and Environmental Policy: Agriculture Perspectives, 1st ed.; Venkatramanan, V., Shah, S., Prasad, R., Eds.; Springer Nature Pte Ltd.: Singapore; pp. 411–422. [Google Scholar]

Digital Globe Agriculture and Rural Development Basic information on the application of remote sensing on agriculture. URL: https://www.eo4idi.eu/eo4sd-knowledge-portal/3-remote-sensing-technology/32-platforms/322-digitalglobe

Droogers, P., Immerzeel, W. W., & Lorite, I. J. (2010). Estimating actual irrigation application by remotely sensed evapotranspiration observations. Agricultural Water Management, 97(9), 1351–1359.

Drusch, M., Del Bello, U., Carlier, S., Colin, O., Fernandez, V., Gascon, F., Hoersch, B., Isola, C., Laberinti, P., Martimort, P., Meygret, A., Spoto, F., Sy, O., Marchese, F., & Bargellini, P. (2012). Sentinel-2: ESA's optical high-resolution mission for GMES operational services. Remote Sensing of Environment, 120, 25–36. ISSN 0034–4257,

DURAND J.H., 1983).- Les sols irrigables : Étude pédologique. Presse Universitaire de France. Collection. Ed. ACCT et CILF. Paris, 339 p

FAO, 2007**:** Perspective alimentaires. Analyse des marches mondiales. http://www.fao.org/ 010/ah864f/ah864f00.html (20.11.2014/13:28).

Farooq, M., Hussain, M., Siddique, K. H. M., & Jabran, K. **(2017)**. Drought stress in plants: An overview. In M. Farooq, K. H. M. Siddique, & N. Ahmad (Eds.), Drought Stress Tolerance in Plants, Vol. 1 (pp. 1-33). Cham: Springer.

Field, C.B.; Barros, V.R.; Dokken, D.J.; Mach, K.J.; Mastrandrea, M.D.; Bilir, T.E.; Chatterjee, M.; Ebi, K.L.; Estrada, Y.O.; Genova, R.C. (2014). IPCC Summary for policymakers. In Climate Change: Impacts, Adaptation, and Vulnerability, Part A: Global and Sectoral Aspects; Contribution of Working Group II to the Fifth Assessment Report of the

Intergovernmental Panel on Climate Change; Cambridge University Press: Cambridge, UK; New York, NY, USA, 2014; pp. 1–32. ISBN 978-92-9169-143-2. [Google Scholar]

Fiwa, L., Vanuytrecht, E., Wiyo, K. A., & Raes, D. (2014). Effect of rainfall variability on the length of the crop growing period over the past three decades in central Malawi. Climate Research, 62, 45–58.

Foley, J.A., Ramankutty, N., Brauman, K.A., Cassidy, E.S., Gerber, J.S., Johnston, M., Mueller, N.D., O'Connell, C., Ray, D.K., West, P.C., Balzer, C., Bennett, E.M., Carpenter, S.R., Hill, J., Monfreda, C., Polasky, S., Rockström, J., Sheehan, J., Siebert, S., Tilman, D., Zaks, D.P.M. (2011). Solutions for a cultivated planet. Nature 478, 337–342.

Foster, T., Gonçalves, I. Z., Campos, I., Neale, C. M. U., & Brozovic, N. (2019). Assessing landscape scale heterogeneity in irrigation water use with remote sensing and in situ monitoring. Environmental Research Letters, 14(2), 024004.

Gao B (1996). NDWI: A normalized difference water index for remote sensing of vegetation liquid water from space. Remote Sensing of Environment, 58(3), 257–266.

Gernez, P., Lafon, V., Lerouxel, A., Curti, C., Lubac, B., Cerisier, S., & Barillé, L. (2015). Toward Sentinel-2 high-resolution remote sensing of suspended particulate matter in very turbid waters: SPOT4 (Take5) experiment in the Loire and Gironde estuaries. Remote Sensing, 7(8), 9507–9528.

Giannakopoulos, C., Le Sager, P., & Bindi, M. (2009). Climate change impacts in the Mediterranean resulting from a 2°C global temperature rise. Report for WWF. Retrieved from

Gonçalves, I. Z., Mekonnen, M. M., Neale, C. M. U., Campos, I., & Neale, M. R. (2020). Temporal and spatial variations of irrigation water use for commercial corn fields in Central Nebraska. Agricultural Water Management, 228, 105924.

Guet G.,2003. Mémento d'agriculture biologique: guide pratique à usage professionnel. 2emeédition. Editions AGRIDECISIONS. Paris. 417P.

Haboudane, D., Miller, J. R., Pattey, E. (2004). Hyperspectral vegetation indices and novel algorithms for predicting green LAI of crop canopies: Modeling and validation in the context of precision agriculture. Remote Sensing of Environment, 90(3), 337–352.

Hanqiu Xu, Xiujuan Hu, Huade Guan, Bobo Zhang, Meiya Wang, Shanmu Chen, and Minghua Chen (2019). Remote Sensing Based Method to Detect Soil Erosion in Forests. ResearchGate, 10.3390/rs11050513.

Hayes, M. J., Svoboda, M. D., Wardlow, B. D., Anderson, M. C., Kogan, F. (2012). Drought monitoring. In: Wardlow, B. D., Anderson, M. C., Verdin, J. P. (Eds.), Remote Sensing of Drought: Innovative Monitoring Approaches. CRC Press, New York.

Hlavackova, P. (2005) : Evaluation du comportement du cuivre et du zinc dans une matrice detype sol à l'aide de différentes méthodologies. Thèse de Doctorat, L'Institut National desSciencesAppliquéesdeLyon, 207p,

Hossam El-Din Fawzy., Adel Sakr, Moustafa El-Enany, Hossam M.Moghazy., 2020. Spatiotemporal assessment of actual evapotranspiration using satellite remote sensing technique in the Nile Delta, Egypt. AEJ - Alexandria Engineering Journal 60(1). https://doi.org/10.1016/j.aej.2020.11.001

Howard, G., Calow, R., Macdonald, A., & Bartram, J. (2016). Climate change, water, and sanitation: impacts and emerging trends for action. Annu. Rev. Environ. Resour, 41(1), 253-276.

Huang, Y., Zhang, X., Li, Y., Li, L., Li, J., & Li, J. (2021). Remote sensing applications in crop disease detection and monitoring: a review. International Journal of Agriculture and Biology, 25(1), 1-9.

Huete, A. R., *& al*. (2019). Advances in Remote Sensing for Agriculture: Context Description, Existing Operational Monitoring Systems, and Major Information Needs. Remote Sensing, 11(19), 2335. doi: 10.3390/rs11192335.

Idso, S. B., Jackson, R. D., Pinter, P. J., (1981). Normalizing the stress-degree-day parameter for environmental variability. Agricultural Meteorology, 24, 45–55.

IPCC (2007) Climate Change (**2007)**: The Physical Science Basis. Contribution of Working Group I to the Fourth Assessment Report of the Intergovernmental Panel on Climate Change [Solomon, S., D. Qin, M. Manning, Z. Chen, M. Marquis, K.B. Averyt, M. Tignor and H.L. Miller (eds.)]. Cambridge University Press, Cambridge, United Kingdom and New York, NY, USA Jamieson PD, Semenov MA, Brooking IR,

IPCC (2014). Climate change 2014: synthesis report. In: Contribution of Working Groups I, II, and III to the Fifth Assessment Report of the Intergovernmental Panel on Climate Change. IPCC, Geneva, Switzerland, pp. 151.

Jackson, T. J., Bindlish, R., Cosh, M. H., Starks, P. J., Bosch, D. D., Seyfried, M. S., ... & Prueger, J. H. (2019). Soil moisture active passive (SMAP) mission soil moisture and temperature validation. Journal of Hydrology, 570, 590-610.

Jalilvand, E., Tajrishy, M., Hashemi, S. A. G. Z., & Brocca, L. (2019). Quantification of irrigation water using remote sensing of soil moisture in a semi-arid region. Remote Sensing of Environment, 231, 111226.

Jasechko, S., Sharp, Z. D., Gibson, J. J., Birks, S. J., Yi, Y., and Fawcett, P. J. (2013). Terrestrial water fluxes dominated by transpiration, Nature, 496, 347 350

Karnieli, A., Agam, N., Pinker, R. T. (2010). Use of NDVI and land surface temperature for drought assessment: Merits and limitations. Journal of Climate, 23(3), 618–633.

Kerrache G. (2011). Caractéristiques et gestion des formations forestières en Algérie. Cours en ligne. Université de Tlemcen.

Kogan, F. N. (1995). Droughts of the late 1980s in the United States as derived from NOAA polar-orbiting satellite data. Bulletin of the American Meteorological Society, 76(5), 655–668.

Kogan, F., Adamenko, T., Guo, W. (2013). Global and regional drought dynamics in the climate warming era. Remote Sensing Letters, 4(4), 364–372.

Kostopoulou E., Jones P. D. (2005). Assessment of climate extremes in the Eastern Mediterranean. Meteorology and Atmospheric Physics, vol. 89, 69–85. DOI 10.1007/s00703-005-0122-2.

Kumar S V, Peters-Lidard C D, Mocko D. (2014). Assimilation of remotely sensed soil moisture and snow depth retrievals for drought estimation. Journal of Hydrometeorology, 15(6), 2446–2469.

L. Karthikeyan, I. Chawla, and A. K. Mishra (2020). A Review of Remote Sensing Applications in Agriculture for Food Security: Crop Growth and Yield, Irrigation, and Crop Losses, J. Hydrol., vol. 586, no. March, doi: 10.1016/j.jhydrol.2020.124905.

Lemaire F., Dartigues A., Charpentier S., Rivière L.M., Morel P., 2003. Cultures en pots et conteneurs : principes agronomiques et applications. 2eme édition.EditionsINRA. Paris. 232P.

Lemma, M., Alemie, A., Habtu, S., & Lemma, C. (2016). Analyzing the impacts of onset, length of growing period, and dry spell length on chickpea production in Adaa District (East Showa Zone) of Ethiopia. Journal of Earth Science and Climatic Change, 7, 349.

Lettenmaier, D. P., Alsdorf, D., Dozier, J., Huffman, G. J., Pan, M., & Wood, E. F. (2015). Inroads of remote sensing into hydrologic science during the WRR era. Water Resources Research, 51, 7309–7342.

Liu Li, Zhou Ying (1998). Drought monitoring based on vegetation supply water index in Guizhou Province. Guizhou Meteorology, 22(6), 17–21. (in Chinese)

Liu, X., Zhu, X., Pan, Y., Li, S., Liu, Y., Ma, Y. (2016). Agricultural drought monitoring: progress, challenges, and prospects. J. Geogr. Sci. 26 (6), 750–767.

Lloyd-Hughes, B. (2014). The impracticality of a universal drought definition. Theory of Applied Climatology 117 (3–4), 607–611.

Lobell, D. B., & Asner, G. P. (2002). Cropland distributions from temporal endmembers using spectral mixture analysis. Remote Sensing of Environment, 80(3), 353-362.

Lobell, D. B., Hammer, G. L., Chenu, K., Zheng, B., McLean, G., & Chapman, S. C. (2015). The shifting influence of drought and heat stress for crops in northeast Australia. Global Change Biology, 21, 4115–4127.

Lopez Valencia, O. M., Johansen, K., Aragon Solorio, B. J. L., Li, T., Houborg, R., Malbeteau, Y., Almashharawi, S., Altaf, M., Fallatah, E. M., Dasari, H. P., Hoteit, I., & McCabe, M. F. (2020). Mapping groundwater abstractions from irrigated agriculture: Big data, inverse modeling and a satellite-model fusion approach. Hydrology and Earth System Sciences Discussions.

MATE (2010), Ministère de l'Aménagement du Territoire et de l'environnement (Ministry of Land Planning and Environment). Seconde communication nationale de l'Algérie sur les changements climatiques à la CCNUCC, projet GEF –PNUD 00039149, 2010, Algiers

MATE (2010), Ministère de l'Aménagement du Territoire et de l'environnement (Ministry of Land Planning and Environment). Seconde communication nationale de l'Algérie sur les changements climatiques à la CCNUCC, projet GEF –PNUD 00039149, 2010, Algiers

McCabe, M. F., Rodell, M., Alsdorf, D. E., Miralles, D. G., Uijlenhoet, R., Wagner, W., Lucieer, A., Houborg, R., Verhoest, N., Franz, T., Shi, J., Gao, H., & Wood, E. F. (2017). The future of earth observation in hydrology. Hydrology and Earth System Sciences Discussions, 21, 3879–3914.

Mendelsohn, R. (2009). The impact of climate change on agriculture in developing countries. J. Nat. Res. Policy Res. 2009, 1, 5–19. [Google Scholar] [CrossRef][Green Version]

MINISTÈRE DE L'AGRICULTURE ET DE LA SOUVERAINETÉ ALIMENTAIRE - LES POLITIQUES AGRICOLES À TRAVERS LE MONDE: ALGÉRIE

Ministry of Agriculture and Rural Development (MADR). (2018). Agriculture statistics yearbook 2017-2018. http://www.interieur.gov.dz/index.php/fr/component/phocadownload/category/211-statistiques-agricoles

Montoroi J.P., 1997. Etude et gestion des sols. Conductivité électrique de lasolution du sol et d'extraits aqueux de sol : application à un sol sulfaté acide salé deBasse-Casamance (Sénégal). Article scientifique 4, (4). Editions AFES. Montpellier. P : 279-298.

Moonen, A. C. (2002). Future climate change and its potential impact on disease transmission in Africa. International Journal of Hygiene and Environmental Health, 205(6), 463-471. doi: 10.1078/1438-4639-00190

Moran M S, Clarke T R, Inoue Y *& al*. (1994). Estimating crop water deficit using the relation between surface-air temperature and spectral vegetation index. Remote Sensing of Environment, 49(3), 246–263.

Msigwa, A., Komakech, H. C., Verbeiren, B., Salvadore, E., Hessels, T., Weerasinghe, I., & Griensven, A. (2019). Accounting for seasonal land use dynamics to improve estimation of agricultural irrigation water withdrawals. Water, 11(12), 2471.

Mu L, Wu B, Yan N *& al*. (2007). Validation of agricultural drought indices and their uncertainty analysis. Bulletin of Soil and Water Conservation, 27(2), 119–122.

Müller, C. (2013). African lessons on climate change risks for agriculture. Annu. Rev. Nutr., 33, 395–411. [Google Scholar] [CrossRef]

Musy A., Higy C., 2004. Hydrologie: 1 Une science de la nature. Editions Presses polytechniques et universitaires romandes. Collection gérer l'environnement. Lausanne.314P.

Nagarajan, R. (2009). Drought Assessment. Springer, Berlin.

Niang, I., Ruppel, O. C., Abdrabo, M. A., Essel, A., Lennard, C., Padgham, J., & Urquhart, P. (2014). Africa. Climate change 2014: impacts, adaptation, and vulnerability. Part B: regional aspects.

Nicolas Da Silva (2018). Autour des relations température-précipitations dans la région Euro Méditerranéenne. Climatologie. Université Paris Saclay, 2018. Français.

Nicolas da silva.(2018). Autour des relations température-précipitations dans la région Euro-Méditerranéenne.192

OAIC ; 2013 : rapport annuelle de L'Office Algérien Interprofessionnel des Céréales.

Oudin, L.(2004). Recherche d'un modèle d'évapotranspiration potentielle pertinent comme entrée d'un modèle pluie-débit global. PhDthesis, ENGREF paris 3.

Ozdogan, M., Yang, Y., Allez, G., Cervantes, C. (2010). Remote sensing of irrigated agriculture: Opportunities and challenges. Remote Sensing, 2, 2274–2304.

Parry, S., Prudhomme, C., Wilby, R.L., Wood, P.J. (2016). Drought termination: concept and characterisation. Prog. Phys. Geogr., 40(6), 743–767.

Peña-Arancibia, J. L., Mainuddin, M., Kirby, J. M., Chiew, F. H. S., McVicar, T. R., & Vaze, J. (2016). Assessing irrigated agriculture's surface water and groundwater consumption by combining satellite remote sensing and hydrologic modelling. Science of the Total Environment, 542, 372–382.

Peng, Y. Stefanidou, A., Gitas, I. Z., Stavrakoudis, D., & Eftychidis, G. (2019). "Remote Sensing-Based Yield Estimation and Prediction of Maize in China: A Review." Remote Sensing, 11(23), 2786. doi: 10.3390/rs11232786

Pereira, L. S., T. Oweis and A. Zairi. (2002). Irrigation management under water scarcity. Agric. Water Manage. 57:175-206.

Petard J., 1993. Les méthodes d'analyse. Tome1,Analyse de sols. Note stechniques. Laboratoire commun d'analyses N°5.Document de travail. Editions ORSTOM (Office de la recherche scientifique et technique outre-mer).Nouvelle Calédonie.196P.

Pousset J.,2002. Engrais vert set fertilité dessols.2eme Edition. Editions Agridécisions. Paris. 305P.

Ralf Waters, Richard Allen, Masahiro Tasumi, Ricardo Trezza, Wim Bastiaanssen. 2002 SEBAL Surface Energy Balance Algorithms for Land Idaho Implementation Advanced Training and Users Manual August, Version 1.0 https://www.posmet.ufv.br/wp-content/uploads/2016/09/MET-479-Waters-et-al-SEBAL.pdf

Romaguera, M., Krol, M. S., Salama, M., Su, Z., Hoekstra, A. Y. (**2014**). Application of a remote sensing method for estimating monthly blue water evapotranspiration in irrigated agriculture. Remote Sensing, 6(10), 10,033–10,050.

Rosenzweig, C., & Hillel, D. (2015). Handbook of climate change and agroecosystems: The agricultural model intercomparison and improvement project (AgMIP) integrated crop and economic assessments. World Scientific: Joint Publication with American Society of Agronomy, Crop Science Society of America, and Soil S.

Rosenzweig, C.; Major, D.C.; Demong, K.; Stanton, C.; Horton, R.; Stults, M. (2007). Managing climate change risks in New York City's water system: Assessment and adaptation planning. Mitig. Adapt. Strat. Glob. Chang. 2007, 12, 1391–1409. [Google Scholar] [CrossRef]

Saadi, S., Todorovic, M., Tanasijevic, L., Pereira, L. S., Pizzigalli, C., & Lionello, P. (**2015**). Climate change and Mediterranean agriculture: Impacts on winter wheat and tomato crop evapotranspiration, irrigation requirements, and yield. Agricultural Water Management, 147, 103–115.

Sandholt I, Rasmussen K, Andersen J (2002). A simple interpretation of the surface temperature/vegetation index space for assessment of surface moisture status. Remote Sensing of Environment, 79(2), 213–224.

Santos, C., Lorite, I. J., Tasumi, M., Allen, R. G., & Fereres, E. (**2010**). Performance assessment of an irrigation scheme using indicators determined with remote sensing techniques. Irrigation Science, 28(6), 461–477.

Sayyad, G., Afyuni, M., Mousavi, S.-F., Abbaspour, K. C., Richards, B. K &SchulinR.(2010) Transport of Cd, Cu, Pb and Zn in a calcareous soil under wheat and safflower cultivation-Acolumn study. Geoderma, vol. 154pp. 311-320, 2010.

Schauberger, B., Archontoulis, S., Arneth, A., Balkovic, J., Ciais, P., Deryng, D. (**2017**). Consistent negative response of US crops to high temperatures in observations and crop models. Nature Communications, 8, 13931.

Segovia-Cardozo, D. A., Rodríguez-Sinobas, L., & Zubelzu, S. (**2019**). Water use efficiency of corn among the irrigation districts across the Duero river basin (Spain): Estimation of local crop coefficients by satellite images. Agricultural Water Management, 212, 241–251.

Seguin B.(2010). Le changement climatique: conséquences pour les végétaux. Quaderni 71 : 27-40.

Sh Kholdorov, Lakshmi Gopakumar, K Katsura, Z Jabbarov, O Jobborov, T Shamsiddinov, and A Khakimov. (**2022**). Soil salinity assessment research using remote sensing techniques: a special focus on recent research. July 2022 IOP Conference Series Earth and Environmental Science, 1068(1), 012037.

Stevens, C.J., Dise, N.B., Mountford, J.O., Gowing, D.J. (**2004**). Impact of nitrogen deposition on the species richness of grasslands. Science, 303, 1876–1879. [Google Scholar] [CrossRef]

Thenkabail, P. S., Knox, J. W., Ozdogan, M., Gumma, M. K., Congalton, R. G., Wu, Z., & Milesi, C. (**2011**). Assessing future risks to agricultural productivity, water resources, and food security: How remote sensing can help? Photogrammetric Engineering & Remote Sensing, 77(9), 973-980.

Tian, J.X.; Qin, J.; Yang, K.;u Zhao, L.; Chen, Y.Y.; Lu, H.; Li, X.; Shi, J.C. (2022). Improving surface soil moisture retrievals through a novel assimilation algorithm to estimate both model and observation errors. Remote Sens. Environ., 269, 112802.

Touitou MOHAMMED Abul Quasem AL-AMIN. (2018). "Climate change and water resources in Algeria: vulnerability, impact, and adaptation strategy". Economic and Environmental Studies Vol. 18, No 1 (45/2018), 411-429.

Ummenhofer, C.C., England, M.H., McIntosh, P.C., Meyers, G.A., Pook, M.J., Risbey, J.S., Gupta, A.S., Taschetto, A.S. (**2009**). What causes Southeast Australia's worst droughts. Geophys. Res. Lett. 36 (4), 1–5.

UNESCO/EOMAP: The portal was developed in the framework of UNESCO-IHP's International Initiative on Water Quality (IIWQ), and a computational system, was developed by EOMAP, Germany.

United Nations Environment Programme (UNEP). (2019). GEO-6: Global Environment Outlook - Summary for Policy Makers. Retrieved from https://www.unenvironment.org/resources/global-environment-outlook-6-summary-policy-makers

Van Dijk, A. I. J. M., & Renzullo, L. J. (2011). Water resource monitoring systems and the role of satellite observations. Hydrology and Earth System Sciences, 15, 39–55.

Van Eekelen, M. W., Bastiaanssen, W. G. M., Jarmain, C., Jackson, B., Ferreira, F., Van der Zaag, P., Okello, A. S., Bosch, J., Dye, P., Bastidas-Obando, E., Dost, R. J. J., & Luxemburg, W. M. J. (2015). A novel approach to estimate direct and indirect water withdrawals from satellite measurements: A case study from the Incomati basin. Agriculture, Ecosystems & Environment, 200, 126–142.

Van Loon, A.F. (2015). Hydrological drought explained. WIREs Water, 2, 359–392.

Van Loon, A.F., Gleeson, T., Clark, J., van Dijk, A.I.J.M., Stahl, K., Hannaford, J., Baldassarre, G.D., Wagener, T., Rangecroft, S., Wanders, N., Van Lanen, H.A.J. (**2016**). Drought in the Anthropocene. Nat. Geosci. 9, 89–91.

Victor Langenberg., Anne van der Heijden., Arjen C de Vos., Beatriz de la Loma Gonzalez (2021). Status of water resources and opportunities in Algeria, Morocco and Tunisia Water in agriculture in three Maghreb countries. March 2021.

Vigneau, N., Ecarnot, M., Rabatel, G., Bendoula, R., & Gorretta, N. (2014). Hyperspectral imaging for monitoring plant pigments. In Hyperspectral Imaging (pp. 261-279). CRC Press.

Vintrou, E.(2012). Cartographie et caracterisation des systemes agricoles au mali par teledetection a moyenne resolution spatiale. Thèse de doctorat. Institut des Sciences et Industries du Vivant et de l'environnement. 204 p .

Vogels, M. F. A., de Jong, S. M., Sterk, G., Wanders, N., Bierkens, M. F. P., & Addink, E. A. (**2020**). An object-based image analysis approach to assess irrigation-water consumption from MODIS products in Ethiopia. International Journal of Applied Earth Observation and Geoinformation, 88, 102067.

Vuolo, F., Essl, L., & Atzberger, C. (2015). Costs and benefits of satellite-based tools for irrigation management. Frontiers in Environmental Science, 3, 52.

Wang Pengxin, Gong Jianya, Li Xiaowen. (2003). Advances in drought monitoring by using remotely sensed normalized difference vegetation index and land surface temperature products. Advance in Earth Sciences, 18(4), 527–533. (in Chinese)

Wang, W., Estsen, M.W., Svoboda, M.D., Hafeez, M. (**2016**). Propagation of drought: from meteorological drought to agricultural and hydrological drought. Adv. Meteorol. 2016, 1–5.

Wang, Y., Zhao, C., Liu, S., Liu, C., & Chen, Y. (2020) : Estimation of maize water consumption using remote sensing data: A case study in the middle reaches of the Heihe River Basin, China. Remote Sensing, 12(5), 780. doi: 10.3390/rs12050780

Werner, B.; Collins, R. et. al., 2012 : Towards efficient use of water resources in Europe. EEA Report | No 1/2012, European Environment Agency, Copenhagen.

World Bank. (2021). data.worldbank.org/country/algeria

World Bank: WB data available in: http://data.worldbank.org/indicator/EN.ATM.CO2E.PC

Xu, H., *& al*. (2019). "Remote Sensing-Based Maize Yield Estimation Using Machine Learning and Feature Selection Methods." Remote Sensing, vol. 11, no. 6, pp. 688. doi: 10.3390/rs11060688.

Yang, C., Everitt, J. H., & Bradford, J. M. (**2018**). Use of unmanned aerial vehicles for crop scouting in agriculture. Agronomy, 8(8), 152.

Yoro, K.O., Daramola, M.O. (2020). Chapter 1—CO2 emission sources, greenhouse gases, and the global warming effect. In Advances in Carbon Capture, 1st ed.; Rahimpour, M.R., Farsi, M., Makarem, M.A., Eds.; Woodhead Publishing: Sawston, UK, 2020; pp. 3–28. ISBN 9780128196571. [Google Scholar]

Yuan, L., Pu, R., Zhang, J., Wang, J., Yang, H., 2015. Using high spatial resolution satellite imagery for mapping powdery mildew at a regional scale. Precis. Agr. 1–17.**Zhang, J., Huang, Y., Yuan, L., Yang, G., Chen, L., Zhao, C., 2015.** Using satellite multispectral imagery for damage mapping of armyworm (Spodoptera frugiperda) in maize at a regional scale. Pest Manage. Sci. 72, 335–348.

Yuei-An Liou,Sanjib kumar kar.(2014) : Evapotranspiration Estimation with Remote Sensing and Various Surface Energy Balance Algorithms.

Zaussinger, F., Dorigo, W., Gruber, A., Tarpanelli, A., Filippucci, P., & Brocca, L. (2019). Estimating irrigation water use over the contiguous United States by combining satellite and reanalysis soil moisture data. Hydrology and Earth System Sciences, 23(2), 897–923.

Zaveri, E., & B Lobell, D. (**2019**). "The role of irrigation in changing wheat yields and heat sensitivity in India." Nature communications, 10(1).

Zhang Renhua, Sun Xiaomin (2001). Regional differentiation of quantitative estimate crop transpiration and soil water use efficiency by using remote sensing. Science in China: Series D, 31(11), 959–968.

Zhang, M. (**2019**). "Advances in Remote Sensing for Crop Growth Monitoring: A Review." Frontiers in Plant Science.

Zhang, W., Ji, Y., Liu, Y., & Wang, Y. (**2021**). A review of remote sensing applications in pest and disease monitoring of crops. Remote Sensing Applications: Society and Environment, 24, 100459.

Zhang, Y., Pan, M., & Wood, E. F. (**2016**). On creating global gridded terrestrial water budget estimates from satellite remote sensing. Surveys in Geophysics, 37(2 SI), 249–268.

Zhang, Y.C., Ma, R.H., Duan, H.T., Loiselle, S.A., Xu, J.D., & Ma, M.X. (**2014**). A Novel Algorithm to Estimate Algal Bloom Coverage to Subpixel Resolution in Lake Taihu. Ieee Journal of Selected Topics in Applied Earth Observations and Remote Sensing, 7, 3060-3068.

Zhao, J., Yang, X., Dai, S., Lv, S., & Wang, J. (**2015**). Increased utilization of lengthening growing season and warming temperatures by adjusting sowing dates and cultivar selection for spring maize in Northeast China. European Journal of Agronomy, 67, 12–19.

Zohaib, M., & Choi, M. (**2020**). Satellite-based global-scale irrigation water use and its contemporary trends. Science of The Total Environment, 714, 136719.

Web sites:

Web master 1: Usgs.gov

Web master 2: climateengine.org

Web master 3: tutiempo.net

Web master 4: google.com

Web master 5: stratfor.com